



LUND UNIVERSITY

Atrial Conduction and P-wave Characteristics: From histology to electrophysiology

Huo, Yan

2015

[Link to publication](#)

Citation for published version (APA):

Huo, Y. (2015). *Atrial Conduction and P-wave Characteristics: From histology to electrophysiology*. [Doctoral Thesis (compilation), Cardiology]. Cardiology, Dept of Clinical Science, Lund, Lund University.

Total number of authors:

1

General rights

Unless other specific re-use rights are stated the following general rights apply:

Copyright and moral rights for the publications made accessible in the public portal are retained by the authors and/or other copyright owners and it is a condition of accessing publications that users recognise and abide by the legal requirements associated with these rights.

- Users may download and print one copy of any publication from the public portal for the purpose of private study or research.
- You may not further distribute the material or use it for any profit-making activity or commercial gain
- You may freely distribute the URL identifying the publication in the public portal

Read more about Creative commons licenses: <https://creativecommons.org/licenses/>

Take down policy

If you believe that this document breaches copyright please contact us providing details, and we will remove access to the work immediately and investigate your claim.

LUND UNIVERSITY

PO Box 117
221 00 Lund
+46 46-222 00 00

Atrial Conduction and P-wave Characteristics

From histology to electrophysiology

YAN HUO, M.D.



LUNDS
UNIVERSITET

DOCTORAL DISSERTATION

by due permission of the Faculty Medicine, Lund University, Sweden.

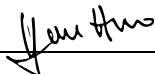
To be defended at Segerfalksalen, BMC, Sölvegatan 19, Lund
on October 16, 2015 at 09:00 AM

Faculty opponent

Docent Nils Edvardsson, Department of Molecular and Clinical Medicine,
University of Gothenburg, Gothenburg, Sweden

Organization: LUND UNIVERSITY	Document name: DOCTORAL DISSERTATION	
Department of Cardiology, Clinical Sciences, Lund	Date of issue: October 16, 2015	
Author: Yan Huo	Sponsoring organization	
Title and subtitle: Atrial Conduction and P-wave Characteristics: From histology to electrophysiology		
<p>Abstract</p> <p>P-wave morphology reflects the projection of the depolarization vector on the electrocardiogram (ECG) lead axes in three-dimensional space and reflects both right and left atrial activation. The main purpose of current thesis was to explore the internal logic between the atrial conduction properties, including intra- and inter- atrial conduction, and P-wave characteristics from the level of histology to electrophysiology.</p> <p>The current thesis consists of four substudies entitled as: (1) P-wave characteristics and histological atrial abnormalities; (2) Effects of baseline P-wave duration and choice of atrial septal pacing site on shortening atrial activation time during pacing; (3) Diagnosis of atrial tachycardia originating from the lower right atrium: importance of P-wave morphology in the precordial leads V3-V6; and (4) Variability of P-wave morphology predicts the outcome of circumferential pulmonary vein isolation in patients with recurrent atrial fibrillation, respectively.</p>		
Key words: Atrial fibrillation, Sinus rhythm, Histology, Electrophysiology, Human, P-wave Morphology, Variability of P-wave morphology, P-wave duration		
Classification system and/or index terms (if any)		
Supplementary bibliographical information	Language: English	
ISSN and key title: ISSN 1652-8220 Lund University, Faculty of Medicine Doctoral Dissertation Series 2015:104	ISBN: 978-91-7619-183-5	
Recipient's notes	Number of pages	Price
	Security classification	

I, the undersigned, being the copyright owner of the abstract of the above-mentioned dissertation, hereby grant to all reference sources permission to publish and disseminate the abstract of the above-mentioned dissertation.

Signature  Date October 16, 2015

Atrial Conduction and P-wave Characteristics

From histology to electrophysiology

YAN HUO, M.D.



LUNDS
UNIVERSITET

Copyright Yan Huo

Department of Cardiology, Clinical Sciences Lund
Faculty of Medicine
Lund University
Sweden

ISBN 978-91-7619-183-5
ISSN 1652-8220

Lund University, Faculty of Medicine Doctoral Dissertation Series 2015:104

Printed in Sweden by Media-Tryck, Lund University
Lund 2015



KLIMATKOMPENSERAT
PAPPER



PAPERS

1. P-wave characteristics and histological atrial abnormality.

Huo Y, Mitrofanova L, Orshanskaya V, Holmberg P, Holmqvist F, Platonov PG. J Electrocardiol. 2014 May-Jun;47(3):275-80.

2. Effects of baseline P-wave duration and choice of atrial septal pacing site on shortening atrial activation time during pacing.

Huo Y, Holmqvist F, Carlson J, Gaspar T, Arya A, Wetzel U, Hindricks G, Piorkowski C, Bollmann A, Platonov PG. Europace. 2012 Sep;14(9):1294-301.

3. Diagnosis of atrial tachycardias originating from the lower right atrium: importance of P-wave morphology in the precordial leads V3-V6.

Huo Y, Braunschweig F, Gaspar T, Richter S, Schönbauer R, Sommer P, Arya A, Rolf S, Bollmann A, Hindricks G, Piorkowski C. Europace. 2013 Apr;15(4):570-7.

4. Variability of P-wave morphology predicts the outcome of circumferential pulmonary vein isolation in patients with recurrent atrial fibrillation.

Huo Y, Holmqvist F, Carlson J, Gaspar T, Hindricks G, Piorkowski C, Bollmann A, Platonov PG. J Electrocardiol. 2015 Mar-Apr;48(2):218-25.

ABBREVIATIONS

AF	-	atrial fibrillation
aIAB	-	advanced interatrial conduction block
CPVI	-	circumferential pulmonary vein isolation
CS	-	coronary sinus
CSo	-	coronary sinus ostium
CT	-	crista terminalis
ECG	-	electrocardiogram
EAT	-	ectopic atrial tachycardia
FO	-	fossa ovalis
HAS	-	high (right) atrial septum
IAC	-	interatrial conduction
IPV	-	inferior pulmonary vein
LA	-	left atrium/atrial
LAA	-	left atrial appendage
pIAB	-	partial interatrial conduction block
PLA	-	posterior left atrium
PTF	-	P-wave terminal force
PV	-	pulmonary vein
PWD	-	P-wave duration
PMV	-	variability of P-wave morphology
PSFO	-	posterior septum behind the FO
RA	-	right atrium/atrial

RAA - right atrial appendage
RFCA - radiofrequency catheter ablation
SR - sinus rhythm
SPV - superior pulmonary vein
TA - tricuspid annulus
3D-EA - three-dimensional electroanatomical

TABLE OF CONTENTS

Papers	4
Abbreviations.....	7
Chapter 1. Introduction.....	11
1.1 Variability of the origin of rhythm.....	11
1.2 Left atrial breakthrough	12
1.3 Interatrial and intraatrial conduction routes.....	13
1.4 Atrial histological abnormalities and atrial conduction.....	14
1.5 Atrial remodeling in patients with atrial fibrillation and variability of P-wave morphology.....	15
1.6 P-wave morphology assessment.....	17
Chapter 2. Aims	19
2.1 Outline of the work	19
2.2 Brief descriptions of the studies and aims.....	19
Chapter 3. Methods.....	21
3.1 Study population	21
3.2 Data acquisition and electrogram analysis	23
3.3 Statistical methods.....	33
Chapter 4. Results	35
4.1 P-wave characteristics and histological atrial abnormality.....	35
4.2 Atrial septal pacing site effect on atrial activation time shortening.....	40
4.3 Atrial tachycardia originating from the lower right atrium	45
4.4 Variability of P-wave morphology.....	53
Chapter 5. Discussion.....	57
5.1 Atrial histology	57
5.2 Interatrial connections and rhythm origin.....	59
5.3 Dynamic P-wave morphology changes.....	62
5.4 Knowledge gaps and clinical implications	64
Chapter 6. Conclusions	67
Acknowledgments.....	69
References.....	71

CHAPTER 1. INTRODUCTION

ATRIAL CONDUCTION AND P-WAVE CHARACTERISTICS

P-wave morphology reflects the projection of the depolarization vector on the electrocardiogram (ECG) lead axes in three-dimensional space and reflects both right (RA) and left atrial (LA) activation. Several factors mainly contribute to the P-wave morphology: (1) the origin of the rhythm (RA breakthrough), which results in RA depolarization and defines the general depolarization vector, (2) the LA breakthrough, which defines the main direction of the LA depolarization vector, (3) interatrial conduction properties, which link to the localization of the LA breakthrough, and (4) the geometry of atrial chambers and histological abnormalities both affect the time of the depolarization process and the course of depolarization propagation.

1.1 Variability of the origin of rhythm

The common perception are often over-simplified illustrations of the sinus node being a relatively small structure located at the superior caval vein opening in the RA. However, the most recent anatomical reconstruction indicates that the compact sinus node may reach 20 mm in length and extend downward in the projection of the terminal groove [1]. These findings are supported by clinical experience of catheter ablation of inappropriate sinus tachycardia in the sinus node region [2]. Interindividual and intraindividual variabilities of P-waves have also been studied. The earliest activation can be located between the most inferior part of the RA pacemaker complex at the level of mid-septal region and the most superior part at the junction with right atrial appendage (RAA) interindividually [3, 4]. Meanwhile, the presence of secondary and tertiary P-wave morphologies intraindividually at rest in one-third of healthy subjects using signal-averaged ECG analysis has also been studied [5]. The variable location of the atrial pacemaker can cause variability of the initial RA activation vector and upward or biphasic P-wave appearance in the inferior leads [3, 6].

A shift in the site of the sinus depolarization wave origin was reported as the possibility of a spontaneous P-wave morphology change [3]. However, whether variability of sinus

rhythm origin is due to the actual switch from one group of pace-making cells within the sinus node to another, or whether variability is caused by a different route of propagation within the sinus node and outside the sinus node via distinct exit routes is still controversial [6]. Further studies reported that the association between heart rate acceleration and the earliest activation site shift to superior-anterior regions of the RA pacemaker complex [7, 8], which are in agreement with P-wave morphology change in healthy subjects during exercise described either as an increase in negative PTF in lead V1 [9] or increase in maximal posterior and inferior component in the orthogonal Z lead [10].

The origin of ‘ectopic’ as used in ‘ectopic atrial tachycardia’ was from the late 19th century: from modern Latin *ectopia* - ‘presence of tissue, cells, etc. in an abnormal place’. Theoretically, the origin of ectopic atrial tachycardia could be anywhere in both atria. However, in reality the localization of atrial tachycardia’s origin mostly clustered around several important atrial structures. The link between P-wave morphology during the ectopic atrial tachycardia (EAT) and the localization of EAT’s origin has been well studied previously [11-13].

1.2 Left atrial breakthrough

The localization of the LA depolarization starting point defines the major vector of LA depolarization and shapes the terminal part of the P-wave alone after the RA depolarization ends. Although Bachmann’s bundle is considered the most important interatrial conduction route, the depolarization breakthrough to the LA may occur in the posteroinferior region of the atrial septum in up to one-third of patients, as reported using noncontact mapping [14, 15]. Further studies, using electro-anatomical mapping in the largest reported patient series to date, confirmed the finding that LA breakthrough occurred outside the Bachmann’s bundle via posterior or inferior interatrial connections in one-third of patients, including 14 of 50 patients in this cohort more than one breakthrough was simultaneously observed in LA [15]. Two factors may be of greatest influence, i.e. high interindividual variability in the structure and location of interatrial routes [16] and their conduction properties, as well as relative proximity of the sinus rhythm origin to the employed interatrial conduction route.

1.3 Interatrial and intraatrial conduction routes

Previous histological studies reported that no special conduction system (i.e. HIS bundle, right bundle branch, left bundle branch, etc.) was found in the atria. However, several special atrial structures were found with a higher conduction velocity, including endocardial and epicardial structures in the septum [17]. Our current understanding of preferential interatrial conduction routes is based mainly on anatomical studies [16, 18, 19] and electrophysiological examinations using 3D electro-anatomic or non-contact mapping during sinus rhythm (SR) [14, 15, 20, 21]. The different modes of intraatrial and interatrial activation have been demonstrated to follow preferential routes located high in the RA septum (i.e. Bachmann's bundle), posteriorly in the intercaval area, and inferiorly in the vicinity of the coronary sinus ostium (CSo) [22-27]. In previous anatomical and radiological studies, Bachmann's bundle was detected in about 90% of specimens in large cohorts, and also in large groups of patients without heart disease using the spiral computed tomography [16, 28], and has been suggested as a region of fast conduction by results of both experimental and human studies [23-25, 29]. Extension of RA myocardial sleeves on the coronary sinus (CS) with distinct connections to the LA myocardium is commonly observed [30]. It has been demonstrated that the CS musculature is electrically connected to the RA and LA, and forms an RA-LA connection in canine hearts [26] and in human hearts [22], which provides further evidence supporting the existence of a preferential route for interatrial conduction near the CSo. Specifically, a single RA breakthrough has been identified around the CSo during distal CS pacing in all studied patients [27]. Furthermore, Ho et al. have described small muscle bridges connecting the LA posterior wall near the ostia of right-sided pulmonary veins to the RA posterior wall at the intercaval area in human hearts [18]. The function of these posterior interatrial connections has also been confirmed by mapping the RA during atrial tachycardia originating from PVs [31] in which the RA breakthrough was identified in the posterior intercaval area. The quantity, length and diameter of interatrial connection fibers vary considerably among individuals [16, 32].

During SR, the preferential interatrial conduction does not seem to be linked to a certain anatomical structure, but rather seems to depend on both the origin of the RA activation [3] and the variability of interatrial connections [16, 32, 33]. The employed interatrial connection during SR was suggested to occur through posterior fibers behind

the FO and / or Bachmann's bundle [20, 34]. However, during pacing in the vicinity of the CSo it has been reported that the preferential interatrial conduction route was likely to be the CS musculature [14, 26]. The retrograde activation of the CS was also studied in detail. During pacing at the left superior PV, the initial breakthrough in the RA was identified at the CSo, which suggests that propagation was through the CS musculature rather than through Bachmann's bundle or the PSFO [25].

Furthermore, conduction properties of interatrial conduction routes were also studied in previous studies involving atrial-pacing technique. Permanent transvenous atrial pacing leads have traditionally been implanted in the RAA and, occasionally, in the RA lateral wall. Pacing from the RAA or free wall can lead to delayed intraatrial and interatrial conduction, and may provoke electromechanical delay in the atria, leading to discoordination of right and LA contraction [35]. Based on the issues raised above, it has been suggested that dual-site RA pacing [36] and biatrial resynchronization [37] are more beneficial than both high RA pacing and antiarrhythmic drug therapies, with regard to atrial fibrillation (AF) prevention by a long-term follow-up. Electrophysiological studies [38] have suggested that reduction in atrial conduction delay and modification of dispersion in atrial refractoriness are important mechanisms in AF prevention, which could be achieved by multisite atrial pacing. Similar results could also be achieved by single-site atrial pacing that does not require any special implantable device. The optimal pacing site for the prevention of paroxysmal AF using single-site pacing is suggested to be the atrial septum [39-42]; however, no detailed studies have been carried out on electrophysiological properties regarding the relation between shortening of P-wave duration (PWD) and pacing site. The limitation of atrial pacing mode was also noticed that the antiarrhythmic efficacy of this specific atrial-pacing mode is rather modest on unselective cohorts, which explains that it remains outside clinical routine. Even though at some centers it is regularly employed.

1.4 Atrial histological abnormalities and atrial conduction

In 1977, Evans and Shaw examined 8 patients with sinus node disease and demonstrated that in 7 of these patients there was increased fibrosis or fatty infiltration in RA musculature. It was the first study offering evidence of widespread RA abnormality in Humans, which revealed an underlying relation between fibro-fatty infiltration and atrial conduction abnormality [43]. Later, in post-mortem materials,

fibrosis extent and fatty infiltration were observed in patients with a history of AF, which was significantly higher in patients with permanent AF as compared to paroxysmal AF [44]. Meanwhile, it revealed that atrial dilatation in AF patients is associated with fibro-fatty replacement of the atrial myocardium that equally affects the atrial walls and the major conduction routes [44]. In this setting, thickness of interatrial routes may be directly linked to the routes' ability to maintain conduction despite myocyte loss. More advanced fibrosis might interrupt conduction over the Bachmann's bundle and result in so-called partial or advanced interatrial block with delayed interatrial conduction through Bachmann's bundle or retrograde LA activation via the inferior interatrial route near the coronary sinus ostium [45-47]. Further studies have also associated abnormal PWD and morphology with AF, ageing and cardiovascular comorbidities [48-54]. Fibro-fatty transformation of atrial walls is believed to be the leading cause of deteriorated atrial conduction [43, 55, 56]. However, any direct assessment of fibrosis extent in the major atrial conduction routes in relation to P-wave characteristics is lacking.

1.5 Atrial remodeling in patients with atrial fibrillation and variability of P-wave morphology

Many studies have explored the mechanism of the initiation and maintenance of AF [57-64]. Over the last decade, studies of radiofrequency catheter ablation for treatment of AF reported higher efficacy rates than studies of antiarrhythmic drug therapy [65-68]. Circumferential PV isolation (CPVI) has been proven as the cornerstone of treatment of AF, regardless of stage of AF. However, CPVI alone has been shown to be insufficient for a considerable proportion of patients with AF [69-71], especially for those with persistent or permanent AF.

In the last two decades, a number of noninvasive markers have been studied in order to evaluate the progress of atrial remodeling in patients with AF, such as atrial fibrosis, LA diameter, PWD and morphology, etc., and these markers further could predict the outcome of AF ablation or affiliate the selection of patients for specific ablation strategies. Previous experimental studies also suggest that interatrial conduction defects play a role in the development of AF [25, 72-74]; the global conduction abnormalities (such as repolarization alternans and conduction slowing) during sinus rhythm in patients or animal models with AF or atrial tachycardia have been also studied [75, 76],

it is also worth noting that in major conduction routes conduction velocity was significantly reduced [77]. These changes are associated with significant increase in AF vulnerability.

The understanding of AF pathophysiology has advanced significantly over the years through increased awareness of the role of atrial remodeling in the development of persistent change in atrial structure or function. Structural remodeling that is consistently seen in models of AF and in patients with AF includes atrial enlargement, cellular hypertrophy, dedifferentiation, fibrosis, apoptosis, and myolysis [78-87]. Recently, the concept of fibrotic atrial cardiomyopathy (FACM) was introduced into the AF field in order to describe the underlying pathophysiological process of human structural atrial remodeling [88, 89]. Fibrotic atrial structural remodeling has been consistently described in AF patients in histological and autopsy studies [44, 90, 91]. The presence of (micro) fibrosis leading to changes in cellular coupling results in spatial “non-uniform anisotropic” impulse propagation, which is a potential cause of atrial activation abnormalities underlying the initiation and perpetuation of re-entrant arrhythmias like AF [92, 93]. Recent clinical research has highlighted the presence of atrial tissue fibrosis using delayed-enhancement magnetic resonance imaging (DE-MRI) and electroanatomical voltage mapping [94, 95]. Importantly, fibrotic atrial changes vary in localization and extent, and are principally bi-atrial findings. A higher mean value of fibrosis was detected in patients with persistent AF versus paroxysmal AF; however, variability in the extent of fibrosis among patients with AF is very high [91]. Additionally, there is indeed limited histological evidence of fibrosis in atrial walls from human atria tissues. Most data came from RA septum biopsies and surgically removed left atrial appendage (LAA) / RAA, not from atrial walls that are believed to harbor electrical circuits maintaining AF.

As assumed above, atrial remodeling is continuously advancing in patients with AF, such as an increase of PWD or LA-diameter or altered P-wave morphology. The variability of P-wave morphology in healthy subjects has been reported very low [96]. Further studies also showed that abnormal P-wave morphology associates with the existence of AF or diseased atria [54, 97]. However, mild or moderate atrial remodeling may not change the P-wave morphology permanently. The P-wave morphology even differ from beat to beat in a short period (The study 4 demonstrates dynamic changes of sinus P-wave morphology in 10 min ECG recordings).

The ability of the atrial depolarization wave to choose one or another intraatrial- or interatrial route during sinus rhythm may be significantly limited by severe atrial structural remodeling (i.e. fibrosis, fatty infiltration etc.) at the end stage of FACM. Regardless of etiological causes, increasing fibrosis etc. would limit both the ability to conduct through different paths and the potential number of exits from the sinus node, thus leading to a more rigid activation pattern during sinus rhythm.

1.6 P-wave morphology assessment

In previous studies, interatrial conduction defects have been suggested to play a role in the development of AF [25, 72-74]. Different P-wave morphologies during SR as displayed on standard ECGs have been postulated to correspond to differences in interatrial conduction [98-100]. A previous study from our group shows that orthogonal P-wave morphology can be used to correctly identify the LA breakthrough site and the corresponding route of interatrial conduction [101]. Accordingly, the orthogonal P-wave morphologies have been present with distinct appearances being linked to age, comorbidities and the risk of AF development.

In our earlier studies using morphology analysis of signal-averaged P-waves [53], we identified that 2 different sinus P-wave morphologies with negative (previously defined Type 1) or biphasic (previously defined Type 2) patterns in lead Z (in the sagittal plane), which are the most common P-wave morphological types, in which both positive patterns in leads X and Y. Sinus P-wave with negative in lead Z is mostly observed in adolescents and young adults [53, 102]; Sinus P-wave with biphasic pattern in lead Z is commonly observed in the elderly [53] and in patients with paroxysmal AF [103, 104]. Furthermore, both 2 sinus P-waves are equally common in middle-aged healthy population [53]. Both above-mentioned 2 types of sinus P-wave morphologies were commonly observed in healthy subjects [53].

On the contrary, advanced interatrial conduction block morphology (previously defined Type 3 P-wave with biphasic in lead Y) has been reported as corresponding to the advanced interatrial block with retrograde LA activation. Previous studies suggested that biphasic P-waves in inferior leads (12-lead ECG) or in Lead Y (orthogonal lead configuration) are most likely due to Bachmann's bundle block producing an advanced interatrial block [100, 105]. In the present study, none of the healthy subjects has Type

3 P-wave morphology, but it is commonly seen in HCM patients [97]. Type 4 morphology has been reported presenting in ARVC patients [106] and patients with paroxysmal AF [107]; however, it has never been observed in healthy subjects [53]. Several reports indicate that P-waves that are negative in lead V1 and positive in inferior and lateral leads are commonly observed in atrial rhythms originating from RAA [11, 108], which suggests a shift of the origin of sinus rhythm toward the anterior part or the RA or the RAA. The variability of the location of sinus rhythm origin including its extreme anterior locations has been reported previously [3].

CHAPTER 2. AIMS

2.1 Outline of the work

The main purpose of the current thesis is to explore the internal logic between atrial conduction properties, including intra- and inter- atrial conduction, and P-wave characteristics from the level of histology to electrophysiology. The thesis consists of the four following sub-studies:

2.2 Brief descriptions of the studies and aims

P-WAVE CHARACTERISTICS AND HISTOLOGICAL ATRIAL ABNORMALITY

As described earlier, fibro-fatty transformation is believed to be the leading cause of deteriorated atrial conduction; however, any direct assessment in relation to P-wave characteristics is lacking. We sought to assess P-wave morphology (PWM) and PWD in relation to histology of the atrial myocardium.

EFFECTS OF BASELINE P-WAVE DURATION AND CHOICE OF ATRIAL SEPTAL PACING SITE ON SHORTENING ATRIAL ACTIVATION TIME DURING PACING

Based on the high variability of the location of interatrial connections, it is reasonable to assume that pacing at the site mainly responsible for interatrial conduction would result in a shorter paced PWD, corresponding to the shorter global atrial activation time in that individual. The aim of this study was thus to assess the effect of different atrial septal pacing sites on P-wave shortening and to identify the pacing site associated with the shortest paced PWD.

DIAGNOSIS OF ATRIAL TACHYCARDIA ORIGINATING FROM THE LOWER RIGHT ATRIUM: IMPORTANCE OF P-WAVE MORPHOLOGY IN THE PRECORDIAL LEADS V3-V6

With respect to the P-wave morphology during EAT originated at RA, multiple factors could influence the P-wave morphology, such as: (1) activation sequence of RA, (2) activation from RA to left atria (LA), which is associated with preferential interatrial

conduction routes (IAC), and in the end (3) activation sequence of LA. This study was done to further establish ECG characteristics of focal atrial tachycardia originating at the lower RA in order to avoid the influence of the superior interatrial conduction route (Bachmann's bundle). We hypothesized that the employment of preferential IAC results in typical P-wave morphology in V3-V6 (horizontal plan).

VARIABILITY OF P-WAVE MORPHOLOGY PREDICTS THE OUTCOME OF CIRCUMFERENTIAL PULMONARY VEIN ISOLATION IN PATIENTS WITH RECURRENT ATRIAL FIBRILLATION

It is commonly held that atrial remodeling is continuously evolving in patients with AF, such as increasing PWD or LA-diameter, or altered P-wave morphology. Furthermore, the sequence of atrial depolarization and the duration of entire atrial depolarization determined the final P-wave morphology beat by beat. Meanwhile, a mild or moderate remodeling may not change the P-wave morphology permanently. So we decided to study the variability of P-wave morphology instead of P-wave morphology directly. We hypothesized that beat-to-beat variability of atrial depolarization route during SR may reflect the degree of atrial remodeling and may thus be associated with the outcome of AF ablation.

CHAPTER 3. METHODS

3.1 Study population

3.1.1 POST MORTEM STUDY MATERIAL (STUDY 1)

Materials for the study were collected in accordance with the protocol described in detail earlier [44]. In short, medical records of consecutive cases of in-hospital deaths referred for post-mortem studies at the Almazov Federal Heart, Blood, and Endocrinology Centre (St. Petersburg, Russia) were screened for AF presence and its clinical type (n=276). Subjects with AF after open-heart surgery or severe valvular pathology were excluded. Three predefined groups of 10 cases each equally were collected, representing subjects with permanent AF, non-permanent AF, and subjects with no documented AF history. A total of 30 subjects were used for histological analysis, of whom 20 either had no AF history or had non-permanent AF, thus being suitable for a study aimed at P-wave analysis. After excluding patients who had ECG tracings with ST-elevation, invisible onset or ending of P-waves (i.e. P-wave on T-wave), unstable baseline of ECG tracing and heart rate <50 or >100/min, 11 subjects remained suitable for analysis. Four out of the 11 subjects had a history of paroxysmal AF. (Table 1)

3.1.2 INVASIVE ELECTROPHYSIOLOGICAL STUDY COHORT (STUDY 2)

Sixty-nine consecutive patients (aged 52 ± 16 years, range 19-79 years, 41 men) undergoing clinically motivated electrophysiological studies due to supraventricular tachycardia were studied. All patients gave written informed consent on the investigational nature of the procedure that was approved by the institutional review committee. None of the patients showed any evidence of underlying structural heart disease as assessed by transthoracic echocardiography. All antiarrhythmic drugs were discontinued at least five half-lives before the study, and none of the patients was taking amiodarone or digitalis. In the current study, the mean diameter of the LA was 39 ± 6 mm; and 25 patients (36%) had an enlarged (>40mm) LA (44 ± 4 mm). 21 of the 69 patients (30%) had a history of paroxysmal AF. 12 of the 21 patients had received flecainide by the 'pill-in-the-pocket' approach, while 9 patients had uncommon arrhythmia episodes and were off all medications. None of paroxysmal AF patients was

treated with PV isolation either before or during index admission. Before the electrophysiological study, the patients with paroxysmal AF had been suspected as carriers of other supraventricular tachycardias with atypical AF-related symptoms, such as atrioventricular nodal reentrant tachycardia (AVNRT) etc.. 10 patients (14%) had a history of typical atrial flutter. 14 patients (20%) were found to have inducible AVNRT, and three patients (4%) had a left-sided accessory pathway. In the rest of the patients (26 patients, 38%) it was not possible to induce tachycardia during the electrophysiological studies. Radiofrequency catheter ablation was successful in patients with induced supraventricular tachycardia.

3.1.3 ATRIAL TACHYCARDIA ABLATION COHORT (STUDY 3)

Between October 2006 and April 2010, 144 consecutive patients underwent radiofrequency catheter ablation (RFCA) due to focal EAT with origin of RA at Heart Center Leipzig. In 28 (aged 52 ± 15 years, 21 men) out of 144 patients (19%), a tachycardia with an origin of lower RA was confirmed using 3-dimensional (3D) electroanatomical (EA) activation mapping and the RFCA procedure. All patients had symptomatic tachycardias and proved refractory to at least one antiarrhythmic agent. All patients signed a written informed consent.

3.1.4 ATRIAL FIBRILLATION ABLATION COHORT (STUDY 4)

Between January 2010 and June 2010, 70 consecutive patients (aged 60 ± 9 years, range 31-79 years, 46 men) undergoing clinically motivated CPVI due to highly symptomatic drug-refractory AF at Heart Center Leipzig were included in this study. All patients gave written informed consent on the investigational nature of the procedure that was approved by the institutional review committee. All antiarrhythmic drugs were discontinued at least five half-lives prior to the study, including beta-blockers and digitalis, and none of the patients were taking amiodarone. Exclusion criteria were: (1) severe valve disease (e.g. greater than mitral insufficiency II°); (2) acute heart failure; (3) any previous ablation procedure affecting the atria; and (4) previous surgery on heart, esophagus or lung. (Table 2)

3.2 Data acquisition and electrogram analysis

3.2.1 OUTLINE OF ECG ANALYSIS

A standard 12-lead ECG was taken for all study subjects for P-wave analysis. For the sub-studies, which involved orthogonal ECG analysis, recordings of standard 12-lead ECGs were transformed to orthogonal leads, and signal-averaged P-wave analysis was performed to estimate P-wave duration. These data were stored for subsequent offline processing. Data analysis was performed using custom software running on MATLAB (The MathWorks, Natick, MA).

P-WAVE ANALYSIS ON PAPER (STUDY 1)

A 12-lead surface ECG was recorded in supine position using a Hellige ECG 153 (Freiburg, Germany) machine. The 12-lead ECG was recorded at a paper speed of 50 mm/s (n=6) or 25 mm/s (n=5), a standard calibration of 10 mm/mV, and a filter of 0.05 - 35 Hz standardization. The PWD was calculated in all 12 leads of the surface ECG. The measurements of the P-wave duration were performed manually by two investigators without knowledge of the histological findings or AF group allocation. To improve accuracy, measurements were performed with calipers and magnifying lens for defining the P-wave deflection, similarly to the approach used by others [109-111]. The P-wave onset was defined as the point of the first visible upward / downward departure of the trace from baseline bottom for positive / negative waves. When the trace returned to the baseline at the bottom of the trace in positive waves or at the top of the trace in negative waves, this point was considered to be the end of the P-wave. All P-waves of sinus rhythm in a 12-lead surface ECG were measured beat-by-beat. The mean values of longest PWDs in any lead obtained from two investigators were used for comparison with the histological findings. Any differences between observers were resolved by consensus.

Definitions

Criteria of interatrial conduction block

- Partial interatrial conduction block (pIAB): Partial interatrial block (pIAB) was defined as prolonged (≥ 120 ms) and bimodal (notched) P-wave in any lead on the standard 12-lead ECG [45-47].
- Advanced interatrial conduction block (aIAB): interatrial block is seen on the

surface ECG as a wide (≥ 120 ms) and biphasic P-wave in the inferior leads [46].

DATA ACQUISITION AND P-WAVE ANALYSIS (STUDY 2)

Standard 12-lead ECG was recorded using the Prucka CardioLab System (GE Medical Systems, Milwaukee, WI, USA) for at least 30 sec at baseline and continuously during pacing. These 12-lead ECGs were transformed to orthogonal leads and signal-averaged P-wave analysis was performed to estimate P-wave duration. These data were stored for subsequent offline processing. Data analysis was performed using custom-made software running on MATLAB (The MathWorks, Natick, MA). The basic method used is described in detail elsewhere [101, 112]. The onset and end of the P-wave were set manually on a magnified signal-averaged P-wave on a computer screen using electronic calipers. In order to ensure unbiased manual settings of P-wave onset and end, all recordings were analyzed in one batch in a blinded fashion so that only computer-generated record number was available at the time of analysis without the possibility of establishing a link between the ECG recordings, pacing sites and patient identity. The onset of the paced P-wave was defined as being directly after the end of the stimulation spike.

P-WAVE ANALYSIS IN ELECTROPHYSIOLOGICAL MAPPING SYSTEM (STUDY 3)

P-wave morphology on the surface ECG was assessed carefully to assist in the tachycardia localization. Particular attention was given to analyzing an unencumbered P-wave during periods of atrioventricular block or after ventricular pacing. Surface 12-lead P-wave morphology was assessed based on the definitions by Tang et al. [13], and was further developed. The P-waves were described on the basis of deviating from baseline during the T-P interval as being: (1) completely positive (+); (2) completely negative (-); (3) biphasic: if there were both positive and negative (+/- or -/+) deflections from baseline; (4) isoelectric: when there was no P-wave deflection from baseline of > 0.05 mV; and (5) isoelectric-positive / isoelectric-negative: isoelectric line after the onset of P-wave 20 ms and then change to positive or negative; positive-isoelectric / negative-isoelectric: positive or negative pattern ended up to the isoelectric line before the end of P-wave 20 ms.

DATA ACQUISITION AND P-WAVE ANALYSIS (STUDY 4)

After sedation using midazolam and propofol, standard 12-lead electrocardiogram (ECG) was recorded continuously using the Prucka CardioLab System (GE Medical Systems, Milwaukee, WI, USA) for 10 minutes at baseline, when patients were in SR at the beginning of the electrophysiological study. In patients with AF at baseline, electrical cardioversion was performed in order to achieve stable SR and analyze P-wave characteristics at SR. These data were stored for subsequent offline processing as previously described in study 2. Data were analyzed using custom software running on MATLAB (The MathWorks, Natick, MA, USA). To enable analysis of orthogonal P-wave morphology, orthogonal-lead ECG data were derived from the 12-lead ECG using the inverse Dower transform [113, 114]. P-wave duration was measured manually by two of the investigators without knowledge of the history of AF. Any differences between observers were resolved by consensus. The method used in this study is described in detail elsewhere [53, 97, 113].

VARIABILITY OF ORTHOGONAL P-WAVE MORPHOLOGY AND CLASSIFICATION OF ORTHOGONAL P-WAVE MORPHOLOGY

After the ECGs were transformed to orthogonal leads, beat-to-beat P-wave morphology was defined automatically depending on P-wave polarity in orthogonal leads (positive / negative / biphasic) in accordance with a pre-defined classification algorithm. The morphology was subsequently classified into one of five pre-defined classes [101]:

1. P-wave with negative deflection in lead Z (Type 1): Positive leads X and Y and negative lead Z
2. P-wave with biphasic deflection in lead Z (Type 2): Positive leads X and Y and biphasic lead Z (-/+)
3. P-wave with positive deflection in lead Z (Type 4): Positive lead X, Y and Z [106]
4. Advanced interatrial conduction block morphology (Type 3): Positive lead X and biphasic signals in leads Y (-/+)
5. Atypical P-wave: Any morphology in lead X, Y and Z, except Type 1 to 4

The four different types are schematically illustrated in Figure 1. The most common P-wave morphology observed in each patient during the 10-minute recording was defined as the dominant morphology. Variability of orthogonal P-wave morphology

(PMV) was defined as the percentage of P-waves with non-dominant morphology in the 10-min sample. All analyses were performed in a blinded fashion. Standard transthoracic echocardiography was performed in association with ablation. Figure 2 was a sample of change of orthogonal P-wave morphology during 10-minute recording.

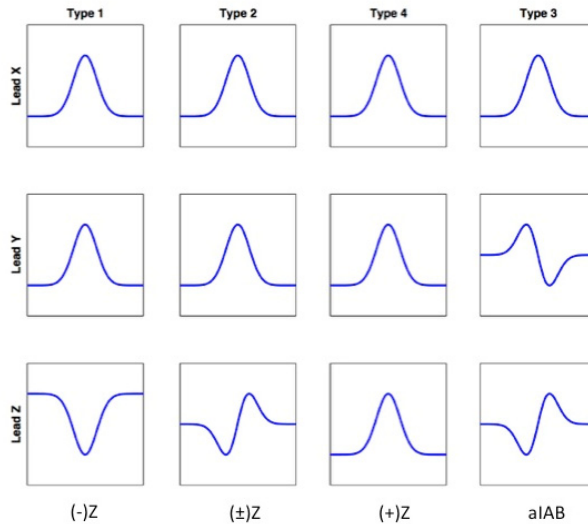


Figure 1. The four different orthogonal P-wave morphology types are schematically illustrated. From left to right: P-waves positive in leads X and Y and variable appearance in lead Z being either negative (also known as Type 1), biphasic (Type 2) or positive (Type 4). The right column depicts advanced interatrial conduction block morphology (Type 3): Positive lead X and biphasic signals in leads Y (-/+) and Z (-/+). aIAB: advanced interatrial block.

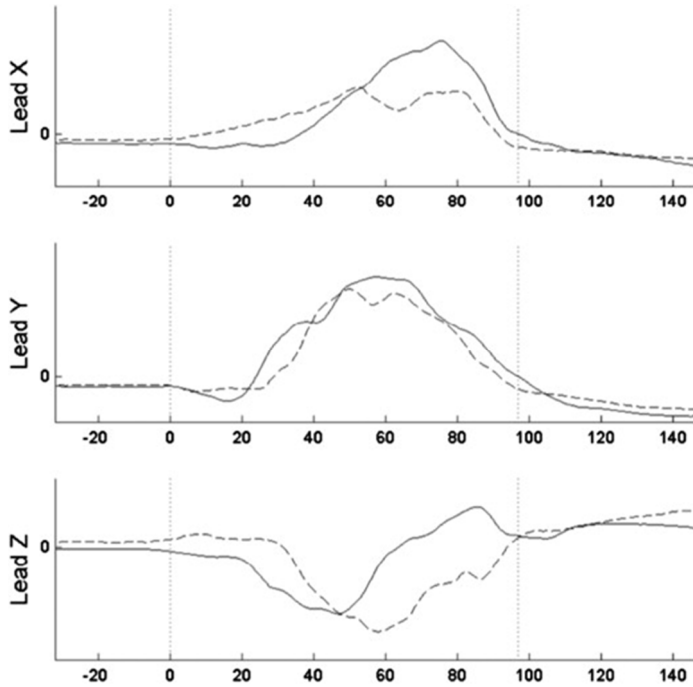


Figure 2. Changing of orthogonal P-wave morphology. P-wave morphology in lead Z from negative / positive switched to completely negative, which presented the change of the dominant type (previously defined Type 2 P-wave, solid line) to the secondary type (previously defined Type 1 P-wave, dashed line).

3.2.2 TISSUE SAMPLE COLLECTION AND HANDLING

Transmural atrial tissue samples of at least 20 mm x 3 mm were collected from 5 locations that included major atrial conduction routes and the posterior LA region in the vicinity of PV ostia. The sites were as follows: crista terminalis (CT) at the RA lateral wall; Bachmann’s bundle from the superior portion of the interatrial groove between the atria; posterior LA wall at the superior PV (SPV) level; centrally between the PV ostia (posterior LA [PLA] wall); and at inferior PVs (IPV) level.

Atrial tissue samples were fixed in 10% buffered formalin and embedded in paraffin. Sections (2 μ m thick) were cut parallel to the atrial wall plane and stained with Masson’s trichrome stain.

Specimens were examined with computer-assisted morphometric analysis using the Leica LAS Image Analysis System (LeicaQWin Plus v3, Leica Microsystems Imaging Solutions, Cambridge, United Kingdom). The percentage of fatty infiltration,

interstitial fibrosis, capillary density, and mean cardiomyocyte diameter from within each sample were assessed at x200 magnification and calculated at 10 fields of view by a single investigator blinded to clinical and demographic data. Epicardial, endocardial, and perivascular fibrosis were excluded in assessing fibrosis percentage. A mean of the 10 measurements for each parameter per location was used for further analysis.

3.2.3 ATRIAL SEPTAL PACING ON SHORTENING ATRIAL ACTIVATION TIME

FLUOROSCOPY-GUIDED CATHETER POSITIONING AND STIMULATION POSITION

First, a 6F, steerable 2-5-2 mm-spaced, 1-mm-tip decapolar electrode catheter was advanced into the superior vena cava. The catheter was torqued toward the atrial septum. Under fluoroscopic guidance (left anterior oblique, LAO 60° and right anterior oblique, RAO 12°), the catheter was pulled caudally to watch for the tip to 'jump' under the aortic knob. This position was considered as high RA septum in the vicinity of the Bachmann's bundle incision (HAS). Posteroseptal position was achieved by pulling the catheter further down until the second 'jump' under the muscular atrial septum onto the fossa ovalis, which was at the same height as the His-bundle catheter, and performing a clockwise-rotation so that the catheter tip pointed posteriorly in the RAO projection, while in the LAO projection the direction of the catheter tip should still face to septum. This position was considered as the posterior septum behind the FO (PSFO). Finally, the catheter was placed into CS and pulled back until its distal bipolar electrodes were located at CS ostium (CSo). Other standard electrode catheters were positioned at the His-bundle and in the right ventricular apex to serve as conventional fluoroscopical landmarks (Figure 1).

STIMULATION PARAMETERS AND PROTOCOL

Distal electrode pairs of the decapolar catheters were used for bipolar stimulation. The stimulus output had a fixed pulse width of 1 ms, and the threshold was set at twice the diastolic threshold. Threshold values ranged from 2 to 5 V for HAS, PSFO, and CSo stimulation. Particular care was taken to ensure continuous capture of the atrial tissue when threshold values were determined. Pacing was performed at each pacing site at fixed cycle lengths, defined by the longest interval (started at 600 ms, 4 patients at 550 ms and 65 patients at 600 ms) without the P-wave merging with the T-wave.

3.2.4 ATRIAL TACHYCARDIA ABLATION

ELECTROPHYSIOLOGICAL STUDY

Electrophysiological procedures were performed according to international standard routines using conventional equipment [116], and the tachycardia mechanism was defined by established criteria [117]. The mode of tachycardia onset and termination was recorded together with the tachycardia cycle length, local activation time at the site of successful ablation, and ratio of atrial to ventricular electrograms as recorded on the ablation catheter at the site of successful ablation.

All antiarrhythmic medications were discontinued at least five half-lives before the study. None of the patients were taking amiodarone or digitalis. If necessary, electrophysiological studies were performed using intravenous midazolam and / or fentanyl. Conventional 12-lead surface ECG and bipolar intracardiac electrogram recordings (filtered between 30 and 500 Hz) were amplified and displayed using the Prucka CardioLab System (GE Medical Systems, Milwaukee, WI, USA). A quadripolar catheter was placed via the left femoral vein in the RV, and a decapolar catheter was placed in the CS with the proximal pole at the ostium. High rate atrial stimulation (or programmed stimulation) and intravenous isoproterenol and / or atropine were used for arrhythmia induction if spontaneous tachycardia was not present at baseline.

MAPPING OF ATRIAL TACHYCARDIA

A mapping and ablation procedure was performed using a 7-F Navistar catheter (Biosense Webster, Diamond Bar, CA, USA; 4-mm tip, 2 bipolar electrode pairs, inter-electrode distance 2 mm) and guided by a 3D-EA mapping system (CARTO-XP, Biosense Webster, diamond Bar, CA, USA) in all patients. Activation mapping during tachycardia was used to identify sites of earliest endocardial activation in the RA and CS. Activation time in the CS relative to the RA activation was used to describe preferential conduction used for impulse propagation from the RA into the LA. The influence on P-wave morphology in V3-V6 was studied.

Activation time was measured from the onset of the first sharp component of the bipolar electrogram on the distal mapping catheter to the earliest deflection of the P-wave on the surface ECG. The target site of ablation was judged using a combination

of the earliest bipolar activation and the shape of the unipolar electrogram (sharply negative pattern).

RFCA AND FOLLOW-UP

RFCA was performed in the RA with continuous temperature feedback control of the power output to achieve a target temperature of 70 °C. The maximum power used was 50 W for a maximum of 60 sec. Acute procedural success was defined by the inability to induce tachycardia 15 min after ablation despite aggressive burst atrial pacing or programmed atrial stimulation and the use of isoproterenol. The patients were followed in their referring clinics in order to assess the return of symptoms or documented tachycardia.

DEFINITIONS OF ANATOMIC LOCATION

The RA location of the tachycardia focus was determined based on findings from 3D-EA activation mapping and termination of tachycardia using RFCA at the putative site.

1. An EAT was considered to arise from the CT when earliest activation was mapped in this region with the aid of fractionated electrograms and the anatomical position was tagged on the 3D-EA map; ablation in this region successfully eliminated the tachycardia.
2. An EAT was considered to arise from the CSo when earliest activation was recorded around the CSo and when ablation within 1 cm of this region successfully eliminated the tachycardia.
3. An EAT was considered to arise from the TA based on the following criteria:
 - a. Ablation catheter positioned in an annular location when viewed in right and left anterior oblique fluoroscopic views with characteristic annular motion of the catheter tip.
 - b. A-V ratio of < 1 .
4. Exclusion of sites around the CSo and parahisian region. TA sectors (Figure 3) are described using anatomical terminology contained in published guidelines [118].
5. Ablation in this region successfully eliminated the tachycardia.

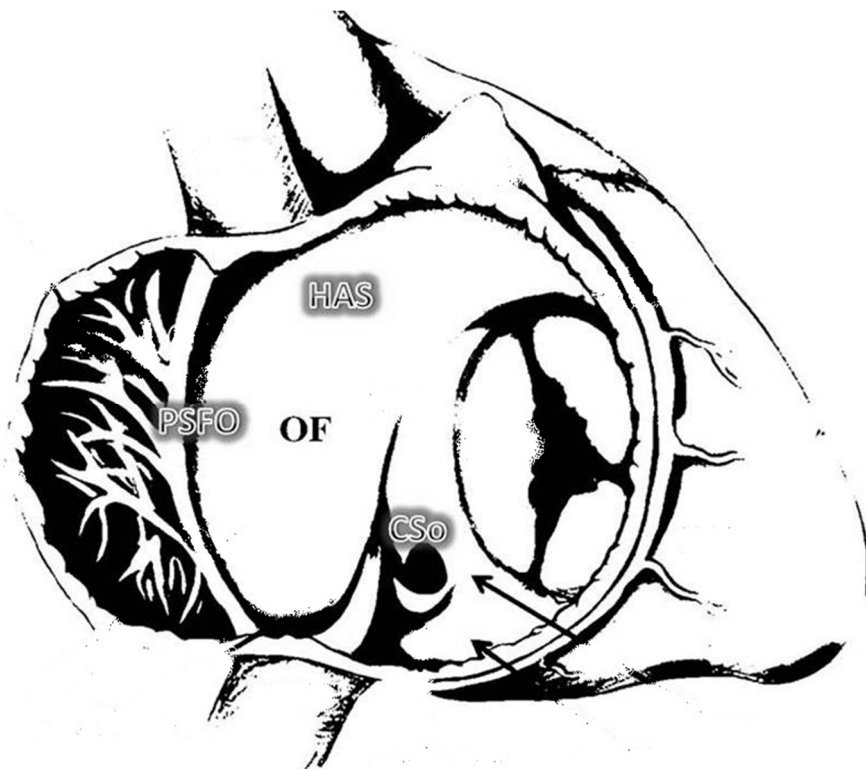


Figure 3. Illustration showing pacing sites. HAS: high atrial septum. PSFO: posterior septum behind fossa ovalis. CSO: coronary sinus ostium. OF: fossa ovalis.

3.2.5 CIRCUMFERENTIAL PULMONARY VEIN ISOLATION PROCEDURE

MAPPING AND ABLATION PROCEDURE

Transesophageal echocardiography was performed to exclude the presence of thrombus within the LA. Patients were studied under deep sedation. Standard catheters were placed in the right ventricular apex and the coronary sinus. Antiarrhythmic drugs were not given for periprocedural rhythm stabilization.

Mapping and ablation were performed under the guidance of 3-D mapping systems (CARTO 3, Biosense Webster, Inc., Diamond Bar, CA, USA or Ensite-Velocity, Endocardial Solutions, Inc., St. Paul, MN, USA) supplemented by 3-D image integration as described previously (CARTO: n=11, NavX: n=59) [119]. A temperature probe in the esophagus (FIAB, St. Jude Medical, Inc., Florence, Italy) at LA level tagged

the esophageal location and provided intraesophageal temperature feedback during the procedure. Ablation lines were adapted to avoid RF delivery in close vicinity to the esophagus [120].

Radiofrequency alternating current was delivered in a unipolar mode between the irrigated tip electrode of the ablation catheter (F-Type, irrigated tip, Navi-Star Thermocool, Biosense Webster, Diamond Bar, California, USA; M-Curve IBI Therapy Cool-Flex, St. Jude Medical, Inc., St. Paul, Minnesota, USA) and the external back-plate electrode. The standard ablation setting consisted of pre-selected catheter tip temperature of 48 °C, power of 40 W, and flow rate of 30 ml/min (17 ml/min for IBI Therapy Cool-Flex catheter). Near the esophagus, power delivery was reduced to 30 W and 20 ml/min, and was further adapted according to actual temperature increase.

Catheter navigation was performed with steerable sheath technology in all patients (Agilis, St. Jude Medical, Inc., St. Paul, Minnesota, USA) [121]. For initial ablation line placement, the catheter tip was dragged along the intended lesion line according to local bipolar amplitude reduction. Therefore, multiple sites were ablated with each initiation of RF energy delivery.

ABLATION LINE CONCEPT AND PROCEDURAL END POINT

Circumferential ablation around both ipsilateral PVs was performed in all patients. The level of ablation was chosen at the atrial side of the PV antrum as indicated by information combined from the integrated 3-D image, the fluoroscopic cardiac silhouette, tactile catheter feedback, catheter impedance changes, and PV–atrium electrogram characteristics.

POST-PROCEDURAL CARE AND FOLLOW-UP

After ablation, a continuous 7-day Holter ECG (Lifecard CF, DelmarReynolds Medical Inc, Irvine, California, USA) was recorded in all patients. The continuous 7-day Holter ECG was repeated after 3 and 6 months. In case of symptoms outside the recording period, patients were advised to contact our institution or the referring physician to obtain ECG documentation. Documentations of AF and / or atypical atrial flutter (AFL) longer than 30 sec were considered to be an episode of sustained AF and/or atypical AFL recurrence. As part of our study protocol, antiarrhythmic medication was discontinued after ablation, and patients received a beta-blocker, if tolerated. Re-ablations for symptomatic drug refractory recurrences of AF and AFL

were scheduled after at least 3 months of follow-up. Starting the day after the ablation procedure, patients received oral anticoagulant with an International Normalized Ratio of 2.0 to 3.0. Anticoagulant was discontinued after 3 months of follow-up according to CHADS₂ score.

3.3 Statistical methods

All data with normal distribution are expressed as means \pm SD. Data without normal distribution are expressed as median. Sample distributions were tested using the Shapiro–Wilk test. A two-independent-sample test (Mann-Whitney test) was used for 2-group comparisons. No correction for multiple testing was applied. Spearman’s correlation coefficient was calculated for analyzing the correlation between quantified histological variables and PWD. Intergroup comparisons were performed using the paired samples t test. Multiple group comparisons (3 groups) were performed by one-way analysis of variance (ANOVA) for continuous variables, followed by a post hoc analysis if the ANOVA test was significant. Possible correlations among pacing sites, baseline PWDs and shortenings of PWDs were tested using the Pearson correlation test.

Data without normal distribution were tested using a non-parametric test. Population proportions are presented as a percentage. Outcome-related values of a set of predictor variables were evaluated by multivariate logistic regression (binary logistic regression). Sensitivity was defined as the probability that a test result will be positive when free of AF after CPVI is present (true positive rate). Specificity was defined as the probability that a test result will be negative when free of AF after CPVI is not present (true negative rate). Positive predictive value (PPV) was defined as the probability that the patient is free of AF after CPVI is present when the test is positive. Negative predictive value (NPV) was defined as the probability that the patient is free of AF after CPVI is not present when the test is negative. A P value of < 0.05 was considered significant. All statistical analyses were performed using IBM SPSS Statistics, version 20.0.0 (SPSS, Chicago, Illinois, USA).

CHAPTER 4. RESULTS

4.1 P-wave characteristics and histological atrial abnormality

4.1.1 PATIENT CHARACTERISTICS

Clinical characteristics of subjects are presented in Table 1. Median age was 73 years (range 54-82 years). All patients died of cardiovascular causes such as acute myocardial infarction (n=9) and pulmonary embolism (n=2) verified by autopsy. There was no difference with regard to the presence of ischemic heart disease, hypertension, stroke, chronic obstructive pulmonary disease, diabetes mellitus, or aortic or mitral valve pathology between patients with AF history and without AF history. The extent of fibrosis, fatty infiltration, capillary density and cardiomyocyte size did not differ among the 5 sampling locations in the atria, in either total material or in subgroup analysis (data not shown).

Table 1. Patients characteristics (Study 1).

ID	Gender	Age (years)	COD	HTN	CHF	DM	AF	Stroke	LVEF%	LA (mm)
1	M	73	AMI	-	+	-	-	-	27	48
2	M	54	AMI	+	+	-	-	+	44	37
3	M	62	AMI	+	+	+	-	-	17	--
4	M	72	AMI	+	+	-	-	-	--	--
5	M	82	AMI	+	+	-	-	-	--	--
6	F	77	AMI	+	+	-	-	-	61	42
7	M	69	AMI	+	+	+	-	-	42	40
8	F	73	AMI	+	+	-	+	+	30	50
9	F	73	AMI	+	+	-	+	-	34	34
10	M	74	PE	+	+	-	+	-	61	42
11	F	72	PE	+	+	-	+	-	--	--

PE: pulmonary embolism. AMI: acute myocardial infarction. COD: cause of death. PTF: P-wave terminal force. PWD: P-wave duration. CHF: chronic heart failure. M: male. F: female. HTN: hypertension. DM: diabetes mellitus. AF: atrial fibrillation. LAD: left atrial diameter. LVEF: left ventricular ejection fraction.

4.1.2 PWD VS. SITE-DEPENDENT HISTOLOGICAL ABNORMALITIES

The median PWD was 160ms (range 120-200ms). The fibrosis extent in CT, SPV and IPV was higher in patients with longer PWD (PWD>160ms) than in patients with shorter PWD. Moreover, the combination of fibrosis extent and fatty tissue in CT, Bachmann's bundle and SPV was greater in the group with longer PWD (PWD>160ms) than in the group with shorter PWD. The average of fibrosis extent or the combination of fibrosis extent and fatty tissue was also significantly greater in the group with longer PWD.

Correlation between PWD and histological variables was assessed at all 5 locations as well as for the mean value of these 5 locations. The fibrosis extent in CT highly correlated to PWD ($r=0.914$, $p<0.001$). The combination of fibrosis extent and fatty tissue in Bachmann's bundle (16%, range 1-41%), CT (18%, range 3-47%) or SPV (15%, range 6-24%) correlated to PWD ($r=0.627$, $p=0.039$; $r=0.795$, $p=0.003$; and $r=0.668$, $p=0.025$, respectively). The average of fibrosis extent or combination of fibrosis extent and fatty tissue at these 5 locations also correlated to PWD ($r=0.747$, $p=0.008$; $r=0.664$, $p=0.026$, respectively). (Table 3)

Table 3. PWD vs. site-dependent histological abnormalities

Location	PWD≤160ms (n=6)	PWD>160ms (n=5)	p-value
Crista terminalis			
Fibrosis extent	6.0% (2.4-9.4%)	19.0% (17.0-40%)	0.004**
Fatty infiltration	2.1% (0.5-13.6%)	9.0% (7.0-17.0%)	0.052
Fibrosis-fatty infiltration	10.1% (3.4-18.4%)	28.0% (26.0-47.0%)	0.004**
Bachmann's Bundle			
Fibrosis extent	7.2% (1.0-12.3%)	15.0% (3.7-26.0%)	0.082
Fatty infiltration	3.5% (0-6.6%)	8.4% (7.0-15.0%)	0.004**
Fibrosis-fatty infiltration	9.4% (1.0-16.8%)	23.4% (10.7-41.0%)	0.017*
Superior PV level			
Fibrosis extent	4.6% (1.9-12.4%)	12.0% (6.0-20%)	0.030*
Fatty infiltration	4.7% (0-6.6%)	6.0% (0-17.0%)	0.537
Fibrosis-fatty infiltration	8.8% (5.8-14.7%)	20% (18.0-24.0%)	0.004**
Center of posterior LA wall			
Fibrosis extent	4.9% (2.5-8.0%)	17.0% (0.7-20.0%)	0.126
Fatty infiltration	3.3% (0-4.7%)	4.0% (0-6.4%)	0.931
Fibrosis-fatty infiltration	9.3% (3.8-12.4%)	21.0% (0.7-22.2%)	0.126
Inferior PV level			
Fibrosis extent	4.0% (1.3-9.2%)	12.8% (5.6-20.6%)	0.017*
Fatty infiltration	5.4% (0-13.9%)	3.8% (0-20.7%)	0.931
Fibrosis-fatty infiltration	9.3% (1.3-18.7%)	21.0% (5.6-41.3%)	0.247
Global atria: 5 sites average			
Fibrosis extent	5.0% (3.6-8.3%)	15.6% (9.4-24.8%)	0.004**
Fatty infiltration	4.5% (0.1-7.6%)	9.2% (3.2-11.4%)	0.082
Fibrosis-fatty infiltration	8.7% (5.2-15.9%)	26.6% (12.6-30.4%)	0.009**

*: A p-value of < 0.05. **: A p-value of < 0.01. LA: left atrium; PV: pulmonary vein.

4.1.3 P-WAVE MORPHOLOGY OF PARTIAL INTERATRIAL CONDUCTION

BLOCK VS. SITE-DEPENDENT HISTOLOGICAL ABNORMALITIES

None of the observed P-wave morphologies fulfilled the criteria of advanced interatrial conduction block. Ten out of 11 subjects had special P-wave morphology that meets the partial interatrial conduction block criteria (Table 4). The extent of fibrosis, fatty infiltration or a combination of fibrosis extent and fatty tissue did not differ between subjects with notches in inferior leads only (n=4) and subjects with notches in both inferior leads and lateral leads (n=4 vs. n=5, all p=0.798), in either the 5 sampling locations in the atria, nor in the average of total 5 sampling locations analysis. However, the only subject who had normal P-wave morphology without pIAB pattern also had the most extensive fibrosis in atrial walls, approaching 40% at CT sampling location (Figure 4b).

Table 4. P-wave morphology (pIAB) vs. site-dependent histological abnormalities

ID	Notch in any lead	Notch in lead I	Notches in lead II, III and aVF	Notch in V1-V6
1	+	-	II, III	V2-V5
2	+	-	II, III, aVF	V4
3	+	+	II, III	V2-V6
4	+	-	II, III, aVF	V4-V6
5	+	-	II, III, aVF	V2, V3
6	+	-	III	V3, V4
7	+	+	III	V3
8	+	-	II, III, aVF	V2-V6
9	-	-	-	-
10	+	-	-	V2, V3
11	+	-	III, aVF	-

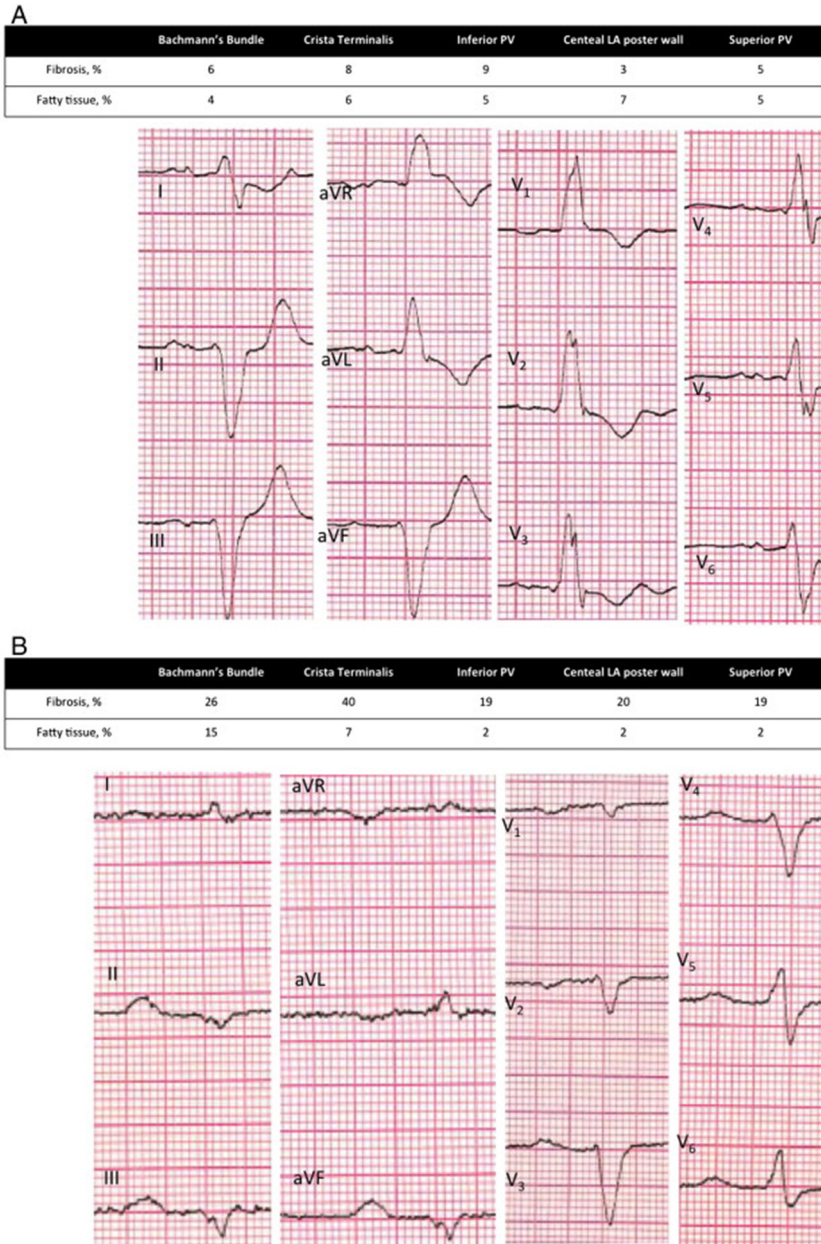


Figure 4. P-wave Morphology on standard 12-lead ECG vs. histological atrial abnormality. A. Notched P-wave (bimodal) in a subject with normal histological findings in atria. B. Normal P-wave morphology (with prolonged P-wave duration) in a subject with abnormal histological findings in atria.

4.2 Atrial septal pacing site effect on atrial activation time shortening

4.2.1 PATIENTS CHARACTERISTICS AND PACED P-WAVE DURATION

Table 2. Comparison of patients with and without recurrence of atrial arrhythmias (Study 4).

Initial Rhythm during procedure	No Recurrence at 6 months (n=53)	Recurrence at 6 months (n=17)	p Value
Age (years)	60±7	58±12	0.356
Gender (male)	32 (60.4%)	14 (82.4%)	0.099
BMI	29±4	28±5	0.360
AF History (months)	56±64	66±74	0.574
Type of AF (paroxysmal AF)	40 (75.5%)	10 (58.8%)	0.189
Hypertension	42 (79.2%)	14 (82.4%)	0.782
Diabetes	8 (15.1%)	1 (5.9%)	0.327
CAD	9 (17.0%)	2 (11.8%)	0.610
CHF	1 (1.9%)	2 (11.8%)	0.070
Mitral valve insufficient	1 (1.9%)	1 (5.9%)	0.393
ECHO			
LA-diameter before CPVI (mm)	43±6	45±5	0.894
LA-Diameter at 6 months after CPVI (mm)	40±5	44±7	0.330
LV-EF% before CPVI	61±8	54±10	0.007*
LV-EF% at 6 months after CPVI	62±5	59±11	0.332
ABLATION			
Initial Rhythm (SR)	37 (69.8%)	11 (64.7%)	0.695
Procedure Time (min)	138±48	142±52	0.773
Fluoroscopy Time (min)	27±11	36±19	0.087

*: A p-value of < 0.05. CAD: coronary artery disease, CHF: chronic heart failure, LA: left atrium, CPVI: circumferential pulmonary vein isolation.

The PWD was significantly shorter when pacing at the CSo (112±15 ms) than when pacing at the HAS (121±14 ms, p<0.001) or the PSFO (124±21 ms, p<0.001), and was also significantly shorter than the baseline PWD (during SR) (128±15 ms, p<0.001). The PWD when pacing at the HAS was also significantly shorter than the PWD during SR (p=0.003), but not significantly shorter than the PWD paced at PSFO (p=0.274) (Figure 5).

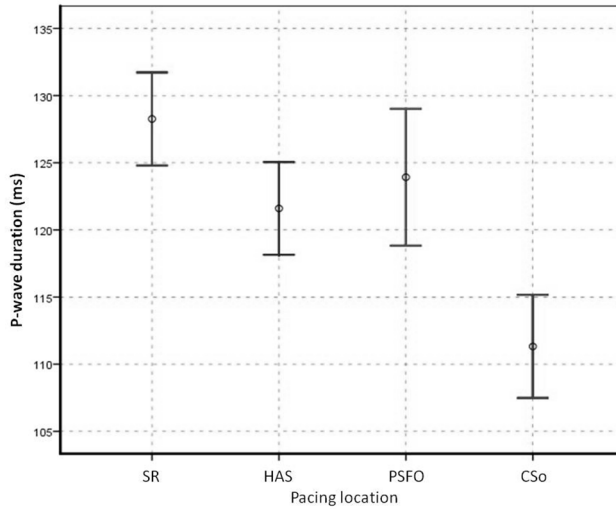


Figure 5. Mean P-wave duration (\pm SE) at baseline (SR) and when paced at different sites in the 69 patients studied. SR: sinus rhythm. HAS: high atrial septum. PSFO: posterior septum of fossa ovalis. CSo: coronary sinus ostium.

PWD shortening (Δ PWD) at each pacing site was defined as the difference between the paced value and the baseline value (Δ PWD=paced PWD-baseline PWD). There was a negative linear correlation between Δ PWD and baseline PWD ($R=-0.64$, -0.63 and -0.72 for HAS, PSFO and CSo pacing respectively, $p<0.001$ for all sites) (Figure 6) with longer P-waves at baseline showing greater shortening during pacing.

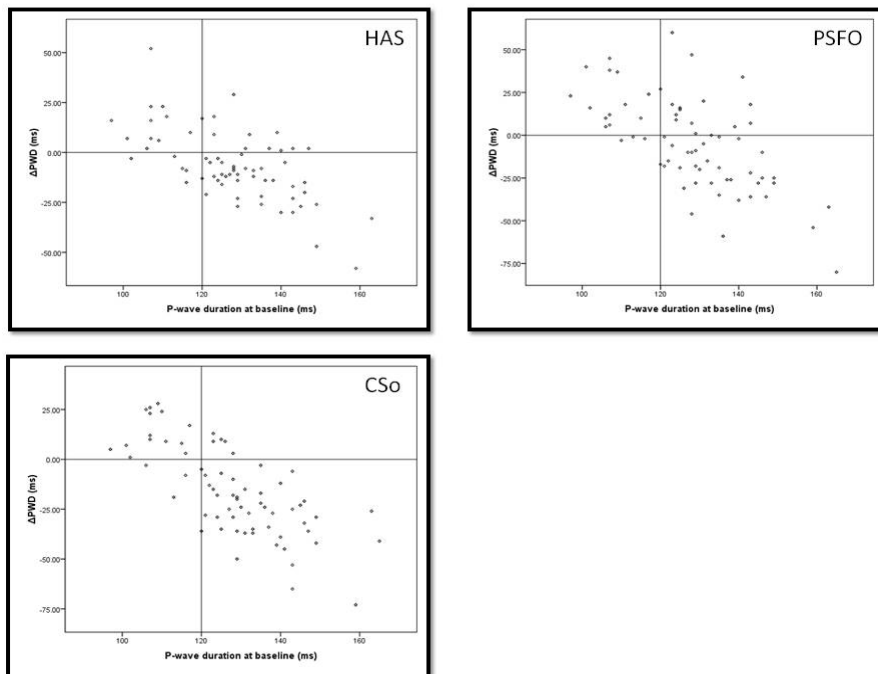


Figure 6. Scatter plot of Δ PWD at three different pacing sites. There were linear correlations between Δ PWD at different pacing sites and baseline PWD (SR) in the group of 69 patients. P-wave shortening (negative Δ PWD) was observed in patients with baseline PWD > 120 ms, while patients with normal PWD at baseline mostly presented with lengthening of pace PWD (positive Δ PWD) regardless of pacing site. HAS: high atrial septum. PSFO: posterior septum of fossa ovalis. CSO: coronary sinus ostium.

4.2.2 NORMAL P-WAVE DURATION VS. PROLONGED P-WAVE DURATION AT BASELINE

19 of the 69 patients had normal PWDs (≤ 120 ms) at baseline. Regardless of pacing site, atrial septal pacing resulted mostly in P-wave shortening in patients with baseline PWD > 120 ms, and P-wave prolongation in patients with normal PWD (Figure 2). Differences in Δ PWD between patients with PWD ≤ 120 ms and PWD > 120 ms were significant at all pacing sites: HAS, 8 ± 17 vs. -12 ± 15 ms ($p < 0.001$), PSFO, 15 ± 17 vs. -12 ± 26 ms ($p < 0.001$) and CSO, 6 ± 16 vs. -25 ± 18 ms ($p < 0.001$) (Figure 7).

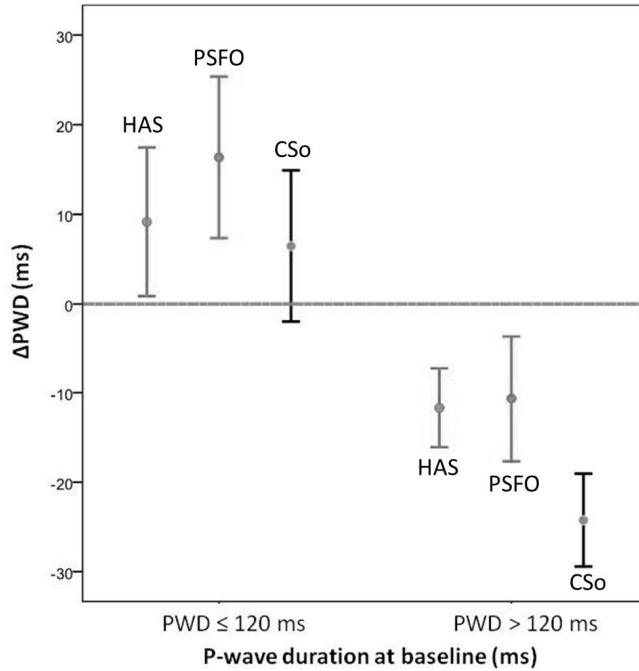


Figure 7. The change in PWD when paced at three different sites, with baseline PWD ≤ 120 ms and > 120 ms. HAS: high atrial septum. PSFO: posterior septum of fossa ovalis. CSo: coronary sinus ostium.

When paced PWD was compared in patients with baseline PWD > 120 ms and baseline PWD ≤ 120 ms, there was no statistically significant difference regardless of pacing site. Patients with baseline PWD > 120 ms had shorter paced PWDs compared with baseline, regardless of pacing sites. Pacing at CSo resulted in a significantly shorter PWD than pacing at HAS or PSFO, but there was no significant difference between the paced PWD at HAS and PSFO. However, in patients with baseline PWD ≤ 120 ms, pacing at PSFO or CSo resulted in a significant prolongation of PWD compared with baseline. In this group, PWD during HAS pacing was similar to baseline, while no difference in PWD was observed among all three septal pacing sites (Table 5).

4.2.3 NORMAL LEFT ATRIUM VS. ENLARGED LEFT ATRIUM

When PWD was compared in patients with enlarged vs. normal LA, there was no difference at baseline, but patients with enlarged LA had a longer paced PWD during HAS or PSFO pacing than patients with normal LA. Pacing at CSo, however, was not

associated with any difference in paced PWD for patients with enlarged or normal LA (Table 5).

When site-related effects of septal pacing were analyzed separately in the subgroup of patients with enlarged LA (median 43 mm, 41-52 mm, n=25), paced PWD was significantly shorter than baseline PWD during CSo pacing, while no significant difference was observed during pacing at HAS or PSFO. The paced PWD during CSo pacing was also significantly shorter than paced PWD at HAS or PSFO. In the subgroup of patients with normal LA (Median 38 mm, 23-40 mm, n=44), paced PWDs were significantly shorter than baseline PWD during septal pacing, regardless of pacing site. The paced PWD during CSo pacing was also significantly shorter than the paced PWD at HAS or PSFO in the subgroup of patients with normal LA. There was no statistically significant difference with regard to the paced PWD during HAS and PSFO (Table 5).

4.2.4 PATIENTS WITH VS. WITHOUT HISTORY OF ATRIAL FIBRILLATION

When PWD was compared in patients with paroxysmal AF (n=21) and without history of paroxysmal AF (n=48), it did not differ either at baseline or during pacing (Table 5). However, LA diameter in patients with paroxysmal AF (42 mm, range 25-52 mm) was significantly greater than in patients without AF history (39 mm, range 23-49, p=0.012).

When site-related effects of septal pacing were analyzed separately in the subgroup of patients without paroxysmal AF history, paced PWDs appeared to be significantly shorter than baseline PWD, regardless of pacing sites. The paced PWD during CSo pacing was also significantly shorter than the paced PWD at HAS or PSFO. There was no statistically significant difference between the paced PWDs during HAS and PSFO. In the subgroup of patients with paroxysmal AF, paced PWDs appeared to be significantly shorter than baseline PWD only during CSo pacing. The paced PWD during CSo pacing was also significantly shorter than the paced PWD at PSFO. There was also no statistically significant difference between the paced PWDs during HAS and PSFO (Table 5).

Table 5. Paced P-wave duration and PWD at baseline.

PWD (ms)	Baseline	HAS pacing	PSFO pacing	CSo pacing
Baseline PWD > 120ms (n=50)	133 (121-165)	121 (100-157) ^{##,***}	120 (77-183) ^{##,***}	110 (78-137) ^{###,*}
Baseline PWD ≤ 120ms (n=19)	108 (97-120)	113 (99-159)	119 (103-152) ^{##}	119 (84-137) [#]
LA diameter >40 mm (n=25)	128 (97-163)	125 (100-159) ^{*,&}	121 (82-183) ^{**,&}	116 (86-137) [#]
LA diameter ≤40 mm (n=44)	129 (101-165)	117 (99-157) ^{##,**}	117 (77-175) ^{##,**}	110 (78-135) ^{###}
History of AF (n=21)	125 (97-165)	120 (102-149)	121 (85-183) [*]	111 (94-137) [#]
No History of AF (n=48)	128 (102-163)	120 (99-159) ^{##,***}	118 (77-175) ^{##,**}	112 (78-137) ^{###}

#: p<0.05 in comparison with baseline PWD; ##: p<0.01 in comparison with baseline PWD; ###: p<0.001 in comparison with baseline PWD; *: p<0.05 in comparison with baseline PWD; **: p<0.01 in comparison with paced PWD during CSo pacing; ***: p<0.001 in comparison with paced PWD during CSo pacing; &: p<0.05 in comparison between normal and enlarged LA. PWD: P-wave duration; HAS: high atrial septum; PSFO: posterior septum behind the fossa ovalis; CSo: coronary sinus ostium, LA: left atrium, PAF: paroxysmal AF. Data presented as median (range).

4.3 Atrial tachycardia originating from the lower right atrium

4.3.1 PATIENT CHARACTERISTICS

We analyzed the results of 28 consecutive patients with a tachycardia origin from the lower part of RA who underwent RFCA for a focal EAT. None received amiodarone. All patients had normal cardiac anatomy on transthoracic echo. LA diameter was 34±5 mm. (Table 6)

Table 6. Patients characteristics.

Patient number	Age	Gender	LA (mm)	HT	DM	CAD	A
1	64	Male	37	-	-	-	PAF, EAT
2	47	Female	39	-	-	-	AVB III, EAT
3	45	Male	33	-	-	-	EAT
4	42	Male	35	-	-	-	EAT
5	58	Male	40	+	-	-	EAT
6	56	Male	41	+	-	-	EAT
7	72	Female	42	-	-	-	PAF, EAT
8	71	Male	39	-	-	-	EAT
9	70	Male	36	-	-	+	EAT
10	60	Male	29	+	-	-	EAT
11	60	Female	37	+	+	-	EAT
12	59	Male	36	+	-	-	EAT
13	56	Male	33	-	-	-	PAF, EAT
14	43	Male	31	+	-	-	EAT
15	48	Male	30	-	-	-	EAT
16	81	Male	40	-	+	-	EAT
17	38	Female	24	-	+	-	EAT
18	27	Male	26	+	-	-	EAT
19	36	Male	33	+	-	+	EAT
20	31	Male	30	+	-	-	EAT
21	33	Male	29	-	-	-	EAT
22	46	Female	34	+	-	+	EAT
23	52	Female	36	-	-	-	EAT
24	66	Male	35	-	-	-	PAF, EAT
25	78	Male	33	+	-	-	EAT
26	55	Male	34	+	-	-	EAT
27	53	Female	27	-	+	+	EAT
28	22	Male	35	-	+	-	EAT

HT: hypertension. DM: diabetes mellitus. LA: left atrium. CAD: coronary arterial disease. A: arrhythmias. Arrhythmia: PAF: paroxysmal atrial fibrillation. EAT: ectopic atrial tachycardia. AVB III°: third degree of atrioventricular block. LA-diameter was measured at parasternal long axis view (antero-posterior in the 2D echo-long axis).

4.3.2 GENERAL FINDINGS

In all 28 patients, EAT origin was located using the 3D-EA mapping system (activation map) and verified by successful RFCA from the lower part of RA, as follows: In 11 patients (39%), EAT origin was along the TA (6 to 9 o'clock), in another 11 patients (39%), EAT origin was around the CSo, 4 patients (14%) had EAT from the lower

CT, and in 2 patients (7%) arrhythmia originated from the lower RA freewall. Multifocal EAT was found in 2 patients (7%) with EAT originating from CSOs; however, neither of these 2 patients had more than one focus from the lower RA. In both patients, the second focal tachycardias originated from the superior CT. Comparing to the EAT originating from upper RA with typically ≥ 2 positive P-waves in inferior leads, EAT with origin of lower RA contained maximal one positive P-wave (up to one lead with completely positive pattern) in inferior leads, which were observed in all 28 EATs.

4.3.3 P-WAVE MORPHOLOGY AND ANATOMIC LOCATION

- NON-SEPTAL TRICUSPID ANNULUS ORIGIN

Nine out of 11 EATs originating at the non-septal TA (6 to 9 o'clock) had a completely negative pattern in the inferior (II, III and aVF) and precordial (V3-V6) leads. However, the remaining 2 EATs, originating from TA at 9 o'clock, had a positive (patient 19) or negative-positive (patient 18) pattern in lead II and an isoelectric pattern in lead III and aVF, and a completely positive pattern in precordial leads V3-V6 (Table 7, Figure 8 and 9).

Table 7. P-wave morphology during ectopic atrial tachycardia.

No.	Localization	I	aVR	aVL	V1	V2	V3	V4	V5	V6
1	L.FW	+	+/-	+	-	-	-/+	-/+	-/+	-/+
2	L.FW	+	iso	+	iso	+	+	+	iso	iso
3	L.CT	+/-	+	-	iso	+	+	+	+	+
4	L.CT	+	-	+	iso	+	+	+	+	+
5	L.CT	-/+	+	-/+	iso	iso	-/+	-/+	-/+	-/+
6	L.CT	-/+	-	+	iso	+	+	+	+	+
7	CSo	-/+	+	+	iso/+	-	-	-	-	-
8	CSo	-/+	+	+	iso	iso	-	-	-	-
9	CSo	iso	+	+	-	-	-	-	-	-
10	CSo	iso	+	+	iso	iso	-	-	-	-
11	CSo	-/+	+	+	-/+	iso	-	-	-	-
12	CSo	-/+	+	+	iso	-	-	-	-	-
13	CSo	-/+	+	+	-/+	-/+	-	-	-	-
14	CSo	-/+	+	+	iso	-/+	-/+	-/+	-	-
15	CSo	-/+	+	+	+/-	-	-	-	-	-
16	CSo	-/+	+	+	+	iso	-/+	-	-	-
17	CSo	iso	+	+	+	iso	-	-	-	-
18	TA 9	-/+	+	-/+	-	-/+	+	+	+	+
19	TA 9	+	-	iso	-	iso	+	+	+	+
20	TA 6	-/+	+	+	-/+	-/+	-	-	-	-
21	TA 7	iso	+	+	-	-	-	-	-	-
22	TA 6	iso/+	+	+	iso	-	-	-	-	-
23	TA 6	-+	+	+	iso	-	-	-	-	-
24	TA 6	-+	+	+	iso	iso/-	-	-	-	-
25	TA 7	+	-	+	-	-/iso	-	-	-	-
26	TA 7	-+	+	+	-	iso	-	-	-	-
27	TA 6	Iso/+	+	+	iso	iso	-	-	-	-
28	TA 6	iso	+	+	+	iso	-	-	-	-

Polarity in lead II, III, aVF were \neq 1 lead with positive P-wave. L.FW: lower free wall. L.CT: lower crista terminalis. CSo: coronary sinus ostium. TA: tricuspid annulus.

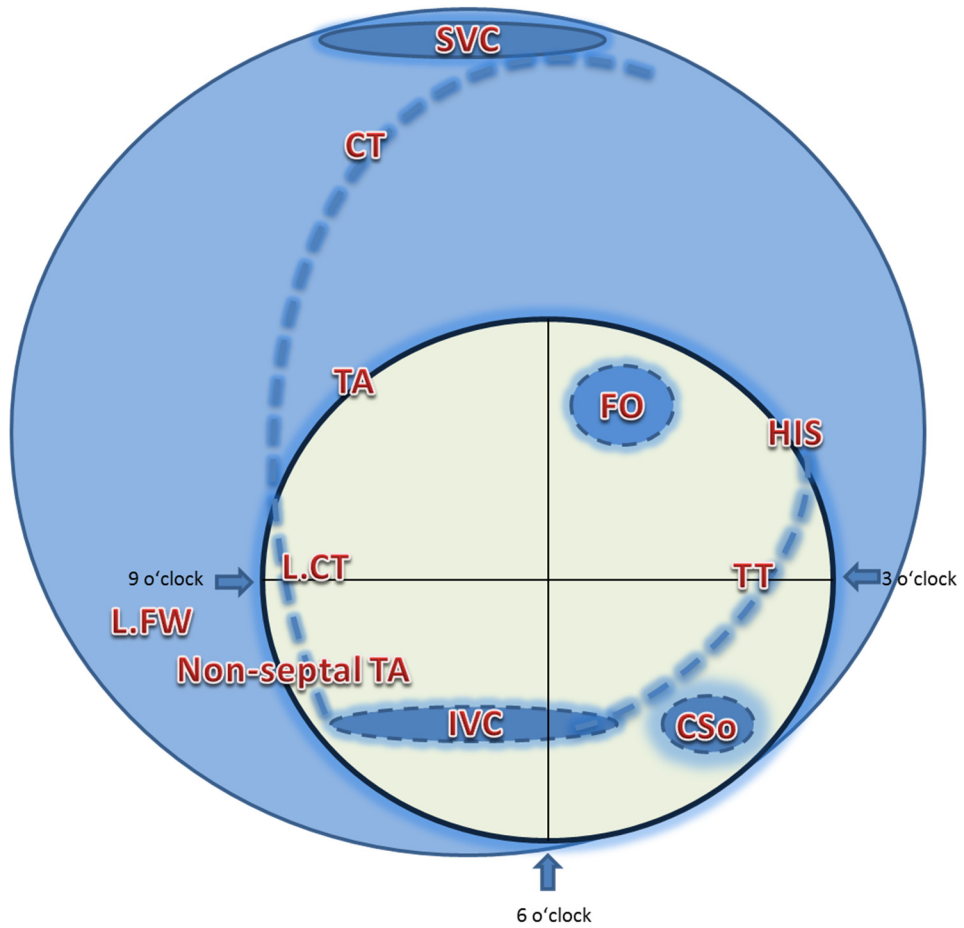


Figure 8. Localization of anatomical structures in the lower right atrium. SVC: superior vena cava. TA: tricuspid annulus. CT: crista terminalis. FO: fossa ovalis. L.FW: lower free wall. L.CT: lower crista terminalis. TT: Tendon of Tudaro. CSo: coronary sinus ostium.

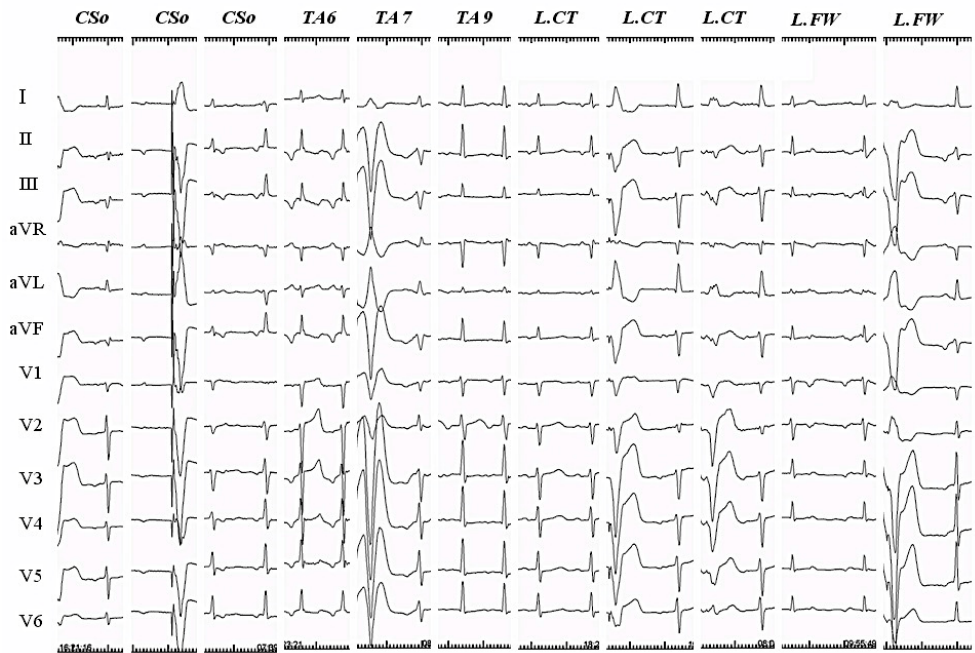


Figure 9. P-wave morphology during ectopic atrial tachycardias (25mm/s). P-wave morphology was shown on a standard 12-lead ECG during ectopic atrial tachycardia originating from the lower right atrium. CSo: coronary sinus ostium. TA: tricuspid annulus. TA6: at 6 o'clock position of TA. TA7: at 7 o'clock position of TA. TA9: at 9 o'clock position of TA. L.CT: lower crista terminalis. L.FW: lower free wall.

- CORONARY SINUS OSTIUM ORIGIN

All 11 EATs originating from CSo had a positive pattern in aVR and aVL, a completely negative pattern in all inferior leads (II, III and aVF). Nine out of 11 EATs had a completely negative pattern in all 4 precordial leads (V3-V6). In the remaining 2 EATs, one (patient 14) had a biphasic pattern (-/+) in both V3 and V4 precordial leads. The other EAT (patient 16) had one biphasic pattern (-/+) in precordial lead V3. All biphasic patterns contained an early negative component.

- LOWER CRISTA TERMINALIS

All 4 EATs originating from the lower CT had isoelectric or biphasic patterns in inferior leads (II, III and aVF); in 3 of 4 EATs there was a positive pattern in all 4 precordial

leads (V3-V6). The remaining EAT had a biphasic pattern (-/+) in all 4 precordial leads (V3-V6).

- LOWER RIGHT ATRIAL FREE WALL

Two EATs originated from the lower RA free wall. One of the EATs had a negative pattern in all inferior leads (II, III and aVF) and biphasic patterns (-/+) in all 4 precordial leads V3-V6. The other EAT had an isoelectric pattern in all inferior leads (II, III, and aVF), a positive pattern in V3 and V4 and an isoelectric pattern in V5 and V6.

4.3.4 POWER OF PRECORDIAL LEADS (V3-V6) TO DISCRIMINATE THE ANATOMICAL EAT ORIGIN

- LOWER TA ORIGIN (ANNULUS FOCI) VS. LOWER CT ORIGIN

P-wave morphology in precordial leads (≥ 2 consecutive leads in V3-V6) showed a negative pattern on EAT origins from the non-septal TA (9/11 patients) or CSo (11/11 patients). P-wave morphology in precordial leads V3-V6 showed a positive pattern on EAT origins from the lower CT (3/4 patients). In electrocardiographic lead V3-V6 (≥ 2 consecutive leads), a negative P-wave demonstrated a sensitivity of 90.9%, a specificity of 100%, a PPV of 100% and a NPV of 75% for an annulus focus, including CSo and non-septal TA; a positive P-wave in all V3-V6 demonstrated a sensitivity of 75%, a specificity of 100%, a PPV of 60% and a NPV of 96% for a lower CT focus.

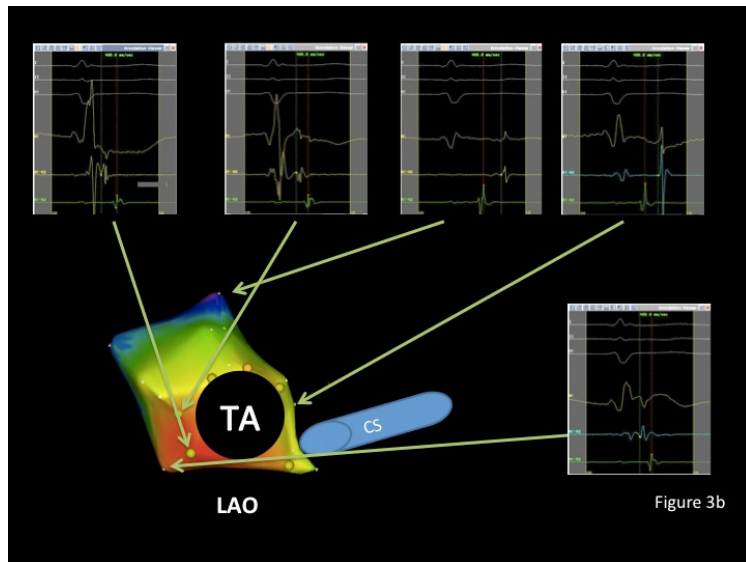
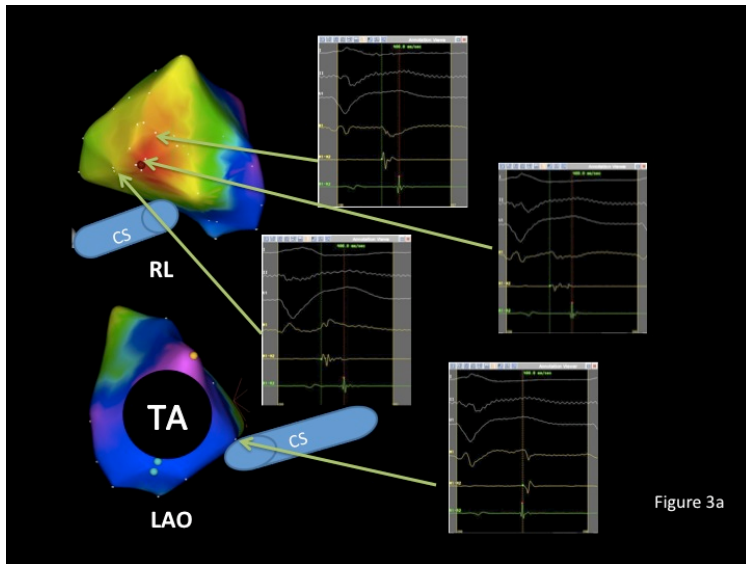
- NON-SEPTAL TA ORIGIN VS. CSO ORIGIN

In the current study, P-wave morphology in precordial leads V3-V6 was not able to discriminate between the EAT of the CSo origin and the EAT of the non-septal TA origin. There were mostly negative P-waves in precordial leads (V3-V6) for both EATs originated from CSo and non-septal TA.

- ACTIVATION MAPPING AND PREFERENTIAL INTERATRIAL CONDUCTION

During all studied EATs, the CS activation was recorded from proximal to distal using the CS catheter, and was compared to the spread of RA activation described in the RA 3D map. During EAT originating from the lower CT, the proximal CS activation (CS 9/10) occurred later than the lower mid-septum of RA, but slightly earlier than the posterior CSo (2/4 patients) or at the same time as the posterior CSo (1/4 patients) in

RA (Figure 10a). However, during EAT originating from the lower TA (20/22 patients), including the non-septal TA (9/11 patients) (Figure 10b) and the CSo (11/11 patients) (Figure 10c), the proximal CS activation (CS 9/10) occurred earlier than the lower mid-septum of RA. These activation patterns indicate differences in LA activation caused by different preferential conduction routes used for interatrial impulse propagation.



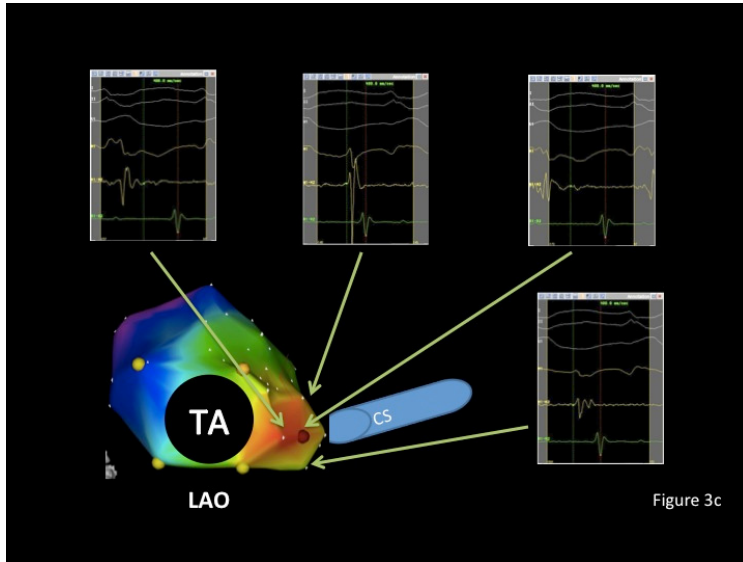


Figure 10. 3D electroanatomical mapping (activation map) and endocardial electrograms during ectopic atrial tachycardias. **Figure 10a.** The ectopic atrial tachycardia originated from the lower CT. The right inferior electrograms show that mid-septum was activated later than the CS ostium. The left superior activation map shows the earliest activation spot with fragmented potentials on the ablation catheter and sharply negative unipolar electrogram. **Figure 10b.** The activation map shows the ectopic atrial tachycardia originating from non-septal TA (7 o'clock). The right superior electrograms show that mid-septum (posterior area of CS ostium) was activated later than the CS ostium. **Figure 10c.** The activation map shows an ectopic atrial tachycardia originating from the CS ostium.

4.4 Variability of P-wave morphology

4.4.1 PATIENTS CHARACTERISTICS AND ABLATION OUTCOME

The patient characteristics are described in Table 2. All patients (n=70) received a CPVI alone without any extra linear ablation. 50 (71%) patients suffered from paroxysmal AF, and 20 patients (29%) suffered from persistent AF. None of the patients with previous diagnosis of heart failure had decompensation during hospital admission or during the 6-month follow-up. 48 of 50 patients with paroxysmal AF had SR at the beginning of the procedure, and 22 patients (2 with paroxysmal AF and 20 with persistent AF) had AF at the beginning of the procedure. In all 70 patients (100%), acute successful PV-Isolation was achieved, and at least 6 months of follow-up were completed. Recurrence of atrial arrhythmias (including recurrence of AF and atypical

atrial flutter) during the 6-month follow-up was observed in 11 patients (22.9%) with paroxysmal AF, and in 6 patients (27.3%) with persistent AF ($p=0.695$).

4.4.2 P-WAVE DURATION AND P-WAVE MORPHOLOGY TYPE

The P-wave duration (PWD) was 150 ± 18 ms in all patients. The PWD in patients with SR at the beginning of the procedure ($n=48$) was significantly shorter than in patients with initial AF ($n=22$) in whom the PWD was measured after cardioversion (144 ± 16 vs. 162 ± 17 ms, $p<0.001$). The PWD in patients with diagnosis of paroxysmal AF ($n=50$) was significantly shorter than in patients with persistent AF ($n=20$) (145 ± 16 vs. 162 ± 17 ms, $p<0.001$). However, there was no significant difference in PWD between patients with recurrence ($n=17$) and those with non-recurrence ($n=53$) during the 6-month follow-up (155 ± 23 vs. 149 ± 16 ms, $p=0.241$).

There was no significant difference in the type of P-waves observed between patients with paroxysmal vs. persistent AF, initial SR vs. AF or recurrence vs. non-recurrence of atrial arrhythmias after CPVI during the 6-month follow-up. (Table 8)

Table 8. Type of P-wave morphology

		Type of P-waves				p-value
		Type 1	Type 2	Type 4	Atypical	
Rhythm at baseline	SR (n=48)	6 (12.5%)	32 (66.7%)	7 (14.6%)	3 (6.3%)	0.359
	AF (n=22)	1 (4.5%)	16 (72.7%)	0 (0%)	5 (22.7%)	
Clinical type of AF	Paroxysmal AF (n=50)	5 (10%)	34 (68%)	7 (14%)	4 (8%)	0.937
	Persistent AF (n=20)	2 (10%)	14 (70%)	0 (0%)	4 (20%)	
FU at 6 months	No Recurrence (n=53)	5 (9.4%)	36 (67.9%)	6 (11.3%)	6 (11.3%)	0.671
	Recurrence (n=17)	2 (11.8%)	12 (70.6%)	1 (5.9%)	2 (11.8%)	

SR: sinus rhythm, AF: atrial fibrillation FU: follow-up.

4.4.3 VARIABILITY OF ORTHOGONAL P-WAVE MORPHOLOGY

The PMV in patients (n=53) without recurrence of atrial arrhythmias after CPVI during the 6-month follow-up was greater than in patients (n=17) with recurrence (19.5±17.1% vs. 8.2±6.7%, p<0.001). However, no significant difference was observed between patients with initial SR (n=48) vs. patients with initial AF (n=22) (14.7±14.0% vs. 21.3±19.1%, p=0.159) or patients with paroxysmal (n=50) vs. patients with persistent AF (n=20) (15.7±15.3% vs. 19.6±17.5%, p=0.351). In the univariate analysis, PMV significantly correlated to AF history duration and baseline LA diameter (R=-0.254, p=0.036; R=-0.355, p=0.005 respectively), but the correlations were weak.

4.4.4 PREDICTOR OF ABLATION OUTCOME

A PMV≥20% (upper tertile) demonstrated a sensitivity of 41.5%, a specificity of 94.1%, a PPV of 96.7%, and an NPV of 34.0% for free of AF after CPVI. In the multivariate logistic regression model, PMV≥20% was the only independent predictor of ablation success (OR=11.4, 95%CI 1.4-92.1, p=0.023). None of the other clinical

characteristics such as age, gender, BMI, LA diameter, type of AF or AF history duration were associated with the outcome.

CHAPTER 5. DISCUSSION

5.1 Atrial histology

Since 1977, the first study, based on 8 human subjects with sinus node disease, demonstrated that in 7 of these patients there was increased fibrosis or fatty infiltration in RA musculature in postmortem, which revealed an underlying relation between fibro-fatty infiltration and atrial conduction abnormality in humans [43]. This study initiated a new era for electrophysiologists and offered a novel pathological tool to further study the missing link between cardiac histology and electrophysiology.

In previous studies, the vast majority of findings linking the pathological P-wave or electrophysiological changes to the related pathophysiological evidences were based on biopsies of the RA septum [55] and surgically removed tissue samples of right or LA appendages [122] [123, 124]. None of these studies were actually performed on the entire LA or RA wall. Further studies, which related to evaluating therapeutic methods or imaging techniques [95, 125, 126], were also based on this speculation that electrophysiological abnormalities directly reflect the underground issue on the level of atrial histology.

Most recently, magnetic resonance imaging (MRI) was employed in order to detect atrial wall fibrosis. As one of the main challenges associated with detecting atrial wall fibrosis relates to the difficulty in imaging the LA wall accurately or reliably due to its thin walls, MRI may be an imaging modality with high temporal and spatial resolution to image the LA [127, 128]. Quantitation of diffuse global and regional interstitial fibrosis within the left ventricular walls has recently been shown to be possible using a novel contrast-enhanced method for detecting and quantifying LA wall fibrosis [94, 129, 130].

Few studies have demonstrated that delayed gadolinium enhancement MRI may potentially be used for identifying LA wall fibrosis in animal models and in human. However, most studies have been limited to animal models. One such study reported a correlation between areas of delayed-gadolinium enhancement on MRI with LA wall fibrosis by histopathology in dogs with radiofrequency-induced lesions [129]. A similar

approach was applied to a group of 23 AF patients who underwent MRI scans at pre-ablation, 1 and 3 months post-ablation, and correlated areas of late gadolinium enhancement within the atrial walls that were ablated [130].

A recent innovative classification system for LA fibrosis was proposed based on the amount of delayed enhancement magnetic resonance imaging of patients [131]. This study also presents evidence highlighting the value of this classification system in terms of likely success of catheter ablation therapy for AF. However, neither the reproducibility, the sensitivity or the specificity of this approach compared to the gold standard (histopathological approach), nor has the long-term prognostic value of this measure been established in humans.

To the best of our knowledge, Bachmann's bundle has been mainly described as the most important preferential interatrial conduction route during sinus rhythm in human and animal studies [20, 132-135]. An impaired conductive property of Bachmann's bundle has been assumed to be an important cause for prolongation of P-wave duration. In 1983, Scott et al. reported a trend for a percentage of fibrosis in the LAA and PWD in lead II, but not amplitude of P-wave in patients with valvular disease who underwent open-heart surgery [136]. In this study, the PWD mostly correlated to the fibrosis extent at the CT site. It could be explained by CT's major role on intraatrial conduction in the RA during sinus rhythm.

In post-mortem, atrial tissues from patients who died of cardiovascular causes (Study 1), the extent of fibrosis and fatty infiltration was strongly associated with PWD, especially in major atrial conduction routes such as Bachmann's bundle and CT; Except Bachmann's bundle and CT, the baseline PWD also highly correlated with the combined count of fibrosis and fatty tissue extent at the site of the LA posterior wall of the superior PV level, which could be explained by the geometry of atrial myocardial fibers at this site and its anatomical origin. In previous anatomical studies in human, the posterior wall of LA at the superior PV level was shown to be covered by extensions from the Bachmann's bundle epicardially [16, 33, 137]. However, no significant correlation was found between histological atrial structural abnormalities and atrial depolarization pattern (e.g. P-wave morphology in sinus rhythm with regard to specific interatrial and/or intraatrial conduction blocks). These findings most likely suggest a causal relationship between atrial structural abnormalities and prolongation of atrial

depolarization during sinus rhythm. The current study is so far the only one attempting to link the PWD to all atrial structural abnormalities in humans; However, this study has its own limitations, such as manual measurements of P-wave characteristics, limited number of observations, and retrospective assessment of clinical characteristics. In particular, the limited number of subjects included in the study suggests caution in interpreting negative findings observed for some of the tested associations. However, to the best of our knowledge, no prior study has been able to evaluate the associations between P-wave appearance on surface ECG and structural characteristics of atrial walls, including major atrial conduction routes.

5.2 Interatrial connections and rhythm origin

What makes the depolarization wave cross the atrial septum boundary at a certain location is not entirely clear. Contributing factors may include high reported inter-individual variability in structure and location of interatrial routes, as well as their conduction properties. Relative proximity of the sinus rhythm origin to the superior interatrial routes (Bachmann's bundle) or posterior/inferior interatrial routes may also affect the route "chosen" for interatrial conduction and, hence, the site of the LA breakthrough. Regardless of the cause, the route used for transseptal conduction determines the P-wave terminal part morphology.

As previously described, the Bachmann bundle is a region of rapid interatrial conduction as confirmed by animal and human studies [20, 27, 31]. In regard to CS, the myocardial coat of CS is commonly observed [138]. It was proven that the CS musculature is electrically connected to the RA and LA, and forms an RA-LA connection in canine hearts [26]. A human study [27] provided further evidence supporting the existence of a preferential route near the CS ostium for interatrial conduction. Later, Ho et al [33] described small muscle bridges connecting the LA posterior wall near the ostia of the right-sided PVs to the RA posterior wall at the intercaval area in human hearts. The function of those posterior interatrial connections was also confirmed by mapping RA during PV tachycardias [31]. Posterior breakthrough at the intercaval area of RA was identified. As recently shown in an extensive study [16], interatrial bundles are not limited to the anteriorly located Bachmann's bundle, but are present in all parts of the interatrial septum, both

posteriorly between the right PVs and inferiorly between the CS and the right inferior PV. Moreover, in the same study, the inferiorly located bundles can be more prominent than the Bachmann's bundle in some hearts [16]. The quantity, length and diameter of interatrial connection fibers vary considerably between human individuals [16, 32].

Due to the high variability of the location of interatrial connections, it is reasonable to assume that pacing at the site mainly responsible for interatrial conduction would result in a shorter paced PWD corresponding to the shorter global atrial activation time in that individual. Meanwhile, we observed that longer PWD at baseline was associated with greater shortening by atrial septal pacing. Specifically, we observed that atrial septal pacing produced shorter PWD in patients with baseline PWD longer than 120 ms, regardless of pacing site location. However, in patients with a baseline PWD shorter than or equal to 120 ms, P-wave prolongation was observed during septal pacing, regardless of pacing site. These findings are in agreement with those of Manolis et al. [139], who described patient-tailored pacing site selection by intraoperative atrial septal mapping aimed at obtaining the shortest atrial activation time between the high RA and the distal CS. These sites were located in the vicinity of the CSo or near the FO in all patients, and not at Bachmann's bundle, which is in agreement with our findings.

Based on the above, it is easy to speculate that atrial septal pacing with regard to AF prevention may benefit only patients with impaired interatrial conduction during sinus rhythm, since such patients are more likely to respond to pacing by PWD shortening and atrial dyssynchrony reduction. In contrast, patients with normal PWD are not likely to demonstrate any improvement in interatrial conduction as a result of atrial septal pacing. If the preventive effect of atrial septal pacing on AF is indeed caused by shortening of the atrial activation time and preserving atrial synchrony [37, 39, 133, 140], then baseline PWD should have an impact on the clinical outcome in atrial septal pacing studies.

Regarding the relation between P-wave morphology and employed interatrial conduction, the preferential interatrial conduction is not always a fixed structure (posterior fibers, Bachmann's bundle or CS), which is typically shown in conduction of EAT beats that depends on relative proximity of the source of activation to each of these routes [25].

P-wave morphologies of EATs are produced by RA and LA activation sequences. Both of these chambers are involved in forming P-wave morphology during EAT. One of the chambers plays as the original chamber (the generator); the other chamber plays a role as a secondary chamber (the follower). The secondary chamber activation sequence during EAT depends on where the propagation starts and also depends on the location of the insertion of the preferential interatrial connection by which propagation conducts into the secondary chamber. Due to the relative long distance between the localization of inferior EAT origin and superoanterior interatrial connection (Bachmann's bundle), EATs from the lower RA have been chosen to study the role of lower preferential conduction routes in forming P-wave morphology. Furthermore, the inferoanterior (musculature in the vicinity of CS) and the posterior interatrial (posterior fibers behind FO) conduction routes are most likely the only two connections involved, and the following chamber (LA) is only activated anteriorly / posteriorly or vice versa. Therefore, the resulting P-wave morphology in precordial leads V3-V6 is either positive or negative depending on the interatrial connection which is reached from the EAT origin first.

The EATs of the lower TA origin were mostly completely negative P-waves or early negative components in leads V3-V6, significantly different from the lower CT origin. Activation mapping suggested one likely explanation that the RA depolarization vector was from the TA to the posterior wall, while LA was activated via the musculature in the vicinity of the CS (one of the three major interatrial conduction routes), and the LA depolarization vector was also backward. In contrast to EATs of lower CT origin, activation mapping showed a reverse depolarization vector pattern in both atria. We speculate that the forward LA depolarization vector may be explained by posterior fibers near the ostia of the right-sided PVs being employed as the preferential interatrial conduction route, thus perhaps explaining P-wave morphology in leads V3-V6.

Regarding the only two EATs of lower freewall origin, our findings may not suffice to describe the whole picture of P-wave morphology of lower freewall EATs. However, none of these two lower freewall EATs had either negative P-waves in leads V3-V6 or positive P-waves in all 4 leads V3-V6. P-wave morphology of lower freewall EATs may be highly variable in leads V3-V6, which may relate to the location of EAT origin, such as closer to lower CT or TA. The interatrial conduction routes used may also play a role.

The properties of intraatrial and interatrial conduction routes may also critically affect AF development. In the current substudy, baseline PWD in patients with persistent AF is prominently longer than PWD in patients with paroxysmal AF, which is in agreement with previous studies [141, 142]. Several studies have also focused on baseline PWD and AF either using standard or signal-averaged ECG [111, 143-145]. Notably, Magnani et al. [145] studied P-wave indices of maximum duration and dispersion in 1,550 Framingham Heart Study participants ≥ 60 years old (58% women) from single-channel ECG recorded from 1968 through 1971. In that analysis, maximum P-wave duration at the upper fifth percentile was associated with long-term AF risk in an elderly community-based cohort. P-wave duration is an electrocardiographic endophenotype for AF. In our study, the vast majority of patients had normal LVEF; most had paroxysmal AF (71%) with mild LA dilatation, while the rest of the cohort had persistent AF (29%) with mild to moderate LA dilatation. This risk profile indicates that the patients in our study had less diseased atria and lower risk of AF recurrence. Due to lack of significantly prolonged P-wave duration at baseline, we may not be able to detect the relationship between the outcome of CPVI and baseline PWD.

Regarding the method of orthogonal P-wave morphology used in the current study (Study 4), the dominant type of orthogonal P-wave morphology was characterized by biphasic P-waves in lead Z (normal SR with biphasic wave in lead Z - Type 2) regardless of AF type, with or without electrical cardioversion or recurrence after CPVI. This corresponds to our previous findings [104, 146]. Moreover, baseline dominant P-wave morphology per se was not related to recurrence of atrial arrhythmias after CPVI. The distribution of P-wave morphology types was compared for patients with initial SR and AF, with paroxysmal and persistent AF, or with and without recurrence of atrial arrhythmias after CPVI. No notable difference was observed in any of the comparisons. We speculate that neither the main type nor the distribution of orthogonal P-wave morphology type predicts the outcome after CPVI.

5.3 Dynamic P-wave morphology changes

Furthermore, even in SR, the employed interatrial conduction routes may alternate the sinus rhythm P-wave morphology. Different P-wave morphologies during SR as displayed on standard ECGs have been postulated to correspond to differences in interatrial

conduction [98-100]. A previous study by our group shows that orthogonal P-wave morphology can be used to correctly identify the LA breakthrough site and the corresponding interatrial conduction route [101]. PMV may be related to a number of factors such as the origin of SR within the RA, the proximity of SR to interatrial connections, and anatomical variabilities of both SR origin and preferential interatrial connection, as reviewed recently [147]. In summary, the PMV in our method likely reflects a switch between different interatrial paths (either due to functional block in any of the paths or due to variability in the sinus rhythm origin). Increasing fibrosis etc. would inhibit the ability to conduct through different paths. and would limit the potential number of exits from sinus node, both leading to a more stable or rigid activation pattern during sinus rhythm. These changes can be quantified.

The causes of a rigid atrial depolarization pattern could be functional or structural, so-called 'remodeling'. Atrial structural remodeling has been considered to be the main contributor for AF initiation and persistence, and may be present before start of AF caused by associated diseases [148-150]. Structural remodeling that is consistently seen in AF models and in patients with AF includes atrial enlargement, cellular hypertrophy, dedifferentiation, fibrosis, apoptosis, and myolysis [78-87]. These structural changes are unlikely to be completely reversible [151].

The PMV may reflect the level of AF substrate deterioration, and, if independently replicated, PMV may be able to identify the appropriate patients for CPVI alone, which could be sufficient for clinical success. High PMV observed in patients who benefited from CPVI may reflect less advanced structural remodeling and greater amount of preserved atrial myocardium that allows variable propagation of sinus pulses across the atria. The exact reason for the high PMV may not completely understood at this time. In our study, we sought to define variability as a switch between the distinct morphological classes of P-waves previously linked to different LA breakthrough sites during SR, which suggest a variation in employment of different interatrial routes [101] that may occur on a beat-to-beat basis.

A recent pathology study documented a strong association between the AF persistency and the extent of structural changes in the atrial myocardium that affect both the RA and the LA, so that the degree of fibro-fatty replacement of atrial myocardium may exceed 50% in patients with long-standing AF [44]. Along with progression of structural remodeling and fibro-fatty replacement of atrial myocardium, the number of

uninterrupted myocardial fibers available for conduction is likely to be reduced, which may lead to reduced variability of atrial activation patterns, i.e., reduced PMV. The strong association between reduced PMV and failure of CPVI suggests that this novel ECG marker of atrial conduction may reflect the degree of atrial remodeling, which is especially important since conventional ECG markers of atrial abnormalities such as P-wave duration or dominant P-wave morphology at baseline failed to identify patients who would benefit from CPVI.

5.4 Knowledge gaps and clinical implications

As briefly mentioned above, there are still great knowledge gaps in histological studies focusing on conduction properties. Currently, no link has been identified between histological abnormalities and particular P-wave morphology (such as partial IAB and advanced IAB, etc.). This may be due to limited sample size, which suggests caution in interpreting negative findings observed for some of the tested associations. Further studies with large cohorts and systematic methods are needed in order to elucidate current findings.

To date, most large-cohort studies on shortening P-wave duration using pacing techniques failed to demonstrate the benefits of shortening PWD in preventing AF, although in some exploratory studies clinical benefit has been reported [152-156]. The current study demonstrates that paced PWD shortening was observed mostly in patients with impaired atrial conduction (prolonged PWD at baseline). By contrast, patients with normal PWD at baseline tended to have a prolonged paced PWD, which suggests that atrial septal pacing may help prevent AF only in patients with impaired interatrial conduction during sinus rhythm, as such patients are more likely to respond to pacing by PWD shortening and atrial dyssynchrony reduction. If the preventive effect of atrial septal pacing on AF is indeed caused by shortening of the atrial activation time and preserving atrial synchrony, then the baseline PWD should impact the clinical outcome in atrial septal pacing studies. Meanwhile, in most studies, P-wave duration prolongation has not been considered to be an inclusion criterion, and no investigation of a possible link between PWD at baseline and the effect of atrial septal pacing has been reported. The current study lays the ground for testing this hypothesis in clinical settings, and may lead to further improvements in assessing patient suitability for atrial septal pacing.

Regarding dynamic P-wave morphology changes, we have taken great care in order to obtain ECG samples with 'good quality' during a 10-minute recording of standard 12-lead ECG. Due to sensitivity to premature atrial contractions, the current method may not totally avoid this interference. Some P-wave morphology variability may be attributed to the variability in the rhythm origin due to PAC. However, a clear switch between sinus P-wave with negative (previously defined as Type 1) and biphasic (previously defined as Type 2) in lead Z has been identified and illustrated, both two types of P-waves are judged to be of sinus origin. The current study shows that P-wave morphology variability could predict the outcome following CPVI, and may reflect the progress of atrial structural remodeling. This study motivates further studies on larger samples in order to independently replicate current findings.

CHAPTER 6. CONCLUSIONS

This study was intended to continue to fill in the gaps between atrial conduction, including intraatrial and interatrial conductions, and P-wave characteristics from histological respects to electrophysiology. We sought to describe the relationship between P-wave characteristics and atrial conduction in order to increase our understanding of atrial conduction following the progressing atrial remodeling and the intrinsic logic between histology and electrophysiology. Based on our findings in the current study, the following conclusions were drawn:

6.1 HISTOLOGICAL ATRIAL ABNORMALITY

Based on the finding that the extent of fibrosis and fatty infiltration demonstrated strong association with PWD, which was particularly apparent for the major atrial conduction routes such as Bachmann's bundle and the terminal crest, we hypothesize that P-wave duration prolongation is most likely explained by structural remodeling on the pathohistological level.

6.2 ATRIAL SEPTAL PACING

Pacing in the vicinity of major interatrial conduction routes may result in shorter global atrial conduction time in patients with impaired atrial conduction, especially when paced at CS ostium, which suggests that septal pacing in terms of P-wave shortening may apply only to patients with prolonged P-wave duration at baseline.

6.3 ECTOPIC ATRIAL TACHYCARDIA AND INTERATRIAL CONDUCTION ROUTE

The current findings suggest that P-wave morphology in precordial leads is likely influenced by the rhythm origin and its employment of preferential conduction routes, and may accurately differentiate the anatomic sites of atrial tachycardia originating from the low RA.

6.4 VARIABILITY OF P-WAVE MORPHOLOGY AND THE OUTCOME OF PULMONARY VEIN ISOLATION

The strong demonstrated relationship between PMV and 6-month CPVI success suggests that low PMV in patients with recurrent AF may reflect severe structural remodeling, and may explain failure of CPVI failure.

ACKNOWLEDGMENTS

Though only my name appears on the cover of this dissertation, a great many people have contributed to its production. I owe my gratitude to all those people who have made this dissertation possible and because of whom my graduate experience has been one that I will cherish forever.

My deepest gratitude is to my advisor, Dr. Pyotr G Platonov. I have been amazingly fortunate to have an advisor who gave me the freedom to explore on my own, and at the same time the guidance to recover when my steps faltered. Pyotr taught me how to question thoughts and express ideas. His patience and support helped me overcome many crisis situations and finish this dissertation. I hope that one day I would become as good an advisor to my students as Pyotr has been to me. I am also thankful to him for encouraging the use of correct grammar and consistent notation in my writings and for carefully reading and commenting on countless revisions of this manuscript.

My colleague, Dr. Jonas Carlson, has been always there to listen and give advice. I am deeply grateful to him for the long discussions that helped me sort out the technical details of my work. I am also thankful maintaining all software functioning efficiently that I never had to worry about losing data or unreliable data-analysis.

Dr. Fredrik Holmqvist's insightful comments and constructive criticisms at different stages of my research were thought-provoking and they helped me focus my ideas. I am grateful to him for holding me to a high research standard and enforcing strict validations for each research result, and thus teaching me how to do research.

Dr. Andreas Bollmann is one of the best teachers that I have had in my life. He sets high standards for his students and he encourages and guides them to meet those standards. I am indebted to him for his continuous encouragement and guidance.

I am grateful to Dr. Christopher Piorkowski for his encouragement and practical advice. I am also thankful to him for reading my manuscripts; commenting on my views and helping me understand and enrich my ideas. As a chief of Department of Electrophysiology in Dresden heart center, he also gives me lots of supports and freedom to dig deeper into my researches.

I am also grateful to the following former or current staff at University of Lund, for their various forms of support during my study, especially Ms. Monica Magnuss.

Many friends have helped me stay sane through these difficult years. Their support and care helped me overcome setbacks and stay focused on my graduate study, especially Dr. Thomas Gaspar. I greatly value their friendship and I deeply appreciate their belief in me.

Most importantly, none of this would have been possible without the love and patience of my family. My family, to whom this dissertation is dedicated to, has been a constant source of love, concern, support and strength all these years. Especially, to my dearest wife, Jingze Xu, for her love, support, and encouragement. I would like to express my heart-felt gratitude to my family. I have to give a special mention for the support given by Dr. Shiwen Yuan. I warmly appreciate the generosity for the stay in Lund.

Finally, I appreciate the financial support from Hjärt-Lungfonden that funded parts of the research discussed in this dissertation.

REFERENCES

1. Sanchez-Quintana, D., et al., Sinus node revisited in the era of electroanatomical mapping and catheter ablation. *Heart*, 2005. **91**(2): p. 189-94.
2. Lee, R.J., et al., Radiofrequency catheter modification of the sinus node for "inappropriate" sinus tachycardia. *Circulation*, 1995. **92**(10): p. 2919-28.
3. Boineau, J.P., et al., Demonstration of a widely distributed atrial pacemaker complex in the human heart. *Circulation*, 1988. **77**(6): p. 1221-37.
4. Schuessler, R.B., J.P. Boineau, and B.I. Bromberg, Origin of the sinus impulse. *J Cardiovasc Electrophysiol*, 1996. **7**(3): p. 263-74.
5. Brody, D.A., M.D. Woolsey, and R.C. Arzbaecher, Application of computer techniques to the detection and analysis of spontaneous P-wave variations. *Circulation*, 1967. **36**(3): p. 359-71.
6. Monfredi, O., et al., The anatomy and physiology of the sinoatrial node--a contemporary review. *Pacing and clinical electrophysiology : PACE*, 2010. **33**(11): p. 1392-406.
7. Boineau, J.P., et al., Quantitative relation between sites of atrial impulse origin and cycle length. *Am J Physiol*, 1983. **245**(5 Pt 1): p. H781-9.
8. Jones, S.B., et al., Comparison of SA nodal and subsidiary atrial pacemaker function and location in the dog. *Am J Physiol*, 1978. **234**(4): p. H471-6.
9. Forfang, K. and J. Erikssen, Significance of P wave terminal force in presumably healthy middle-aged men. *Am Heart J*, 1978. **96**(6): p. 739-43.
10. Yokota, M., et al., Analysis of the exercise-induced orthogonal P wave changes in normal subjects and patients with coronary artery disease. *Jpn Heart J*, 1986. **27**(4): p. 443-60.
11. Kistler, P.M., et al., P-wave morphology in focal atrial tachycardia: development of an algorithm to predict the anatomic site of origin. *J Am Coll Cardiol*, 2006. **48**(5): p. 1010-7.
12. Gonzalez, M.D., et al., Left atrial tachycardia originating from the mitral annulus-aorta junction. *Circulation*, 2004. **110**(20): p. 3187-92.
13. Tang, C.W., et al., Use of P wave configuration during atrial tachycardia to predict site of origin. *J Am Coll Cardiol*, 1995. **26**(5): p. 1315-24.

14. Betts, T.R., P.R. Roberts, and J.M. Morgan, High-density mapping of left atrial endocardial activation during sinus rhythm and coronary sinus pacing in patients with paroxysmal atrial fibrillation. *J Cardiovasc Electrophysiol*, 2004. **15**(10): p. 1111-7.
15. Markides, V., et al., Characterization of left atrial activation in the intact human heart. *Circulation*, 2003. **107**(5): p. 733-9.
16. Platonov, P.G., et al., Substrates for intra-atrial and interatrial conduction in the atrial septum: anatomical study on 84 human hearts. *Heart Rhythm*, 2008. **5**(8): p. 1189-95.
17. Mitrofanova, L.B., et al., Evidence of specialized tissue in human interatrial septum: histological, immunohistochemical and ultrastructural findings. *PLoS One*, 2014. **9**(11): p. e113343.
18. Ho, S.Y., et al., Anatomy of the left atrium: implications for radiofrequency ablation of atrial fibrillation. *J Cardiovasc Electrophysiol*, 1999. **10**(11): p. 1525-33.
19. James, T.N. and L. Sherf, Specialized tissues and preferential conduction in the atria of the heart. *The American journal of cardiology*, 1971. **28**(4): p. 414-27.
20. Lemery, R., et al., Human study of biatrial electrical coupling: determinants of endocardial septal activation and conduction over interatrial connections. *Circulation*, 2004. **110**(15): p. 2083-9.
21. De, P.R., et al., Electroanatomic analysis of sinus impulse propagation in normal human atria. *J Cardiovasc Electrophysiol*, 2002. **13**(1): p. 1-10.
22. Chauvin, M., et al., The anatomic basis of connections between the coronary sinus musculature and the left atrium in humans. *Circulation*, 2000. **101**(6): p. 647-52.
23. Hayashi, H., et al., Relation of canine atrial activation sequence to anatomic landmarks. *Am J Physiol*, 1982. **242**(3): p. H421-8.
24. Dolber, P.C. and M.S. Spach, Structure of canine Bachmann's bundle related to propagation of excitation. *Am J Physiol*, 1989. **257**(5 Pt 2): p. H1446-57.
25. O'Donnell, D., J.P. Bourke, and S.S. Furniss, Interatrial transseptal electrical conduction: comparison of patients with atrial fibrillation and normal controls. *J Cardiovasc Electrophysiol*, 2002. **13**(11): p. 1111-7.
26. Antz, M., et al., Electrical conduction between the right atrium and the left atrium via the musculature of the coronary sinus. *Circulation*, 1998. **98**(17): p. 1790-5.

27. Hertervig, E., et al., Global dispersion of right atrial repolarization in healthy pigs and patients. *Scand Cardiovasc J*, 2003. 37(6): p. 329-33.
28. Saremi, F., et al., Bachmann Bundle and its arterial supply: imaging with multidetector CT--implications for interatrial conduction abnormalities and arrhythmias. *Radiology*, 2008. 248(2): p. 447-57.
29. Yu, W.C., et al., Prevention of the initiation of atrial fibrillation: mechanism and efficacy of different atrial pacing modes. *Pacing Clin Electrophysiol*, 2000. 23(3): p. 373-9.
30. Lüdinghausen, M., N. Ohmachi, and C. Boot, Myocardial coverage of the coronary sinus and related veins. *Clinical Anatomy*, 1992. 5(1): p. 1-15.
31. Dong, J., et al., Catheter ablation of left atrial focal tachycardia guided by electroanatomic mapping and new insights into interatrial electrical conduction. *Heart Rhythm*, 2005. 2(6): p. 578-91.
32. Ho, S.Y., R.H. Anderson, and D. Sanchez-Quintana, Atrial structure and fibres: morphologic bases of atrial conduction. *Cardiovasc Res*, 2002. 54(2): p. 325-36.
33. Ho, S.Y. and D. Sanchez-Quintana, The importance of atrial structure and fibers. *Clin Anat*, 2009. 22(1): p. 52-63.
34. Lemery, R., et al., Normal atrial activation and voltage during sinus rhythm in the human heart: an endocardial and epicardial mapping study in patients with a history of atrial fibrillation. *J Cardiovasc Electrophysiol*, 2007. 18(4): p. 402-8.
35. Ovsyshcher, I.E., Toward physiological pacing: optimization of cardiac hemodynamics by AV delay adjustment. *Pacing Clin Electrophysiol*, 1997. 20(4 Pt 1): p. 861-5.
36. Saksena, S., et al., Prevention of recurrent atrial fibrillation with chronic dual-site right atrial pacing. *J Am Coll Cardiol*, 1996. 28(3): p. 687-94.
37. D'Allonnes, G.R., et al., Long-term effects of biatrial synchronous pacing to prevent drug-refractory atrial tachyarrhythmia: a nine-year experience. *J Cardiovasc Electrophysiol*, 2000. 11(10): p. 1081-91.
38. Prakash, A., et al., Acute effects of dual-site right atrial pacing in patients with spontaneous and inducible atrial flutter and fibrillation. *J Am Coll Cardiol*, 1997. 29(5): p. 1007-14.
39. Padeletti, L., et al., Interatrial septum pacing: a new approach to prevent recurrent atrial fibrillation. *J Interv Card Electrophysiol*, 1999. 3(1): p. 35-43.

40. Hemels, M.E., et al., Right atrial preventive and antitachycardia pacing for prevention of paroxysmal atrial fibrillation in patients without bradycardia: a randomized study. *Europace*, 2008. **10**(3): p. 306-13.
41. Padeletti, L., et al., Combined efficacy of atrial septal lead placement and atrial pacing algorithms for prevention of paroxysmal atrial tachyarrhythmia. *J Cardiovasc Electrophysiol*, 2003. **14**(11): p. 1189-95.
42. Miyazaki, H., et al., Atrial septal pacing to resynchronize atrial contraction and improve atrial transport function. *J Cardiol*, 2005. **45**(6): p. 239-46.
43. Evans, R. and D.B. Shaw, Pathological studies in sinoatrial disorder (sick sinus syndrome). *British heart journal*, 1977. **39**(7): p. 778-86.
44. Platonov, P.G., et al., Structural abnormalities in atrial walls are associated with presence and persistency of atrial fibrillation but not with age. *Journal of the American College of Cardiology*, 2011. **58**(21): p. 2225-32.
45. Husson, J., [Partial interatrial block]. *Arch Mal Coeur Vaiss*, 1983. **76**(8): p. 959-63.
46. Bayes de Luna, A., et al., Interatrial conduction block and retrograde activation of the left atrium and paroxysmal supraventricular tachyarrhythmia. *Eur Heart J*, 1988. **9**(10): p. 1112-8.
47. Bayes de Luna, A., M.C. Oter, and J. Guindo, Interatrial conduction block with retrograde activation of the left atrium and paroxysmal supraventricular tachyarrhythmias: influence of preventive antiarrhythmic treatment. *Int J Cardiol*, 1989. **22**(2): p. 147-50.
48. Marconi, P., et al., [A "signal averaging" analysis of the P wave in patients with a history of isolated paroxysmal atrial fibrillation]. *G Ital Cardiol*, 1991. **21**(10): p. 1075-81.
49. Falk, R.H. and A. Pollak, Signal-averaged P wave duration and atrial fibrillation. *J Am Coll Cardiol*, 1994. **23**(2): p. 549-50.
50. Raitt, M.H., K.D. Ingram, and S.M. Thurman, Signal-averaged P wave duration predicts early recurrence of atrial fibrillation after cardioversion. *Pacing Clin Electrophysiol*, 2000. **23**(2): p. 259-65.
51. Bachman, S., D. Sparrow, and L.K. Smith, Effect of aging on the electrocardiogram. *Am J Cardiol*, 1981. **48**(3): p. 513-6.

52. Stafford, P.J., I. Turner, and R. Vincent, Quantitative analysis of signal-averaged P waves in idiopathic paroxysmal atrial fibrillation. *Am J Cardiol*, 1991. **68**(8): p. 751-5.
53. Havmoller, R., et al., Age-related changes in P wave morphology in healthy subjects. *BMC Cardiovasc Disord*, 2007. **7**: p. 22.
54. Holmqvist, F., et al., Abnormal P-wave morphology is a predictor of atrial fibrillation development and cardiac death in MADIT II patients. *Ann Noninvasive Electrocardiol*, 2010. **15**(1): p. 63-72.
55. Frustaci, A., et al., Histological substrate of atrial biopsies in patients with lone atrial fibrillation. *Circulation*, 1997. **96**(4): p. 1180-4.
56. Nguyen, B.L., et al., Histopathological substrate for chronic atrial fibrillation in humans. *Heart rhythm : the official journal of the Heart Rhythm Society*, 2009. **6**(4): p. 454-60.
57. Olsson, S.B., et al., Spontaneous reversion from long-lasting atrial fibrillation to sinus rhythm. *Acta Med Scand*, 1980. **207**(1-2): p. 5-20.
58. Chen, J., et al., Dynamics of wavelets and their role in atrial fibrillation in the isolated sheep heart. *Cardiovascular research*, 2000. **48**(2): p. 220-32.
59. Anyukhovskiy, E.P., et al., Age-associated changes in electrophysiologic remodeling: a potential contributor to initiation of atrial fibrillation. *Cardiovascular research*, 2005. **66**(2): p. 353-63.
60. Roberts-Thomson, K.C., et al., Anatomically determined functional conduction delay in the posterior left atrium relationship to structural heart disease. *Journal of the American College of Cardiology*, 2008. **51**(8): p. 856-62.
61. Rha, S.W., et al., Mechanisms responsible for the initiation and maintenance of atrial fibrillation assessed by non-contact mapping system. *International journal of cardiology*, 2008. **124**(2): p. 218-26.
62. Yamazaki, M., et al., Mechanisms of stretch-induced atrial fibrillation in the presence and the absence of adrenergic stimulation: interplay between rotors and focal discharges. *Heart rhythm : the official journal of the Heart Rhythm Society*, 2009. **6**(7): p. 1009-17.
63. Yamabe, H., et al., Analysis of the mechanisms initiating random wave propagation at the onset of atrial fibrillation using noncontact mapping: role of complex fractionated electrogram region. *Heart rhythm : the official journal of the Heart Rhythm Society*, 2011. **8**(8): p. 1228-36.

64. Olgin, J.E., et al., Heterogeneous atrial denervation creates substrate for sustained atrial fibrillation. *Circulation*, 1998. **98**(23): p. 2608-14.
65. Reynolds, M.R., et al., Cost-effectiveness of radiofrequency catheter ablation compared with antiarrhythmic drug therapy for paroxysmal atrial fibrillation. *Circulation. Arrhythmia and electrophysiology*, 2009. **2**(4): p. 362-9.
66. Calkins, H., et al., Treatment of atrial fibrillation with antiarrhythmic drugs or radiofrequency ablation: two systematic literature reviews and meta-analyses. *Circulation. Arrhythmia and electrophysiology*, 2009. **2**(4): p. 349-61.
67. Khaykin, Y., et al., Cost comparison of ablation versus antiarrhythmic drugs as first-line therapy for atrial fibrillation: an economic evaluation of the RAAFT pilot study. *Journal of cardiovascular electrophysiology*, 2009. **20**(1): p. 7-12.
68. Jons, C., et al., The Medical ANtiarrhythmic Treatment or Radiofrequency Ablation in Paroxysmal Atrial Fibrillation (MANTRA-PAF) trial: clinical rationale, study design, and implementation. *Europace : European pacing, arrhythmias, and cardiac electrophysiology : journal of the working groups on cardiac pacing, arrhythmias, and cardiac cellular electrophysiology of the European Society of Cardiology*, 2009. **11**(7): p. 917-23.
69. Mulder, A.A., et al., Pulmonary vein isolation and left atrial complex-fractionated atrial electrograms ablation for persistent atrial fibrillation with phased radio frequency energy and multi-electrode catheters: efficacy and safety during 12 months follow-up. *Europace : European pacing, arrhythmias, and cardiac electrophysiology : journal of the working groups on cardiac pacing, arrhythmias, and cardiac cellular electrophysiology of the European Society of Cardiology*, 2011. **13**(12): p. 1695-702.
70. Hayward, R.M., et al., Pulmonary vein isolation with complex fractionated atrial electrogram ablation for paroxysmal and nonparoxysmal atrial fibrillation: A meta-analysis. *Heart rhythm : the official journal of the Heart Rhythm Society*, 2011. **8**(7): p. 994-1000.
71. Willems, S., et al., Substrate modification combined with pulmonary vein isolation improves outcome of catheter ablation in patients with persistent atrial fibrillation: a prospective randomized comparison. *European heart journal*, 2006. **27**(23): p. 2871-8.
72. Papageorgiou, P., et al., Electrophysiology of atrial fibrillation and its prevention by coronary sinus pacing. *Semin Interv Cardiol*, 1997. **2**(4): p. 227-32.

73. Papageorgiou, P., et al., Coronary sinus pacing prevents induction of atrial fibrillation. *Circulation*, 1997. **96**(6): p. 1893-8.
74. Agarwal, Y.K., et al., Association of interatrial block with development of atrial fibrillation. *The American journal of cardiology*, 2003. **91**(7): p. 882.
75. Monigatti-Tenkorang, J., et al., Intermittent atrial tachycardia promotes repolarization alternans and conduction slowing during rapid rates, and increases susceptibility to atrial fibrillation in a free-behaving sheep model. *J Cardiovasc Electrophysiol*, 2014. **25**(4): p. 418-27.
76. Lalani, G.G., et al., Atrial conduction slows immediately before the onset of human atrial fibrillation: a bi-atrial contact mapping study of transitions to atrial fibrillation. *J Am Coll Cardiol*, 2012. **59**(6): p. 595-606.
77. Medi, C., et al., Atrial electrical and structural changes associated with longstanding hypertension in humans: implications for the substrate for atrial fibrillation. *J Cardiovasc Electrophysiol*, 2011. **22**(12): p. 1317-24.
78. Ausma, J., et al., Structural changes of atrial myocardium due to sustained atrial fibrillation in the goat. *Circulation*, 1997. **96**(9): p. 3157-63.
79. Li, D., et al., Promotion of atrial fibrillation by heart failure in dogs: atrial remodeling of a different sort. *Circulation*, 1999. **100**(1): p. 87-95.
80. Schoonderwoerd, B.A., et al., Atrial ultrastructural changes during experimental atrial tachycardia depend on high ventricular rate. *Journal of cardiovascular electrophysiology*, 2004. **15**(10): p. 1167-74.
81. Anne, W., et al., Self-terminating AF depends on electrical remodeling while persistent AF depends on additional structural changes in a rapid atrially paced sheep model. *Journal of molecular and cellular cardiology*, 2007. **43**(2): p. 148-58.
82. Morillo, C.A., et al., Chronic rapid atrial pacing. Structural, functional, and electrophysiological characteristics of a new model of sustained atrial fibrillation. *Circulation*, 1995. **91**(5): p. 1588-95.
83. Everett, T.H.t., et al., Electrical, morphological, and ultrastructural remodeling and reverse remodeling in a canine model of chronic atrial fibrillation. *Circulation*, 2000. **102**(12): p. 1454-60.
84. Bauer, A., A.D. McDonald, and J.K. Donahue, Pathophysiological findings in a model of persistent atrial fibrillation and severe congestive heart failure. *Cardiovascular research*, 2004. **61**(4): p. 764-70.

85. Moe, G.W., et al., Matrix metalloproteinase inhibition attenuates atrial remodeling and vulnerability to atrial fibrillation in a canine model of heart failure. *Journal of cardiac failure*, 2008. **14**(9): p. 768-76.
86. Boyden, P.A., et al., Effects of left atrial enlargement on atrial transmembrane potentials and structure in dogs with mitral valve fibrosis. *The American journal of cardiology*, 1982. **49**(8): p. 1896-908.
87. Boyden, P.A., et al., Mechanisms for atrial arrhythmias associated with cardiomyopathy: a study of feline hearts with primary myocardial disease. *Circulation*, 1984. **69**(5): p. 1036-47.
88. Kottkamp, H., Human atrial fibrillation substrate: towards a specific fibrotic atrial cardiomyopathy. *Eur Heart J*, 2013. **34**(35): p. 2731-8.
89. Kottkamp, H., Catheter Ablation of Atrial Fibrillation: On the Pathophysiology of the Arrhythmia and the Impact of Cardiac Risk Factor Management. *J Am Coll Cardiol*, 2014. **64**(21): p. 2232-4.
90. Kostin, S., et al., Structural correlate of atrial fibrillation in human patients. *Cardiovascular research*, 2002. **54**(2): p. 361-79.
91. Boldt, A., et al., Fibrosis in left atrial tissue of patients with atrial fibrillation with and without underlying mitral valve disease. *Heart*, 2004. **90**(4): p. 400-5.
92. Spach, M.S. and P.C. Dolber, Relating extracellular potentials and their derivatives to anisotropic propagation at a microscopic level in human cardiac muscle. Evidence for electrical uncoupling of side-to-side fiber connections with increasing age. *Circ Res*, 1986. **58**(3): p. 356-71.
93. Spach, M.S. and J.P. Boineau, Microfibrosis produces electrical load variations due to loss of side-to-side cell connections: a major mechanism of structural heart disease arrhythmias. *Pacing and clinical electrophysiology : PACE*, 1997. **20**(2 Pt 2): p. 397-413.
94. Oakes, R.S., et al., Detection and quantification of left atrial structural remodeling with delayed-enhancement magnetic resonance imaging in patients with atrial fibrillation. *Circulation*, 2009. **119**(13): p. 1758-67.
95. McGann, C., et al., Atrial fibrillation ablation outcome is predicted by left atrial remodeling on MRI. *Circ Arrhythm Electrophysiol*, 2014. **7**(1): p. 23-30.
96. Havmoller, R., et al., Evolution of P-wave morphology in healthy individuals: a 3-year follow-up study. *Ann Noninvasive Electrocardiol*, 2009. **14**(3): p. 226-33.

97. Holmqvist, F., et al., Variable interatrial conduction illustrated in a hypertrophic cardiomyopathy population. *Ann Noninvasive Electrocardiol*, 2007. **12**(3): p. 227-36.
98. Husson, J. and C. Froment, [Partial interatrial block due to a conduction defect of the preferential middle interatrial depolarization pathway]. *Arch Mal Coeur Vaiss*, 1985. **78**(10): p. 1569-74.
99. Ariyarajah, V., et al., Specific electrocardiographic markers of P-wave morphology in interatrial block. *J Electrocardiol*, 2006. **39**(4): p. 380-4.
100. Bayes de Luna, A., et al., Electrocardiographic and vectorcardiographic study of interatrial conduction disturbances with left atrial retrograde activation. *J Electrocardiol*, 1985. **18**(1): p. 1-13.
101. Holmqvist, F., et al., Interatrial conduction can be accurately determined using standard 12-lead electrocardiography: validation of P-wave morphology using electroanatomic mapping in man. *Heart Rhythm*, 2008. **5**(3): p. 413-8.
102. Dilaveris, P., et al., Prevalence of interatrial block in healthy school-aged children: definition by P-wave duration or morphological analysis. *Ann Noninvasive Electrocardiol*, 2010. **15**(1): p. 17-25.
103. Holmqvist, F., et al., Altered interatrial conduction detected in MADIT II patients bound to develop atrial fibrillation. *Ann Noninvasive Electrocardiol*, 2009. **14**(3): p. 268-75.
104. Platonov, P.G., et al., Detection of inter-atrial conduction defects with unfiltered signal-averaged P-wave ECG in patients with lone atrial fibrillation. *Europace*, 2000. **2**(1): p. 32-41.
105. Ariyarajah, V. and D.H. Spodick, Advanced interatrial block: a classic electrocardiogram. *Cardiology*, 2005. **104**(1): p. 33-4.
106. Platonov, P.G., et al., Abnormal atrial activation is common in patients with arrhythmogenic right ventricular cardiomyopathy. *Journal of electrocardiology*, 2011. **44**(2): p. 237-41.
107. Huo, Y., et al., Variability of P-wave morphology predicts the outcome of circumferential pulmonary vein isolation in patients with recurrent atrial fibrillation. *J Electrocardiol*, 2014.
108. Zhang, T., et al., Focal atrial tachycardia arising from the right atrial appendage: electrophysiologic and electrocardiographic characteristics and catheter ablation. *Int J Clin Pract*, 2009. **63**(3): p. 417-24.

109. Dilaveris, P.E., et al., Simple electrocardiographic markers for the prediction of paroxysmal idiopathic atrial fibrillation. *Am Heart J*, 1998. **135**(5 Pt 1): p. 733-8.
110. Weber, U.K., et al., Selective versus non-selective antiarrhythmic approach for prevention of atrial fibrillation after coronary surgery: is there a need for pre-operative risk stratification? A prospective placebo-controlled study using low-dose sotalol. *European heart journal*, 1998. **19**(5): p. 794-800.
111. Steinberg, J.S., et al., Value of the P-wave signal-averaged ECG for predicting atrial fibrillation after cardiac surgery. *Circulation*, 1993. **88**(6): p. 2618-22.
112. Carlson, J., et al., Can orthogonal lead indicators of propensity to atrial fibrillation be accurately assessed from the 12-lead ECG? *Europace*, 2005. **7 Suppl 2**: p. 39-48.
113. Carlson, J., et al., Can orthogonal lead indicators of propensity to atrial fibrillation be accurately assessed from the 12-lead ECG? *Europace : European pacing, arrhythmias, and cardiac electrophysiology : journal of the working groups on cardiac pacing, arrhythmias, and cardiac cellular electrophysiology of the European Society of Cardiology*, 2005. **7 Suppl 2**: p. 39-48.
114. Edenbrandt, L. and O. Pahlm, Vectorcardiogram synthesized from a 12-lead ECG: superiority of the inverse Dower matrix. *Journal of electrocardiology*, 1988. **21**(4): p. 361-7.
115. Holmqvist, F., et al., Signal-averaged P wave analysis for delineation of interatrial conduction - further validation of the method. *BMC Cardiovasc Disord*, 2007. **7**: p. 29.
116. Akhtar, M., et al., Clinical competence in invasive cardiac electrophysiological studies. A statement for physicians from the ACP/ACC/AHA Task Force on Clinical Privileges in Cardiology. *Circulation*, 1994. **89**(4): p. 1917-20.
117. Blomstrom-Lundqvist, C., et al., ACC/AHA/ESC guidelines for the management of patients with supraventricular arrhythmias--executive summary. a report of the American college of cardiology/American heart association task force on practice guidelines and the European society of cardiology committee for practice guidelines (writing committee to develop guidelines for the management of patients with supraventricular arrhythmias) developed in collaboration with NASPE-Heart Rhythm Society. *Journal of the American College of Cardiology*, 2003. **42**(8): p. 1493-531.

118. Cosio, F.G., et al., ESCWGA/NASPE/P experts consensus statement: living anatomy of the atrioventricular junctions. A guide to electrophysiologic mapping. Working Group of Arrhythmias of the European Society of Cardiology. North American Society of Pacing and Electrophysiology. *J Cardiovasc Electrophysiol*, 1999. **10**(8): p. 1162-70.
119. Piorkowski, C., et al., Computed tomography model-based treatment of atrial fibrillation and atrial macro-re-entrant tachycardia. *Europace : European pacing, arrhythmias, and cardiac electrophysiology : journal of the working groups on cardiac pacing, arrhythmias, and cardiac cellular electrophysiology of the European Society of Cardiology*, 2008. **10**(8): p. 939-48.
120. Kottkamp, H., et al., Topographic variability of the esophageal left atrial relation influencing ablation lines in patients with atrial fibrillation. *Journal of cardiovascular electrophysiology*, 2005. **16**(2): p. 146-50.
121. Piorkowski, C., et al., Steerable sheath catheter navigation for ablation of atrial fibrillation: a case-control study. *Pacing and clinical electrophysiology : PACE*, 2008. **31**(7): p. 863-73.
122. Krul, S.P., et al., Atrial fibrosis and conduction slowing in the left atrial appendage of patients undergoing thoracoscopic surgical pulmonary vein isolation for atrial fibrillation. *Circ Arrhythm Electrophysiol*, 2015. **8**(2): p. 288-95.
123. Kataoka, T., et al., Left atrium volume index and pathological features of left atrial appendage as a predictor of failure in postoperative sinus conversion. *Journal of cardiology*, 2010. **55**(2): p. 274-82.
124. Saito, T., et al., Histopathological features of the resected left atrial appendage as predictors of recurrence after surgery for atrial fibrillation in valvular heart disease. *Circulation journal : official journal of the Japanese Circulation Society*, 2007. **71**(1): p. 70-8.
125. Sramko, M., et al., Clinical value of assessment of left atrial late gadolinium enhancement in patients undergoing ablation of atrial fibrillation. *Int J Cardiol*, 2015. **179**: p. 351-7.
126. Rolf, S., et al., Tailored atrial substrate modification based on low-voltage areas in catheter ablation of atrial fibrillation. *Circ Arrhythm Electrophysiol*, 2014. **7**(5): p. 825-33.

127. Carpen, M., et al., First experience of 3D rotational angiography fusion with NavX electroanatomical mapping to guide catheter ablation of atrial fibrillation. *Heart Rhythm*, 2013. **10**(3): p. 422-7.
128. Messroghli, D.R., et al., Myocardial T1 mapping: application to patients with acute and chronic myocardial infarction. *Magn Reson Med*, 2007. **58**(1): p. 34-40.
129. Daccarett, M., et al., Association of left atrial fibrosis detected by delayed-enhancement magnetic resonance imaging and the risk of stroke in patients with atrial fibrillation. *Journal of the American College of Cardiology*, 2011. **57**(7): p. 831-8.
130. Peters, D.C., et al., Detection of pulmonary vein and left atrial scar after catheter ablation with three-dimensional navigator-gated delayed enhancement MR imaging: initial experience. *Radiology*, 2007. **243**(3): p. 690-5.
131. Mahnkopf, C., et al., Evaluation of the left atrial substrate in patients with lone atrial fibrillation using delayed-enhanced MRI: implications for disease progression and response to catheter ablation. *Heart rhythm : the official journal of the Heart Rhythm Society*, 2010. **7**(10): p. 1475-81.
132. Waldo, A.L., K.J. Vitikainen, and B.F. Hoffman, The sequence of retrograde atrial activation in the canine heart. Correlation with positive and negative retrograde P waves. *Circulation research*, 1975. **37**(2): p. 156-63.
133. Bailin, S.J., S. Adler, and M. Giudici, Prevention of chronic atrial fibrillation by pacing in the region of Bachmann's bundle: results of a multicenter randomized trial. *J Cardiovasc Electrophysiol*, 2001. **12**(8): p. 912-7.
134. Dolber, P.C. and M.S. Spach, Structure of canine Bachmann's bundle related to propagation of excitation. *The American journal of physiology*, 1989. **257**(5 Pt 2): p. H1446-57.
135. Lemery, R., Bi-atrial mapping of atrial arrhythmias. *Card Electrophysiol Rev*, 2002. **6**(4): p. 378-82.
136. Scott, C.C., et al., The effect of left atrial histology and dimension on P wave morphology. *J Electrocardiol*, 1983. **16**(4): p. 363-6.
137. Ho, S.Y., R.H. Anderson, and D. Sanchez-Quintana, Atrial structure and fibres: morphologic bases of atrial conduction. *Cardiovascular research*, 2002. **54**(2): p. 325-36.

138. Maros, T.N., et al., Contributions to the morphology of the human coronary sinus. *Anat Anz*, 1983. 154(2): p. 133-44.
139. Manolis, A.G., et al., Prevention of atrial fibrillation by inter-atrial septum pacing guided by electrophysiological testing, in patients with delayed interatrial conduction. *Europace*, 2002. 4(2): p. 165-74.
140. Hermida, J.S., et al., Atrial septal versus atrial appendage pacing: feasibility and effects on atrial conduction, interatrial synchronization, and atrioventricular sequence. *Pacing Clin Electrophysiol*, 2003. 26(1 Pt 1): p. 26-35.
141. Santoni-Rugiu, F., et al., Signal-averaged P-wave ECG discriminates between persistent and paroxysmal atrial fibrillation. *J Electrocardiol*, 2001. 34(3): p. 189-95.
142. Vincenti, A., et al., A noninvasive index of atrial remodeling in patients with paroxysmal and persistent atrial fibrillation: a pilot study. *Journal of electrocardiology*, 2012. 45(2): p. 109-15.
143. Ogawa, H., et al., The signal-averaged electrocardiogram of P wave in patients with documented atrial fibrillation or flutter and in patients with left or right atrial overload without atrial fibrillation. *Japanese heart journal*, 1993. 34(1): p. 29-39.
144. Van Beeumen, K., et al., Changes in P-wave area and P-wave duration after circumferential pulmonary vein isolation. *Europace*, 2010.
145. Magnani, J.W., et al., P wave duration and risk of longitudinal atrial fibrillation in persons \geq 60 years old (from the Framingham Heart Study). *The American journal of cardiology*, 2011. 107(6): p. 917-921 e1.
146. Holmqvist, F., et al., Abnormal atrial activation in young patients with lone atrial fibrillation. *Europace : European pacing, arrhythmias, and cardiac electrophysiology : journal of the working groups on cardiac pacing, arrhythmias, and cardiac cellular electrophysiology of the European Society of Cardiology*, 2011. 13(2): p. 188-92.
147. Platonov, P.G., P-wave morphology: underlying mechanisms and clinical implications. *Ann Noninvasive Electrocardiol*, 2012. 17(3): p. 161-9.
148. Anne, W., et al., Matrix metalloproteinases and atrial remodeling in patients with mitral valve disease and atrial fibrillation. *Cardiovascular research*, 2005. 67(4): p. 655-66.

149. Sanders, P., et al., Electrical remodeling of the atria in congestive heart failure: electrophysiological and electroanatomic mapping in humans. *Circulation*, 2003. **108**(12): p. 1461-8.
150. Vaziri, S.M., et al., Influence of blood pressure on left atrial size. The Framingham Heart Study. *Hypertension*, 1995. **25**(6): p. 1155-60.
151. Kourliouros, A., et al., Current concepts in the pathogenesis of atrial fibrillation. *American heart journal*, 2009. **157**(2): p. 243-52.
152. Naito, S., et al., Biatial epicardial pacing prevents atrial fibrillation and confers hemodynamic benefits after coronary artery bypass surgery. *Pacing and clinical electrophysiology : PACE*, 2005. **28 Suppl 1**: p. S146-9.
153. Healey, J.S., et al., Relevance of electrical remodeling in human atrial fibrillation: results of the asymptomatic atrial fibrillation and stroke evaluation in pacemaker patients and the atrial fibrillation reduction atrial pacing trial mechanisms of atrial fibrillation study. *Circulation. Arrhythmia and electrophysiology*, 2012. **5**(4): p. 626-31.
154. Padeletti, L., et al., Duration of P-wave is associated with atrial fibrillation hospitalizations in patients with atrial fibrillation and paced for bradycardia. *Pacing Clin Electrophysiol*, 2007. **30**(8): p. 961-9.
155. Kristensen, L., et al., Sinus and paced P wave duration and dispersion as predictors of atrial fibrillation after pacemaker implantation in patients with isolated sick sinus syndrome. *Pacing Clin Electrophysiol*, 2004. **27**(5): p. 606-14.
156. Katsivas, A., et al., Atrial septal pacing to synchronize atrial depolarization in patients with delayed interatrial conduction. *Pacing Clin Electrophysiol*, 1998. **21**(11 Pt 2): p. 2220-5.

Paper I



P-wave characteristics and histological atrial abnormality

Yan Huo, MD,^{a, b, *} Lubov Mitrofanova, MD,^c Victoria Orshanskaya, MD,^c
Petter Holmberg, MD,^a Fredrik Holmqvist, MD, PhD,^a
Pyotr G. Platonov, MD, PhD, FHRS, FESC^a

^aDepartment of Cardiology, Lund University Hospital, Lund University, Lund, Sweden

^bDepartment of Electrophysiology, Heart Center Dresden, Dresden University of Technology, Dresden, Germany

^cAlmazov Federal Center for Heart, Blood and Endocrinology, St. Petersburg, Russia

Abstract

Background: Fibro-fatty transformation is believed to be the leading cause of deteriorated atrial conduction; however, any direct assessment in relation to P-wave characteristics is lacking. We sought to assess P-wave morphology (PWM) and duration (PWD) in relation to histology of the atrial myocardium.

Objective: Atrial specimens were collected from 11 patients who died from cardiovascular causes (7 men; median age 73 years).

Methods: Tissue samples were taken at the level of superior and inferior PVs, center of posterior left atrial wall, terminal crest (CT) and Bachmann's bundle (BB) for assessment of fibro-fatty tissue extent. Standard 12-lead ECGs in sinus rhythm recorded during hospital stay were used for manual assessment of P-wave. Partial interatrial block (pIAB) was defined as a prolonged (≥ 120 ms) and bimodal P-wave in any lead on 12-lead ECG.

Results: The median PWD was 160 (120–200) ms. Fibrosis extent in CT highly correlated to PWD ($r = 0.914$, $p < 0.001$). The combination of fibrosis extent and fatty tissue in BB (16%, range 1%–41%), CT (18%, range 3%–47%) or superior PV (15%, range 6%–24%) correlated to PWD ($r = 0.627$, $p = 0.039$; $r = 0.795$, $p = 0.003$; and $r = 0.668$, $p = 0.025$, respectively). pIAB pattern was observed in 10 subjects; however, it was not associated with either fibrosis or fatty tissue content at any sampling location.

Conclusions: Our findings further support causal association between PWD and the extent of structural abnormalities in the atrial myocardium and the major atrial conduction routes.

© 2014 Elsevier Inc. All rights reserved.

Keywords:

Fibro-fatty transformation; P-wave morphology; P-wave duration

Introduction

In 1977, Evans and Shaw examined 8 patients with sinus node disease and demonstrated that in 7 of these patients there was increased fibrosis or fatty infiltration in right atrial musculature. It was the first study offering evidence of widespread right atrial abnormality, which revealed an underlying relation between fibro-fatty infiltration and atrial conduction abnormality [1]. Later, in post-mortem materials, fibrosis extent and fatty infiltration were observed in patients with history of atrial fibrillation (AF), which were significantly higher in patients with permanent AF as compared to paroxysmal AF [2].

Meanwhile, earlier studies have associated abnormal P-wave duration (PWD) and morphology with AF, aging and cardiovascular comorbidities [3–9]. Fibro-fatty transformation of atrial walls is believed to be the leading cause of deteriorated atrial conduction [1,10,11]. However, any direct assessment of fibrosis extent in the major atrial conduction routes in relation to P-wave characteristics is lacking. We hypothesized that P-wave morphology and duration may be related to histological abnormality of the atrial myocardium.

Method

Patient population

Material for the study was collected in accordance with the protocol described in detail earlier [2]. To summarize, medical records of consecutive cases of in-hospital deaths

* Corresponding author at: Department of Cardiology, Lund University, SE-211 85, Lund, Sweden.

E-mail address: dr.huoyan@googlemail.com

referred for post-mortem studies at the Federal Heart, Blood, and Endocrinology Centre (St. Petersburg, Russia) were screened for AF presence and its clinical type ($n = 276$). Subjects with AF after open-heart surgery or severe valvular pathology were excluded. Three predefined groups of 10 cases each equally were collected, representing subjects with permanent AF, non-permanent AF, and subjects with no documented AF history. A total of 30 subjects were used for histological analysis.

Exclusive criteria of ECG tracings included ST-elevation, invisible onset or ending of P-waves (i.e. P-wave on T-wave), unstable baseline of ECG tracing and heart rate <50 or >100 /min. Accordingly, of the 20 subjects who did not have permanent AF, the medical records contained at least a standard 12-lead ECG recorded in sinus rhythm, and were thus suitable for P-wave analysis in 11 cases. Four out of 11 subjects had a history of paroxysmal AF.

ECG analysis

A 12-lead surface ECG was recorded in supine position using a Hellige ECG 153 (Freiburg, Germany) machine. The 12-lead ECG was recorded at a paper speed of 50 mm/s ($n = 6$) or 25 mm/s ($n = 5$), a standard calibration of 10 mm/mV, and a filter of 0.05–35 Hz standardization. The P-wave duration (PWD) was calculated in all 12 leads of the surface ECG. The measurements of the P-wave duration were performed manually by two investigators without knowledge of the histological findings or AF group allocation. To improve accuracy, measurements were performed with calipers and magnifying lens for defining the P-wave deflection, similarly to the approach used by others [12–14]. P-wave onset was defined as the point of the first visible upward/downward departure of the trace from baseline bottom for positive/negative waves. When the trace returned to the baseline at the bottom of the trace in positive waves or at the top of the trace in negative waves, this point was considered to the end of the P-wave. All P-waves of sinus rhythm in a 12-lead surface ECG were measured beat-by-beat. The mean values of longest PWDs in any lead obtained from two investigators were used for comparison with the histological findings. Any differences between observers were resolved by consensus.

Definitions

Criteria of interatrial conduction block

- Partial interatrial conduction block (pIAB): Partial interatrial block (pIAB) was defined as prolonged (≥ 120 ms) and bimodal (notched) P-wave in any lead on the standard 12-lead ECG [15–17].
- Advanced interatrial conduction block (aIAB): interatrial block is seen on the surface ECG as a wide (≥ 120 ms) and biphasic P-wave in the inferior leads [17].

Criteria of left atrial abnormality

- P-wave terminal force (PTF): defined as the product of duration (D) and amplitude (A) of the P-wave terminal phase in lead V1; $PTF > 0.04$ mV \times ms has been

found to be a specific but less sensitive ECG marker of left atrial enlargement [18,19].

Tissue sample collection and handling

Transmural atrial tissue samples of at least 20 mm \times 3 mm were collected from 5 locations that included major atrial conduction pathways and the posterior left atrial (LA) region in the vicinity of pulmonary vein ostia. The sites were as follows: crista terminalis (CT) at the right atrium lateral wall; Bachmann's bundle (BB) from the superior portion of the interatrial groove between the atria; posterior LA wall at the superior pulmonary vein (SPV) level; centrally between the pulmonary vein ostia (posterior left atrial [PLA] wall); and at inferior pulmonary veins (IPV) level.

Atrial tissue samples were fixed in 10% buffered formalin and embedded in paraffin. Sections (2 μ m thick) were cut parallel to the atrial wall plane and stained with Masson's trichrome stain.

Specimens were examined with computer-assisted morphometric analysis using the Leica LAS Image Analysis System (LeicaQWin Plus v3, Leica Microsystems Imaging Solutions, Cambridge, United Kingdom). The percentage of fatty infiltration, interstitial fibrosis, capillary density, and mean cardiomyocyte diameter from within each sample were assessed at $\times 200$ magnification and calculated at 10 fields of view by a single investigator blinded to clinical and demographic data. Epicardial, endocardial, and perivascular fibrosis were excluded in assessing fibrosis percentage. A mean of the 10 measurements for each parameter per location was used for further analysis.

Statistical analyses

Data are expressed as the median and range. All statistical analyses were performed using IBM SPSS Statistics, version 20.0.0 (SPSS, Chicago, IL). A two-independent-sample test (Mann–Whitney test) was used for 2-group comparisons. No correction for multiple testing was applied. Spearman's correlation coefficient was calculated for analyzing correlation between quantified histological variables and PWD. All data without normal distribution were tested using non-parametric tests. All tests were 2-sided, and a p of < 0.05 was considered statistically significant.

Results

Patient characteristics

Clinical characteristics of subjects are presented in Table 1. Median age was 73 years (range 54–82 years). All patients died of cardiovascular causes such as acute myocardial infarction ($n = 9$) and pulmonary embolism ($n = 2$) verified by autopsy. There was no difference with regard to the presence of ischemic heart disease, hypertension, stroke, chronic obstructive pulmonary disease, diabetes mellitus, or aortic or mitral valve pathology between patients with AF history and without AF history. The extent of fibrosis, fatty infiltration, capillary density and cardiomyocyte size did not differ among the 5 sampling locations in the atria, in either total material or in subgroup analysis (data not shown).

Table 1
Patients' characteristics.

ID	Gender	Age (year)	COD	HTN	CHF	DM	AF	Stroke	LVEF %	LAD (mm)
1	M	73	AMI	-	+	-	-	-	27	48
2	M	54	AMI	+	+	-	-	+	44	37
3	M	62	AMI	+	+	+	-	-	17	-
4	M	72	AMI	+	+	-	-	-	-	-
5	M	82	AMI	+	+	-	-	-	-	-
6	F	77	AMI	+	+	-	-	-	61	42
7	M	69	AMI	+	+	+	-	-	42	40
8	F	73	AMI	+	+	-	+	+	30	50
9	F	73	AMI	+	+	-	+	-	34	34
10	M	74	PE	+	+	-	+	-	61	42
11	F	72	PE	+	+	-	+	-	-	-

PE: pulmonary embolism. AMI: acute myocardial infarction. COD: cause of death. CHF: chronic heart failure. M: male. F: female. HTN: hypertension. DM: diabetes mellitus. AF: atrial fibrillation. LAD: left atrial diameter. LVEF: left ventricular ejection fraction.

P-wave terminal force vs. site-dependent histological abnormalities in LA

The P-waves in 8 out of 11 subjects had abnormal PTF (> 0.04 mV × ms). There was no significant difference between subjects with and without abnormal PTF with regard to their clinical or demographical characteristics. The extent of fibrosis, fatty infiltration or the combination of fibrosis and fatty tissue did not differ in the 5 sampling locations in the atria, regardless of abnormal PTF (Table 3). There is no significant difference in the absolute value of PTF between subjects with AF and without AF (0.06, 0.04–0.09 mV × ms vs. 0.06, 0.03–0.30 mV × ms; p = 0.648). There is no correlation between the absolute value of PTF and the extent of fibrosis, fatty infiltration, or the combination of fibrosis and fatty tissue in all 5 sampling locations.

PWD vs. site-dependent histological abnormalities (Table 2)

The median PWD was 160 ms (range 120–200 ms). The fibrosis extent in CT, SPV and IPV was higher in patients with longer PWD (PWD > 160 ms) as compared to patients with shorter PWD. Moreover, the combination of fibrosis extent and fatty tissue in CT, BB and SPV was greater in the group with longer PWD (PWD > 160 ms) as compared to the group with shorter PWD. The average of fibrosis extent or the combination of fibrosis extent and fatty tissue was also significantly greater in the group with longer PWD.

Correlation between PWD and histological variables was assessed at all 5 locations as well as for the mean value of these 5 locations. The fibrosis extent in CT highly correlated to PWD (r = 0.914, p < 0.001). The combination of fibrosis extent and fatty tissue in BB (16%, range 1%–41%), CT (18%, range 3%–47%) or SPV (15%, range 6%–24%) correlated to PWD (r = 0.627, p = 0.039; r = 0.795, p = 0.003; and r = 0.668, p = 0.025, respectively). The average of fibrosis extent or combination of fibrosis extent and fatty tissue at these 5 locations also correlated to PWD (r = 0.747, p = 0.008; r = 0.664, p = 0.026, respectively).

P-wave morphology of partial interatrial conduction block vs. site-dependent histological abnormalities

None of the observed P-wave morphologies fulfilled the criteria of advanced interatrial conduction block. Ten out of 11 subjects had the special P-wave morphology that meets the partial interatrial conduction block criteria. The extent of fibrosis, fatty infiltration or the combination of fibrosis extent and fatty tissue did not differ between subjects with notches in inferior leads only (n = 4) and notches in both inferior leads and lateral leads (n = 4 vs. n = 5, all p = 0.798), in either the 5 sampling locations in the atria, or in the average of total 5 sampling locations analysis. However, the only subject who had normal P-wave morphology without pIAB pattern also had the most extensive fibrosis in atrial walls, approaching 40% at CT sampling location (Fig. 1b).

Discussion

Main finding

In post-mortem atrial tissues from patients who died of cardiovascular causes, the extent of fibrosis and fatty infiltration was strongly associated with PWD, especially in major atrial conduction routes such as BB and CT, thus suggesting a causal relationship between atrial structural abnormalities and prolongation of atrial depolarization during sinus rhythm.

Table 2
PWD vs. site-dependent histological abnormalities.

Location	PWD < =160 ms (n = 6)	PWD > 160 ms (n = 5)	P-value
CT			
Fibrosis extent	6.0% (2.4%–9.4%)	19.0% (17.0%–40%)	0.004**
Fatty infiltration	2.1% (0.5%–13.6%)	9.0% (7.0%–17.0%)	0.052
Fibrosis–fatty infiltration	10.1% (3.4%–18.4%)	28.0% (26.0%–47.0%)	0.004**
BB			
Fibrosis extent	7.2% (1.0%–12.3%)	15.0% (3.7%–26.0%)	0.082
Fatty infiltration	3.5% (0%–6.6%)	8.4% (7.0%–15.0%)	0.004**
Fibrosis–fatty infiltration	9.4% (1.0%–16.8%)	23.4% (10.7%–41.0%)	0.017*
Level of superior PVs			
Fibrosis extent	4.6% (1.9%–12.4%)	12.0% (6.0%–20%)	0.030*
Fatty infiltration	4.7% (0%–6.6%)	6.0% (0%–17.0%)	0.537
Fibrosis–fatty infiltration	8.8% (5.8%–14.7%)	20% (18.0%–24.0%)	0.004**
Center of posterior wall in LA			
Fibrosis extent	4.9% (2.5%–8.0%)	17.0% (0.7%–20.0%)	0.126
Fatty infiltration	3.3% (0%–4.7%)	4.0% (0%–6.4%)	0.931
Fibrosis–fatty infiltration	9.3% (3.8%–12.4%)	21.0% (0.7%–22.2%)	0.126
Level of inferior PVs			
Fibrosis extent	4.0% (1.3%–9.2%)	12.8% (5.6%–20.6%)	0.017*
Fatty infiltration	5.4% (0%–13.9%)	3.8% (0%–20.7%)	0.931
Fibrosis–fatty infiltration	9.3% (1.3%–18.7%)	21.0% (5.6%–41.3%)	0.247
Global atria (average of 5 locations)			
Fibrosis extent	5.0% (3.6%–8.3%)	15.6% (9.4%–24.8%)	0.004**
Fatty infiltration	4.5% (0.1%–7.6%)	9.2% (3.2%–11.4%)	0.082
Fibrosis–fatty infiltration	8.7% (5.2%–15.9%)	26.6% (12.6%–30.4%)	0.009**

* A p-value of < 0.05.
** A p-value of < 0.01.



Fig. 1. P-wave Morphology on standard 12-lead ECG vs. histological atrial abnormality. A. Notched P-wave (bimodal) in a subject with normal histological findings in atria. B. Normal P-wave morphology (with prolonged P-wave duration) in a subject with abnormal histological findings in atria.

P-wave duration vs. site-dependent atrial histological abnormalities

BB has been mainly described as the most important preferential interatrial conduction pathway during sinus rhythm in human and animal studies [20–24]. An impaired

conductive property of BB has been assumed to be an important cause for prolongation of P-wave duration. In 1983, Scott et al. reported a trend for a percentage of fibrosis in left atrial appendage and PWD in lead II, but not amplitude of P-wave in patients with valvular disease who underwent open-heart surgery [25]. In this study, the PWD

Table 3
PTF vs. site-dependent histological abnormalities.

Location	PTF <= 0.04 mV*ms (n = 3)	PTF > 0.04 mV*ms (n = 8)	P-value
CT			
Fibrosis	2.9% (2.4%–20.0%)	13.2% (4.8%–40.0%)	0.376
Fatty infiltration	1.2% (0.5%–17.0%)	8.0% (0.6%–13.6%)	0.630
Fibrosis–fatty infiltration	3.6% (3.4%–37.0%)	22.2% (10.0%–47.0%)	0.376
BB			
Fibrosis	8.0% (3.2%–22.0%)	10.7% (1.0%–26.0%)	0.921
Fatty infiltration	3.4% (1.0%–7.0%)	6.8% (0%–15.0%)	0.279
Fibrosis–fatty infiltration	9.0% (6.6%–29.0%)	16.4% (1.0%–41.0%)	0.630
Level of superior PVs			
Fibrosis	4.4% (3.6%–6.0%)	9.5% (1.9%–20.0%)	0.194
Fatty infiltration	6.6% (3.9%–13.3%)	3.9% (0%–17.0%)	0.279
Fibrosis–fatty infiltration	11.0% (7.5%–19.3%)	16.4% (5.8%–24.0%)	0.776
Center of posterior wall in LA			
Fibrosis Extent	5.0% (2.5%–17.0%)	7.5% (0.7%–20.0%)	0.776
Fatty infiltration	4.0% (1.3%–7.4%)	3.3% (0%–7.3%)	0.630
Fibrosis–fatty infiltration	12.4% (3.8%–21.0%)	10.7% (0.7%–22.2%)	1.000
Level of inferior PVs			
Fibrosis	5.5% (3.1%–12.8%)	5.6% (1.3%–20.6%)	0.921
Fatty infiltration	6.3% (2.8%–15.7%)	4.6% (0%–20.7%)	0.497
Fibrosis–fatty infiltration	11.8% (5.9%–28.5%)	12.0% (1.3%–41.3%)	0.921
Global atria (average of 5 locations)			
Fibrosis extent	4.5% (3.6%–15.6%)	8.8% (4.9%–24.8%)	0.279
Fatty infiltration	4.3% (2.6%–11.4%)	5.6% (0.1%–9.9%)	0.921
Fibrosis–fatty infiltration	7.9% (7.1%–27.0%)	14.2% (5.2%–30.4%)	0.630

mostly correlated to the fibrosis extent at the site of CT. It could be explained by CT's major role on intraatrial conduction in the right atrium during sinus rhythm.

Except BB and CT, the baseline PWD also highly correlated with the combined count of fibrosis and fatty tissue extent at the site of LA posterior wall of superior PV level, which might link to its anatomical origin. In previous anatomical studies, the posterior wall of LA at the superior PV level was shown to be covered by extensions from the BB epicardially [26–28].

P-wave terminal force and site-dependent atrial histological abnormalities

Previous studies have suggested that PTF is a predictor of LA enlargement with low sensitivity [18,19,29]. Later, PTF was considered to be part of the definition of LA-abnormality [30,31]. In this study, we could find no association between the histological findings and the left atrial abnormality pattern.

Limitation

We are aware of the limitations in our study, such as manual measurements of P-wave characteristics, the limited number of observations, and retrospective assessment of clinical characteristics. In particular, the limited number of subjects included in the study urges to caution in interpreting negative findings observed for some of the tested associations. However, to the best of our knowledge, no prior study has been able to evaluate the associations between P-wave appearance on surface ECG and structural characteristics of atrial walls, including major atrial conduction routes.

Conclusion

In *post-mortem* atrial tissues from patients who died of cardiovascular causes, the extent of fibrosis and fatty infiltration demonstrated strong association with PWD, which was particularly apparent for the major atrial conduction routes such as Bachmann's bundle and terminal crest. This suggests that fibrosis–fatty infiltration of BB and CT may play a major role of inter- and intra-atrial conduction on prolongation of PWD.

Conflict of interest disclosures

None.

Funding sources: The study was supported by the Swedish Heart-Lung Foundation and donation funds at the Skåne University Hospital, Lund, Sweden.

References

- [1] Evans R, Shaw DB. Pathological studies in sinoatrial disorder (sick sinus syndrome). *Br Heart J* 1977;39:778–86.
- [2] Platonov PG, Mitrofanova LB, Orshanskaya V, Ho SY. Structural abnormalities in atrial walls are associated with presence and persistency of atrial fibrillation but not with age. *J Am Coll Cardiol* 2011;58:2225–32.
- [3] Marconi P, Castelli G, Montereggi A, Marioni C. A "signal averaging" analysis of the p wave in patients with a history of isolated paroxysmal atrial fibrillation. *G Ital Cardiol* 1991;21:1075–81.
- [4] Falk RH, Pollak A. Signal-averaged p wave duration and atrial fibrillation. *J Am Coll Cardiol* 1994;23:549–50.
- [5] Raitt MH, Ingram KD, Thurman SM. Signal-averaged p wave duration predicts early recurrence of atrial fibrillation after cardioversion. *Pacing Clin Electrophysiol* 2000;23:259–65.
- [6] Bachman S, Sparrow D, Smith LK. Effect of aging on the electrocardiogram. *Am J Cardiol* 1981;48:513–6.

- [7] Stafford PJ, Turner I, Vincent R. Quantitative analysis of signal-averaged p waves in idiopathic paroxysmal atrial fibrillation. *Am J Cardiol* 1991;68:751–5.
- [8] Havmoller R, Carlson J, Holmqvist F, Herreros A, Meurling CJ, Olsson B, et al. Age-related changes in p wave morphology in healthy subjects. *BMC Cardiovasc Disord* 2007;7:22.
- [9] Holmqvist F, Platonov PG, McNitt S, Polonsky S, Carlson J, Zareba W, et al. Abnormal p-wave morphology is a predictor of atrial fibrillation development and cardiac death in madit ii patients. *Ann Noninvasive Electrocardiol* 2010;15:63–72.
- [10] Frustaci A, Chimenti C, Bellocci F, Morgante E, Russo MA, Maseri A. Histological substrate of atrial biopsies in patients with lone atrial fibrillation. *Circulation* 1997;96:1180–4.
- [11] Nguyen BL, Fishbein MC, Chen LS, Chen PS, Masroor S. Histopathological substrate for chronic atrial fibrillation in humans. *Heart Rhythm* 2009;6:454–60.
- [12] Dilaveris PE, Gialafos EJ, Sideris SK, Theopistou AM, Andrikopoulos GK, Kyriakidis M, et al. Simple electrocardiographic markers for the prediction of paroxysmal idiopathic atrial fibrillation. *Am Heart J* 1998;135:733–8.
- [13] Weber UK, Osswald S, Huber M, Buser P, Skarvan K, Stulz P, et al. Selective versus non-selective antiarrhythmic approach for prevention of atrial fibrillation after coronary surgery: is there a need for pre-operative risk stratification? A prospective placebo-controlled study using low-dose sotalol. *Eur Heart J* 1998;19:794–800.
- [14] Steinberg JS, Zelenkofske S, Wong SC, Gelernt M, Sciacca R, Menchavez E. Value of the p-wave signal-averaged ECG for predicting atrial fibrillation after cardiac surgery. *Circulation* 1993;88:2618–22.
- [15] Husson J. Partial interatrial block. *Arch Mal Coeur Vaiss* 1983;76:959–63.
- [16] Bayes de Luna A, Oter MC, Guindo J. Interatrial conduction block with retrograde activation of the left atrium and paroxysmal supraventricular tachyarrhythmias: influence of preventive antiarrhythmic treatment. *Int J Cardiol* 1989;22:147–50.
- [17] Bayes de Luna A, Cladellas M, Oter R, Torner P, Guindo J, Marti V, et al. Interatrial conduction block and retrograde activation of the left atrium and paroxysmal supraventricular tachyarrhythmia. *Eur Heart J* 1988;9:1112–8.
- [18] Waggoner AD, Adyanthaya AV, Quinones MA, Alexander JK. Left atrial enlargement. Echocardiographic assessment of electrocardiographic criteria. *Circulation* 1976;54:553–7.
- [19] Munuswamy K, Alpert MA, Martin RH, Whiting RB, Mechlin NJ. Sensitivity and specificity of commonly used electrocardiographic criteria for left atrial enlargement determined by m-mode echocardiography. *Am J Cardiol* 1984;53:829–32.
- [20] Waldo AL, Vitikainen KJ, Hoffman BF. The sequence of retrograde atrial activation in the canine heart. Correlation with positive and negative retrograde p waves. *Circ Res* 1975;37:156–63.
- [21] Bailin SJ, Adler S, Giudici M. Prevention of chronic atrial fibrillation by pacing in the region of Bachmann's bundle: results of a multicenter randomized trial. *J Cardiovasc Electrophysiol* 2001;12:912–7.
- [22] Dolber PC, Spach MS. Structure of canine Bachmann's bundle related to propagation of excitation. *Am J Physiol* 1989;257:H1446–57.
- [23] Lemery R. Bi-atrial mapping of atrial arrhythmias. *Card Electrophysiol Rev* 2002;6:378–82.
- [24] Lemery R, Soucie L, Martin B, Tang AS, Green M, Healey J. Human study of biatrial electrical coupling: determinants of endocardial septal activation and conduction over interatrial connections. *Circulation* 2004;110:2083–9.
- [25] Scott CC, Leier CV, Kilman JW, Vasko JS, Unverferth DV. The effect of left atrial histology and dimension on p wave morphology. *J Electrocardiol* 1983;16:363–6.
- [26] Ho SY, Anderson RH, Sanchez-Quintana D. Atrial structure and fibres: morphologic bases of atrial conduction. *Cardiovasc Res* 2002;54:325–36.
- [27] Ho SY, Sanchez-Quintana D. The importance of atrial structure and fibers. *Clin Anat* 2009;22:52–63.
- [28] Platonov PG, Mitrofanova L, Ivanov V, Ho SY. Substrates for intra-atrial and interatrial conduction in the atrial septum: anatomical study on 84 human hearts. *Heart Rhythm* 2008;5:1189–95.
- [29] Koehler NR, Velho FJ, Collar IC, Zouvi JP, Behr PB. Left arterial overload. Electro-echocardiographic correlations. *Arq Bras Cardiol* 1993;60:247–51.
- [30] Pohjola S, Siltanen P, Romo M. The prognostic value of the p wave morphology in the discharge ECG in a 5-year follow-up study after myocardial infarction. *Am Heart J* 1979;98:32–8.
- [31] Alpert MA, Munuswamy K. Electrocardiographic diagnosis of left atrial enlargement. *Arch Intern Med* 1989;149:1161–5.

Paper II

Effects of baseline P-wave duration and choice of atrial septal pacing site on shortening atrial activation time during pacing

Yan Huo^{1,3*}, Fredrik Holmqvist^{1,2}, Jonas Carlson¹, Thomas Gaspar³, Arash Arya³, Ulrike Wetzel³, Gerhard Hindricks³, Christopher Piorkowski³, Andreas Bollmann³, and Pyotr G. Platonov^{1,2}

¹Department of Cardiology and Center for Integrative Electrophysiology at Lund University (CIEL), Lund University, SE-221 85 Lund, Sweden; ²Arrhythmia Clinic, Skåne University Hospital, Lund, Sweden; and ³Department of Electrophysiology, Leipzig Heart Center, Leipzig University, Leipzig, Germany

Received 21 October 2011; accepted after revision 21 February 2012; online publish-ahead-of-print 21 March 2012

Background

Atrial septal pacing (ASP) has been shown to shorten P-wave duration (PWD) and reduce recurrence of atrial fibrillation (AF) in patients with bradyarrhythmias. However, variability of interatrial connections and atrial conduction properties may explain ASP's modest clinical benefit. The aim of this study was to assess the effect of ASP site on the duration of the paced P wave.

Methods and results

Atrial septal pacing at high atrial septum (HAS), posterior septum behind the fossa ovalis (PSFO), and coronary sinus ostium (CSo) was performed in 69 patients admitted for electrophysiological study (52 ± 16 years, 41 men). Twelve-lead electrocardiogram was recorded at baseline and during pacing, signal-averaged for analysis of PWD and P-wave shortening achieved by ASP (Δ PWD = paced PWD-baseline PWD). Baseline PWD was 128 ± 15 ms. The shortest PWD during pacing was achieved at CSo (112 ± 15 ms) followed by HAS (122 ± 14 ms, $P < 0.001$ vs. CSo) and PSFO (124 ± 21 ms, $P < 0.001$ vs. CSo). P wave was shortened during pacing in patients with baseline PWD of > 120 ms ($n = 50$), whereas those with PWD of ≤ 120 ms showed PWD lengthening ($n = 19$) when paced at HAS (8 ± 17 vs. -12 ± 15 ms, $P < 0.001$), PSFO (15 ± 17 vs. -12 ± 26 ms, $P < 0.001$) and CSo (6 ± 16 vs. -25 ± 18 ms, $P < 0.001$).

Conclusion

Pacing at CSo is associated with the shortest PWD. P-wave shortening is greatest in patients with baseline PWD of > 120 ms regardless of the pacing site. The results may have implications on the selection of candidates for ASP and the placement of the atrial septal lead, and warrant further evaluation in cases of permanent pacing in patients with paroxysmal AF.

Keywords

Baseline P-wave duration • Atrial septal pacing • Interatrial conduction

Introduction

Permanent transvenous atrial pacing leads have traditionally been implanted in the right atrial appendage (RAA) and, occasionally, in the right atrial (RA) lateral wall. Pacing from the RAA or free wall can lead to delayed intraatrial and interatrial conduction, and may provoke electromechanical delay in the atria, leading to discoordination of right and left atrial contraction.¹ It has been suggested that dual-site RA pacing² and batrial resynchronization³ are

more beneficial than both high RA pacing and antiarrhythmic drug therapies, based on long-term follow-up, with regard to atrial fibrillation (AF) prevention. Electrophysiological studies⁴ have suggested that the reduction in atrial conduction delay and modification of dispersion in atrial refractoriness are important mechanisms in AF prevention, which can be achieved by multisite atrial pacing. Similar results can be achieved by single-site atrial pacing that does not require any special implantable device. The optimal pacing site for the prevention of paroxysmal atrial

* Corresponding author. Tel: +46 46 172435; fax: +46 46 157857; Email: dr.huoyan@googlemail.com

Published on behalf of the European Society of Cardiology. All rights reserved. © The Author 2012. For permissions please email: journals.permissions@oup.com.

fibrillation (PAF) using single-site pacing is suggested to be the atrial septum;^{5–8} however, no detailed studies have been carried out on the electrophysiological properties regarding the shortening of P-wave duration (PVD) with respect to pacing site. Previous anatomical studies have identified three major pathways responsible for interatrial conduction, i.e. Bachmann's bundle (BB),⁹ the posterior fibres behind the fossa ovalis (FO),¹⁰ and the coronary sinus (CS).¹¹ As recently shown in an extensive study,¹⁰ interatrial bundles are not limited to the anteriorly located BB, but are present in all parts of the interatrial septum, both posteriorly between the right pulmonary veins and inferiorly between the CS and the right inferior pulmonary vein. Moreover, in some hearts, the inferiorly located bundles can be more prominent than the BB.¹⁰ The quantity, length, and diameter of interatrial connection fibres vary considerably between individuals.^{10,12}

On the basis of the high variability of the location of interatrial connections, it is reasonable to assume that pacing at the site mainly responsible for interatrial conduction would result in a shorter-paced PWD, corresponding to the shorter global atrial activation time in that individual. The aim of this study was thus to assess the effect of different atrial septal pacing sites on P-wave shortening and to identify the pacing site associated with the shortest paced PWD.

Methods

Study group

Sixty-nine consecutive patients (aged 52 ± 16 years, range 19–79 years, 41 men) undergoing clinically motivated electrophysiological studies due to supraventricular tachycardia (SVT) were studied. All patients gave written informed consent on the investigational nature of the procedure that was approved by the institutional review committee. None of the patients showed any evidence of underlying structural heart disease as assessed by transthoracic echocardiography. All antiarrhythmic drugs were discontinued at least five half-lives before the study, and none of the patients was taking amiodarone or digitalis. In this study, the mean diameter of the left atrium (LA) was 39 ± 6 mm; and 25 patients (36%) had an enlarged (>40 mm) LA (44 ± 4 mm).

Twenty-one of the 69 patients (30%) had a history of PAF. Twelve of the 21 patients had received flecainide by the 'pill-in-the-pocket' approach whereas nine patients had uncommon arrhythmia episodes and were off medications. None of PAF patients was treated with pulmonary vein isolation either before or during index admission. Before electrophysiological study, these patients with PAF had been suspected as carriers of other SVTs with atypical AF-related symptom, such as atrioventricular nodal reentrant tachycardia (AVNRT). Ten patients (14%) had a history of typical atrial flutter. Fourteen patients (20%) were found to have inducible AVNRT, and three patients (4%) had a left-sided accessory pathway. In the rest of the patients (26 patients, 38%) it was not possible to induce tachycardia during the electrophysiological studies. Radiofrequency catheter ablation was successful in the patients with induced SVT.

Fluoroscopy-guided catheter positioning and stimulation position

Firstly, a 6F, steerable 2-5-2 mm-spaced, 1 mm-tip decapolar electrode catheter was advanced into the superior vena cava. The catheter was

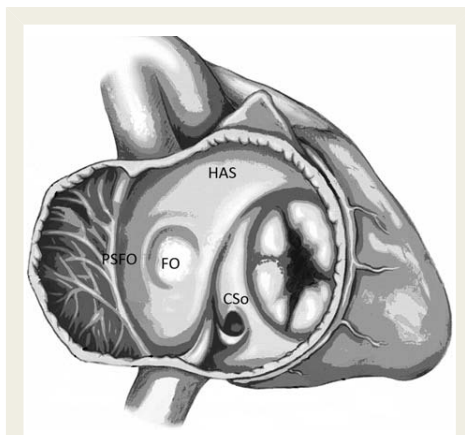


Figure 1 Schematic Diagram: Illustration showing pacing sites. HAS, high atrial septum; PSFO, posterior septum behind fossa ovalis; CSo, coronary sinus ostium; FO, fossa ovalis.

torqued towards the atrial septum. Under fluoroscopic guidance (left anterior oblique, LAO 60° and right anterior oblique, RAO 12°), the catheter was pulled caudally to watch for the tip to 'jump' under the aortic knob. This position was considered as high RA septum in the vicinity of the BB incision (high atrial septum, HAS). Posteroseptal position was achieved by pulling the catheter further down until the second 'jump' under the muscular atrial septum onto the FO, which was in the same height as the His bundle catheter, and clockwise rotation so that the catheter tip pointed posteriorly in the RAO projection and in the LAO projection the direction of the catheter tip should still face to the septum. This position was as the posterior septum behind the FO (PSFO). Finally, the catheter was placed into CS and pulled back until its distal bipolar electrodes were located at CS ostium (CSo). Other standard electrode catheters were positioned at the His bundle and in the right ventricular apex to serve as conventional fluoroscopic landmarks (Figure 1).

Stimulation parameters and protocol

The distal electrode pairs of the decapolar catheters were used for bipolar stimulation. The stimulus output had a fixed pulse width of 1 ms, and the threshold was set at twice the diastolic threshold. The threshold values ranged from 2 to 5 V for HAS, PSFO, and CSo stimulation. Particular care was taken to ensure continuous capture of the atrial tissue when threshold values were determined. Pacing was performed at each pacing site at fixed cycle lengths, defined by the longest interval (started at 600 ms, 4 patients at 550 ms and 65 patients at 600 ms) without the P-wave merging with the T wave.

Data acquisition and P-wave analysis

Standard 12-lead electrocardiogram (ECG) was recorded using the Prucka CardioLab System (GE Medical Systems, Milwaukee, WI, USA) for at least 30 s at baseline and continuously during pacing. These 12-lead ECGs were transformed to orthogonal leads and signal-averaged P-wave analysis was performed to estimate the

P-wave duration. These data were stored for subsequent offline processing. Data analysis was performed using custom-made software running on MATLAB (The MathWorks, Natick, MA, USA). The basic method used is described in detail elsewhere.^{13,14} The onset and end of the P wave were set manually on a magnified signal-averaged P wave on a computer screen using electronic calipers. In order to ensure unbiased manual settings of P wave onset and end, all recordings were analysed in one batch in a blinded manner so that only computer-generated record number was available at the time of analysis without possibility to establish a link between the ECG recordings, pacing sites, and patient identity. The onset of the paced P wave was defined as being directly after the end of the stimulation spike.

Statistics

All data with normal distribution are expressed as mean \pm SD. Data without normal distribution are expressed as median. The distributions of samples were tested using the Shapiro–Wilk test. Inter-group comparisons were performed using the paired samples *t* test. Multiple group comparisons (three groups) were performed by one-way analysis of variance (ANOVA) for continuous variables, followed by a *post hoc* analysis if the ANOVA test was significant. Possible correlations among pacing sites, baseline PWDs, and shortenings of PWDs were tested using the Pearson correlation test. Data without normal distribution were tested using a non-parametric test. A *P* value of < 0.05 was considered significant.

Results

The PWD was significantly shorter when pacing at the CSo (112 ± 15 ms) than when pacing at the HAS (121 ± 14 ms, $P < 0.001$) or the PSFO (124 ± 21 ms, $P < 0.001$), and was also significantly shorter than the baseline PWD (during sinus rhythm, SR) (128 ± 15 ms, $P < 0.001$). The PWD when pacing at the

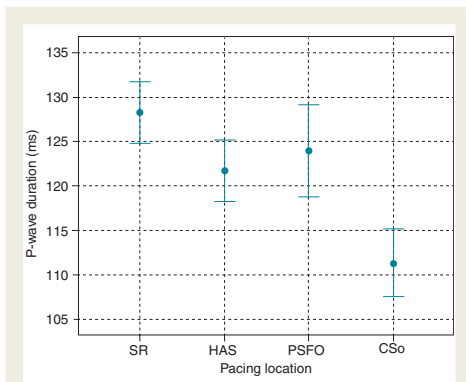


Figure 2 Mean P-wave duration (\pm SD) at baseline (sinus rhythm) and when paced at different sites in the 69 patients studied. SR, sinus rhythm; HAS, high atrial septum; PSFO, posterior septum of fossa ovalis; CSo, coronary sinus ostium.

HAS was also significantly shorter than the PWD during SR ($P = 0.003$), but not significantly shorter than the PWD paced at PSFO ($P = 0.274$) (Figure 2).

The shortening of the PWD (Δ PWD) at each pacing site was defined as the difference between the paced and the baseline values (Δ PWD = paced PWD–baseline PWD). There was a negative linear correlation between Δ PWD and baseline PWD ($R = -0.64, -0.63$ and -0.72 for HAS, PSFO, and CSo pacing, respectively, $P < 0.001$ for all sites) (Figure 3) with longer P waves at baseline showing a greater shortening during pacing.

Normal P-wave duration vs. prolonged P-wave duration at baseline

Nineteen of the 69 patients had normal PWDs (≤ 120 ms) at baseline. Regardless of the pacing site, atrial septal pacing resulted mostly in P-wave shortening in patients with baseline PWD of > 120 ms, and P-wave prolongation in patients with normal PWD (Figure 3). Differences in Δ PWD between patients with PWD of ≤ 120 ms and > 120 ms were significant at all pacing sites: HAS, 8 ± 17 vs. -12 ± 15 ms ($P < 0.001$), PSFO, 15 ± 17 vs. -12 ± 26 ms ($P < 0.001$) and CSo, 6 ± 16 vs. -25 ± 18 ms ($P < 0.001$) (Figure 4).

When paced PWD was compared between patients with baseline PWD of > 120 ms and baseline PWD of ≤ 120 ms, there was no statistically significant difference regardless of the pacing site. Patients with baseline PWD of > 120 ms had shorter paced PWDs compared with baseline, regardless of pacing sites. Pacing at CSo resulted in a significantly shorter PWD than pacing at HAS or PSFO, but there was no significant difference between the paced PWD at HAS and PSFO. However, in patients with baseline PWD of ≤ 120 ms pacing at PSFO or CSo resulted in a significant prolongation of PWD compared with the baseline. In this group, PWD during HAS pacing was similar to baseline, whereas no difference in PWD was observed between all three septal pacing sites (Table 1).

Normal left atrium vs. enlarged left atrium

When PWD was compared between patients with enlarged vs. normal LA, there was no difference at baseline, but patients with enlarged LA had a longer paced PWD during HAS or PSFO pacing than patients with normal LA. Pacing at CSo, however, was not associated with any difference in paced PWD between patients with enlarged or normal LA (Table 1).

When site-related effects of septal pacing were analysed separately in the subgroup of patients with enlarged LA (median 43 mm, 41–52 mm, $n = 25$), the paced PWD was significantly shorter than baseline PWD during CSo pacing while no significant difference was observed during pacing at HAS or PSFO. The paced PWD during CSo pacing was also significantly shorter than paced PWD at HAS or PSFO. In a subgroup of patients with normal LA (median 38 mm, 23–40 mm, $n = 44$), paced PWDs were significantly shorter than the baseline PWD during septal pacing, regardless of pacing site. The paced PWD during CSo pacing was also significantly shorter than the paced PWD at HAS or

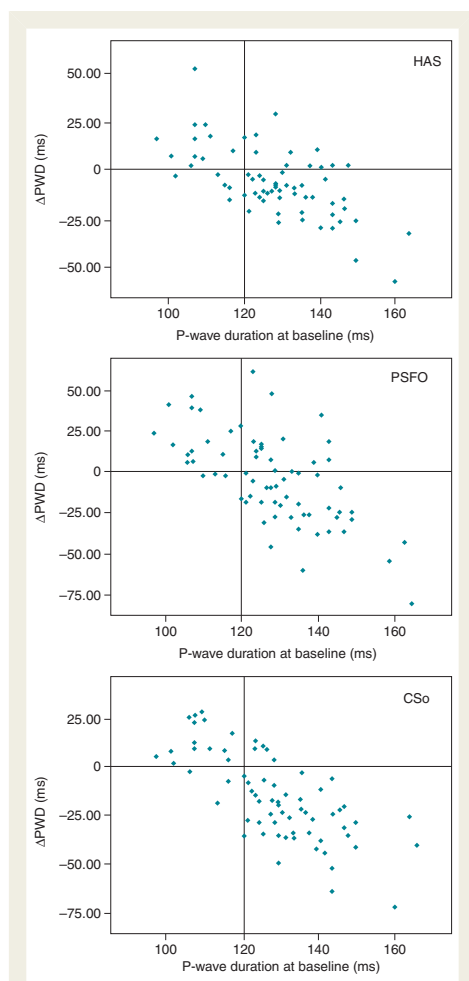


Figure 3 Scatter plot of Δ PWD at three different pacing sites. There were linear correlations between Δ PWD at different pacing sites and the baseline P-wave duration (sinus rhythm) in the group of 69 patients. P-wave shortening (negative Δ PWD) was observed in patients with baseline P-wave duration of >120 ms, whereas patients with normal P-wave duration at baseline mostly presented with lengthening of pace P-wave duration (positive Δ PWD) regardless of pacing site. HAS, high atrial septum; PSFO, posterior septum behind the fossa ovalis; CSO, coronary sinus ostium; PWD, P-wave duration.

PSFO in the subgroup of patients with normal LA. There was no statistically significant difference with regard to the paced PWD during HAS and PSFO (Table 1).

History of paroxysmal atrial fibrillation

When PWD was compared between patients with PAF ($n = 21$) and without a history of AF ($n = 48$), it did not differ either at baseline or during pacing (Table 1). However, the LA diameter in patients with PAF (42 mm, range 25–52 mm) was significantly greater than in patients without a history of PAF (39 mm, range 23–49, $P = 0.012$).

When site-related effects of septal pacing were analysed separately in a subgroup of patients without a history of PAF, paced PWDs appeared to be significantly shorter than the baseline PWD, regardless of pacing sites. The paced PWD during CSO pacing was also significantly shorter than the paced PWD at HAS or PSFO. There was no statistically significant difference between the paced PWDs during HAS and PSFO. In a subgroup of patients with PAF, paced PWDs appeared to be significantly shorter than the baseline PWD only during CSO pacing. The paced PWD during CSO pacing was also significantly shorter than the paced PWD at PSFO. There was no statistically significant difference between the paced PWDs during HAS and PSFO either (Table 1).

Discussion

Main findings

Our results indicate that pacing at any of the septal pacing sites investigated (HAS, PSFO, or CSO) results in a P-wave shortening only if the baseline PWD exceeds 120 ms. HAS and CSO pacing leads to significantly reduced PWDs compared with the baseline. The maximal shortening of PWD is associated with CSO pacing and is particularly prominent in patients with left atrial enlargement. Atrial septal pacing in patients with baseline PWD of ≤ 120 ms does not result in P-wave shortening and, on the contrary, is likely to result in P-wave prolongation.

Properties of interatrial conduction pathways

Our current understanding of preferential interatrial conduction pathways is based mainly on anatomical studies^{9,10,15} and electrophysiological examinations using three-dimensional (3D) electro-anatomic or non-contact mapping during SR.^{16–19} The different modes of intra-atrial and interatrial activation have been demonstrated to follow preferential pathways located high in the RA septum (BB), posteriorly in the intercalval area, and inferiorly in the vicinity of the CSO.^{11,20–24} In previous anatomical and radiological studies, BB has been detected in about 90% of specimens in large studies, and also in large groups of patients without heart disease, studied by spiral computed tomography,^{10,25} and has been suggested as a region of fast conduction by results of both experimental and human studies.^{20–22,26} Extension of RA myocardial sleeves on the CS, with distinct connections to the left atrial myocardium, is commonly observed.²⁷ It has been demonstrated that the CS musculature is electrically connected to the RA and LA, and forms an RA–LA connection in canine hearts²³ and in human hearts,¹¹ which provides further evidence supporting the existence of a preferential pathway for interatrial conduction near the CSO. Specifically, a single RA breakthrough

has been identified around the CSo during distal CS pacing in all patients studied.²⁴ Furthermore, Ho et al.⁹ have described small muscle bridges connecting the LA posterior wall near the ostia of the right-sided pulmonary veins to the RA posterior wall at the intercaval area in human hearts. The function of these

posterior interatrial connections has also been confirmed by mapping the RA during atrial tachycardia originating from pulmonary veins,²⁸ in which the RA breakthrough was identified in the posterior intercaval area.

During SR, the preferential interatrial conduction does not seem to be linked to a certain anatomical structure, but rather seems to depend on both the origin of the RA activation²⁹ and the variability of interatrial connections.^{10,12,30} The employed interatrial connection during SR was suggested to occur through posterior fibres behind the FO and/or BB.^{16,31} However, during pacing in the vicinity of the CSo, it has been reported that the preferential interatrial conduction pathway was likely to be the CS musculature.^{17,23} The retrograde activation of the CS was also studied in detail. During pacing at the left superior pulmonary vein, the initial breakthrough in the RA was identified at the CSo, which suggests that propagation was through the musculature of the CS rather than through BB or the PSFO.²² In this study, pacing at the CSo led to a shorter PWD than pacing at the HAS or the PSFO. This suggests that during CSo, pacing the LA can be activated via the CS musculature and myocardial sleeves in its vicinity much faster than during HAS and PSFO pacing.

Thus, both posterior fibres behind the FO (possibly combined with BB) and the muscular sleeves surrounding the CS provide a reliable pathway for interatrial conduction. Whether the posterior fibres behind the FO, BB, or the CS are responsible for the conduction of atrial beats probably depends on the relative proximity of the source of activation to each of these pathways.

The variable effects of septal pacing on P-wave duration in similar studies

In previous studies aimed at evaluating the effects of atrial septal pacing on PWD, P-wave shortening was observed when pacing

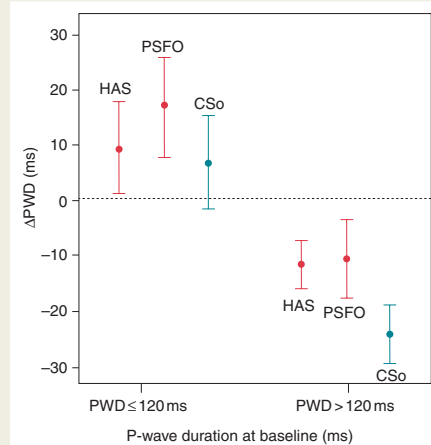


Figure 4 The change in P-wave duration when paced at three different sites, with baseline P-wave duration of ≤ 120 and > 120 ms. HAS, high atrial septum; PSFO, posterior septum of fossa ovalis; CSo, coronary sinus ostium; PWD, P-wave duration.

Table 1 Paced P-wave duration with regard to its duration at baseline, the size of the left atrium, and the history of paroxysmal atrial fibrillation

PWD (ms)	Baseline	HAS pacing	PSFO pacing	CSo pacing
Baseline PWD > 120 ms (n = 50)	133 (121–165)	121 (100–157) ^{####}	120 (77–183) ^{###}	110 (78–137) ^{###}
Baseline PWD ≤ 120 ms (n = 19)	108 (97–120)	113 (99–159)	119 (103–152) ^{##}	119 (84–137) [#]
LA diameter > 40 mm (n = 25)	128 (97–163)	125 (100–159) ^{*&}	121 (82–183) ^{*&}	116 (86–137) [#]
LA diameter ≤ 40 mm (n = 44)	129 (101–165)	117 (99–157) ^{###}	117 (77–175) ^{##}	110 (78–135) ^{###}
PAF (n = 21)	125 (97–165)	120 (102–149)	121 (85–183) [*]	111 (94–137) [#]
No history of AF (n = 48)	128 (102–163)	120 (99–159) ^{###}	118 (77–175) ^{##}	112 (78–137) ^{###}

Data presented as median (range).

[#] $P < 0.05$ in comparison with baseline PWD; ^{##} $P < 0.01$ in comparison with baseline PWD; ^{###} $P < 0.001$ in comparison with baseline PWD; ^{*} $P < 0.05$ in comparison with baseline PWD; ^{**} $P < 0.01$ in comparison with paced PWD during CSo pacing; ^{***} $P < 0.001$ in comparison with paced PWD during CSo pacing; [&] $P < 0.05$ in comparison between normal and enlarged LA.

PWD, P-wave duration; HAS, high atrial septum; PSFO, posterior septum behind the fossa ovalis; CSo, coronary sinus ostium; LA, left atrium; PAF, paroxysmal AF.

(i) *P* values (baseline PWD > 120 and ≤ 120 ms): HAS: $P = 0.108$; PSFO: $P = 0.598$; CSo: $P = 0.085$. Baseline PWD > 120 ms: (1) SR vs. HAS: $P < 0.001$; SR vs. PSFO: $P = 0.002$; SR vs. CSo: $P < 0.001$; CSo vs. HAS: $P < 0.001$; CSo vs. PSFO: $P < 0.001$; HAS vs. PSFO: $P = 0.787$. Baseline PWD ≤ 120 ms: (2) SR vs. HAS: $P = 0.083$; SR vs. PSFO: $P = 0.002$; SR vs. CSo: $P = 0.015$; CSo vs. HAS: $P = 0.777$; CSo vs. PSFO: $P = 0.164$; HAS vs. PSFO: $P = 0.116$.

(ii) *P* values (LA diameter > 40 and ≤ 40 mm): Baseline: $P = 0.817$; HAS: $P = 0.049$; PSFO: $P = 0.023$; CSo: $P = 0.253$. LA > 40 mm: (1) SR vs. HAS: $P = 0.394$; SR vs. PSFO: $P = 0.764$; SR vs. CSo: $P = 0.011$; CSo vs. HAS: $P = 0.022$; CSo vs. PSFO: $P = 0.005$; HAS vs. PSFO: $P = 0.260$. LA diameter ≤ 40 mm: (2) SR vs. HAS: $P = 0.001$; SR vs. PSFO: $P = 0.019$; SR vs. CSo: $P < 0.001$; CSo vs. HAS: $P = 0.001$; CSo vs. PSFO: $P = 0.006$; HAS vs. PSFO: $P = 0.664$.

(iii) *P* values (PAF and non-PAF): Baseline: $P = 0.720$; HAS: $P = 0.851$; PSFO: $P = 0.229$; CSo: $P = 0.518$. PAF: (1) SR vs. HAS: $P = 0.537$; SR vs. PSFO: $P = 0.917$; SR vs. CSo: $P = 0.016$; CSo vs. HAS: $P = 0.122$; CSo vs. PSFO: $P = 0.023$; HAS vs. PSFO: $P = 0.133$. Non-PAF: (2) SR vs. HAS: $P = 0.002$; SR vs. PSFO: $P = 0.043$; SR vs. CSo: $P < 0.001$; CSo vs. HAS: $P < 0.001$; CSo vs. PSFO: $P = 0.001$; HAS vs. PSFO: $P = 0.909$.

BB^{32–35} and the CSo/triangle of Koch.^{36–38} There may be several explanations of the considerable variation in septal pacing effects on P-wave shortening. The first explanation is related to clinical characteristics of study subjects, such as history of AF, burden or type of AF, size of atria, etc.^{34,39} For example, Lewicka-Nowak *et al.*⁴⁰ reported a specific group of patients with extremely prolonged P waves (145 ± 17 ms), symptomatic of documented recurrent AF. Pacing at BB or the CSo did not lead to significantly shorter PWDs compared with SR, which contrasts our findings and those of Manolis.³⁹ However, the combination of BB and CSo pacing can lead to significantly shorter PWDs.⁴⁰ Yu *et al.*²⁶ reported a group of patients (15 patients) with similar baseline clinical characteristics that were paced in the vicinity of BB. The results showed BB pacing offered shorter-paced PWD, comparing to pacing at PSFO, which is in agreement with our findings. The second explanation of the variation in results is that the exact location of the septal pacing sites is either not explicitly defined or not reported in some studies.^{5,40,41} Third, different methods are used to evaluate the global atrial activation time, including invasive and non-invasive approaches. Measurement of PWD allows non-invasive assessment of total atrial activation time from surface ECG using a standard 12-lead configuration,^{40,42} 65-lead ECG,³⁴ or the approach used in this study. Clearly, ECG approaches that utilize information from a higher number of ECG leads for PWD measurement or cover orthogonal planes have an advantage compared with a single-lead analysis²⁶ that is likely to underestimate the true duration of atrial activation.

Clinical implications

Despite the reported clinical benefit,^{6,39,43,44} a considerable number of patients do not benefit from septal pacing with regard to preventing AF. Padeletti *et al.*⁴⁵ reported that shorter baseline PWD may be indicative of a lower risk of persistent AF requiring cardioversion or AF-related hospitalization, regardless of whether pacing takes place at the RAA or the atrial septum. In previous pacing studies,^{5–7,43,46} atrial septal pacing resulted in a shorter PWD and was associated with a significant decrease in AF compared with RAA pacing or antiarrhythmic drugs.

In this study, we observed that longer PWD at baseline was associated with greater shortening by atrial septal pacing. Specifically, we observed that atrial septal pacing produced a shorter PWD in patients with a baseline PWD longer than 120 ms, regardless of location of pacing site. However, in patients with a baseline PWD shorter than or equal to 120 ms, prolongation of the P wave was observed during septal pacing, regardless of the pacing site. These findings are in agreement with those of Manolis *et al.*,³⁹ who described patient-tailored pacing site selection by intraoperative atrial septal mapping, aimed at obtaining the shortest atrial activation time between the HRA and the distal CS. These sites were located in the vicinity of the CSo or near the FO in all patients, and not at BB, which is in agreement with our findings.

Based on the above, we are inclined to speculate that the benefit of atrial septal pacing with regard to AF prevention may be confined to patients with impaired interatrial conduction during sinus rhythm, as such patients are more likely to respond to pacing by shortening of the PWD and reduction of atrial dyssynchrony. In contrast, patients with normal PWD are not likely to

demonstrate any improvement in interatrial conduction as a result of atrial septal pacing. If the preventive effect of atrial septal pacing on AF is indeed caused by shortening of the atrial activation time and preserving atrial synchrony,^{3,5,32,41} then the baseline PWD should have an impact on the clinical outcome in atrial septal pacing studies. To the best of our knowledge, atrial pacing studies reported to date^{2–4,32,36} have not provided any information in this regard. P-wave duration prolongation has not been considered as an inclusion criterion, with the exception of one study,³⁹ and no investigation of a possible link between PWD at baseline and the effect of atrial septal pacing has been reported. We believe our study provides the grounds for testing this hypothesis in clinical settings, as this may lead to further improvements in assessing patient suitability for atrial septal pacing.

Recently, Dabrowska-Kugacka *et al.*⁴⁷ reported that single-site BB pacing resulted in restoring atrial contraction synchrony, whereas CS pacing resulted in reduced RA filling, shortened mechanical atrioventricular delay in the right heart, and reduced right ventricular inflow, thus inducing echocardiographic pacemaker syndrome in the right heart. However, pacemaker syndrome has not been reported in any previous studies involving permanent CSo pacing.^{5,39,40} Pacing at BB may indeed produce mechanical contraction sequences close to those in natural SR, but the risks associated with CSo pacing have not been investigated. The superiority of CSo pacing site in the clinical settings is further supported by recently published results from EPASS study that found that low atrial septal pacing is associated prevention of paroxysmal AF progression to persistent or permanent AF compared with RAA pacing in patients with sinus node dysfunction.⁴⁸

Limitations

Our study was intended to assess whether pacing at any specific atrial septal site is associated with the shortest P-wave duration as a measure of global atrial activation time. The use of 3D mapping systems would allow more accurate verification of the atrial activation propagation, but it was not used in our study as left atrial catheterization could not be ethically justified in the majority of study subjects included in our cohort. As a minority of patients in the study had a history of AF, it is not clear how the results would apply to a population of patients with AF and sinus node dysfunction who would be eligible for such pacing on a permanent basis.

Conclusions

The optimal atrial septal pacing site with respect to the shortening of global atrial activation time can be identified by using the baseline P-wave duration. Furthermore, the impact of pacing on PWD is most pronounced in patients with a baseline PWD of >120 ms, and the shortest PWD is usually obtained by pacing at the CSo, rather than the HAS or the PSFO. Our findings underline the need for further investigation aimed at better selection of patients suitable for atrial septal pacing in order to improve the clinical benefit with regard to preventing AF in patients with indications for a pacemaker.

Funding

The study was supported by research grants from The Swedish Heart-Lung Foundation, donation funds at Skåne University Hospital, and government funding of clinical research within the Swedish National Health Service.

References

- Ovshyscher IE. Toward physiological pacing: optimization of cardiac hemodynamics by AV delay adjustment. *Pacing Clin Electrophysiol* 1997;**20**:861–5.
- Saksena S, Prakash A, Hill M, Krol RB, Munsif AN, Mathew PP et al. Prevention of recurrent atrial fibrillation with chronic dual-site right atrial pacing. *J Am Coll Cardiol* 1996;**28**:687–94.
- D'Alonnes GR, Pavin D, Leclercq C, Ecker JE, Jauvert G, Mabo P et al. Long-term effects of batrial synchronous pacing to prevent drug-refractory atrial tachyarrhythmia: a nine-year experience. *J Cardiovasc Electrophysiol* 2000;**11**:1081–91.
- Prakash A, Saksena S, Hill M, Krol RB, Munsif AN, Giorgberizze I et al. Acute effects of dual-site right atrial pacing in patients with spontaneous and inducible atrial flutter and fibrillation. *J Am Coll Cardiol* 1997;**29**:1007–14.
- Padeletti L, Porciani MC, Michelucci A, Colella A, Ticci P, Vena S et al. Interatrial septum pacing: a new approach to prevent recurrent atrial fibrillation. *J Interv Card Electrophysiol* 1999;**3**:35–43.
- Hemels ME, Ruiters JH, Molhoek GP, Veeger NJ, Wieselhof AC, Rancho AV et al. Right atrial preventive and antitachycardia pacing for prevention of paroxysmal atrial fibrillation in patients without bradycardia: a randomized study. *Europace* 2008;**10**:306–13.
- Padeletti L, Purerfellner H, Adler SW, Waller TJ, Harvey M, Horvitz L et al. Combined efficacy of atrial septal lead placement and atrial pacing algorithms for prevention of paroxysmal atrial tachyarrhythmia. *J Cardiovasc Electrophysiol* 2003;**14**:1189–95.
- Miyazaki H, Noma K, Date T, Kobayashi A, Koga A, Kuno M et al. Atrial septal pacing to resynchronize atrial contraction and improve atrial transport function. *J Cardiol* 2005;**45**:239–46.
- Ho SY, Sanchez-Quintana D, Cabrera JA, Anderson RH. Anatomy of the left atrium: implications for radiofrequency ablation of atrial fibrillation. *J Cardiovasc Electrophysiol* 1999;**10**:1525–33.
- Platonov PG, Mitrofanova L, Ivanov V, Ho SY. Substrates for intra-atrial and interatrial conduction in the atrial septum: anatomical study on 84 human hearts. *Heart Rhythm* 2008;**5**:1189–95.
- Chauvin M, Shah DC, Haissaguerre M, Marcellin L, Brechenmacher C. The anatomic basis of connections between the coronary sinus musculature and the left atrium in humans. *Circulation* 2000;**101**:647–52.
- Ho SY, Anderson RH, Sanchez-Quintana D. Atrial structure and fibres: morphological bases of conduction. *Cardiovasc Res* 2002;**54**:325–36.
- Holmqvist F, Husser D, Tapanainen JM, Carlsson J, Jurkko R, Xia Y et al. Interatrial conduction can be accurately determined using standard 12-lead electrocardiography: validation of P-wave morphology using electroanatomic mapping in man. *Heart Rhythm* 2008;**5**:413–8.
- Carlson J, Havmoller R, Herreros A, Platonov P, Johansson R, Olsson B. Can orthogonal lead indicators of propensity to atrial fibrillation be accurately assessed from the 12-lead ECG? *Europace* 2005;**7**(Suppl. 2):39–48.
- James TN, Sherf L. Specialized tissues and preferential conduction in the atria of the heart. *Am J Cardiol* 1971;**28**:414–27.
- Lemery R, Soucie L, Martin B, Tang AS, Green M, Healey J. Human study of biatrial electrical coupling: determinants of endocardial septal activation and conduction over interatrial connections. *Circulation* 2004;**110**:2083–9.
- Betts TR, Roberts PR, Morgan JM. High-density mapping of left atrial endocardial activation during sinus rhythm and coronary sinus pacing in patients with paroxysmal atrial fibrillation. *J Cardiovasc Electrophysiol* 2004;**15**:1111–7.
- Markides V, Schilling RJ, Ho SY, Chow AW, Davies DW, Peters NS. Characterization of left atrial activation in the intact human heart. *Circulation* 2003;**107**:733–9.
- De PR, Ho SY, Salerno-Uriarte JA, Tritto M, Spadacini G. Electroanatomic analysis of sinus impulse propagation in normal human atria. *J Cardiovasc Electrophysiol* 2002;**13**:1–10.
- Hayashi H, Lux RL, Wyatt RF, Burgess MJ, Abildskov JA. Relation of canine atrial activation sequence to anatomic landmarks. *Am J Physiol* 1982;**242**:H421–8.
- Dolber PC, Spach MS. Structure of canine Bachmann's bundle related to propagation of excitation. *Am J Physiol* 1989;**257**:H1446–57.
- O'Donnell D, Bourke JP, Furniss SS. Interatrial transeptal electrical conduction: comparison of patients with atrial fibrillation and normal controls. *J Cardiovasc Electrophysiol* 2002;**13**:1111–7.
- Antz M, Otomo K, Arruda M, Schlerlag BJ, Pitha J, Tondo C et al. Electrical conduction between the right atrium and the left atrium via the musculature of the coronary sinus. *Circulation* 1998;**98**:1790–5.
- Hertervig E, Li Z, Kongstad O, Holm M, Olsson SB, Yuan S. Global dispersion of right atrial repolarization in healthy pigs and patients. *Scand Cardiovasc J* 2003;**37**:329–33.
- Saremi F, Channul S, Krishnan S, Gurudevan SV, Narula J, Abolhoda A. Bachmann Bundle and its arterial supply: imaging with multidetector CT—implications for interatrial conduction abnormalities and arrhythmias. *Radiology* 2008;**248**:447–57.
- Yu WC, Tsai CF, Hsieh MH, Chen CC, Tai CT, Ding YA et al. Prevention of the initiation of atrial fibrillation: mechanism and efficacy of different atrial pacing modes. *Pacing Clin Electrophysiol* 2000;**23**:373–9.
- Lüdinghausen M, Ohmachi N, Boot C. Myocardial coverage of the coronary sinus and related veins. *Clin Anat* 1992;**5**:1–15.
- Dong J, Zrenner B, Schreieck J, Deisenhofer I, Karch M, Schneider M et al. Catheter ablation of left atrial focal tachycardia guided by electroanatomic mapping and new insights into interatrial electrical conduction. *Heart Rhythm* 2005;**2**:578–91.
- Boineau JP, Canavan TE, Schuessler RB, Cain ME, Corr PB, Cox JL. Demonstration of a widely distributed atrial pacemaker complex in the human heart. *Circulation* 1988;**77**:1221–37.
- Ho SY, Sanchez-Quintana D. The importance of atrial structure and fibers. *Clin Anat* 2009;**22**:52–63.
- Lemery R, Birnie D, Tang AS, Green M, Gollub M, Hendry M et al. Normal atrial activation and voltage during sinus rhythm in the human heart: an endocardial and epicardial mapping study in patients with a history of atrial fibrillation. *J Cardiovasc Electrophysiol* 2007;**18**:402–8.
- Bailin SJ, Adler S, Giudici M. Prevention of chronic atrial fibrillation by pacing in the region of Bachmann's bundle: results of a multicenter randomized trial. *J Cardiovasc Electrophysiol* 2001;**12**:912–7.
- Bailin SJ. Is Bachmann's Bundle the only right site for single-site pacing to prevent atrial fibrillation? Results of a multicenter randomized trial. *Card Electrophysiol Rev* 2003;**7**:325–8.
- Gozolits S, Fischer G, Berger T, Hanser F, Abou-Harb M, Tilg B et al. Global P wave duration on the 65-lead ECG: single-site and dual-site pacing in the structurally normal human atrium. *J Cardiovasc Electrophysiol* 2002;**13**:1240–5.
- Noguchi H, Kumagai K, Tojo H, Yasuda T, Saku K. Effect of Bachmann's bundle pacing on atrial fibrillation: electrophysiologic assessment. *Clin Cardiol* 2004;**27**:50–3.
- Padeletti L, Pieragnoli P, Ciapetti C, Colella A, Musilli N, Porciani MC et al. Randomized crossover comparison of right atrial appendage pacing versus interatrial septum pacing for prevention of paroxysmal atrial fibrillation in patients with sinus bradycardia. *Am Heart J* 2001;**142**:1047–55.
- Kutarski A, Glowniak A, Szczesniak D, Rucinski P. Coronary sinus pacing: Its influence on external and intraatrial signal-averaged P wave time domain parameters. *Cardiol J* 2007;**14**:470–81.
- Papageorgiou P, Monahan K, Anselme F, Kirchhof C, Josephson ME. Electrophysiology of atrial fibrillation and its prevention by coronary sinus pacing. *Semin Interv Cardiol* 1997;**2**:227–32.
- Manolis AG, Katsivas AG, Vassilopoulos C, Koutsogeorgis D, Louvros NE. Prevention of atrial fibrillation by inter-atrial septum dual-site pacing guided by electrophysiological testing, in patients with delayed interatrial conduction. *Europace* 2002;**4**:165–74.
- Lewicka-Nowak E, Kutarski A, Dabrowska-Kugacka A, Rucinski P, Zagodzko P, Raczak G. A novel method of multisite atrial pacing, incorporating Bachmann's bundle area and coronary sinus ostium, for electrical atrial resynchronization in patients with recurrent atrial fibrillation. *Europace* 2007;**9**:805–11.
- Hermida JS, Carpentier C, Kubala M, Otmami A, Delonca J, Jarry G et al. Atrial septal versus atrial appendage pacing: feasibility and effects on atrial conduction, interatrial synchronization, and atrioventricular sequence. *Pacing Clin Electrophysiol* 2003;**26**:26–35.
- Endoh Y, Nakamura A, Suzuki T, Mizuno M, Takara A, Ota Y et al. Clinical significance of prolonged P wave width after right atrial appendage pacing in sick sinus syndrome. *Circ J* 2003;**67**:485–9.
- Hermida JS, Kubala M, Lescure FX, Delonca J, Clerc J, Otmami A et al. Atrial septal pacing to prevent atrial fibrillation in patients with sinus node dysfunction: results of a randomized controlled study. *Am Heart J* 2004;**148**:312–7.
- Kale M, Bennett DH. Atrial septal pacing in the prevention of paroxysmal atrial fibrillation refractory to antiarrhythmic drugs. *Int J Cardiol* 2002;**82**:167–75.
- Padeletti L, Santini M, Boriani G, Botto G, Ricci R, Spampinato A et al. Duration of P-wave is associated with atrial fibrillation hospitalizations in patients with

- atrial fibrillation and paced for bradycardia. *Pacing Clin Electrophysiol* 2007;**30**: 961–9.
46. Padeletti L, Michelucci A, Pieragnoli P, Colella A, Musilli N. Atrial septal pacing: a new approach to prevent atrial fibrillation. *Pacing Clin Electrophysiol* 2004;**27**: 850–4.
47. Dabrowska-Kugacka A, Lewicka-Nowak E, Rucinski P, Kozlowski D, Raczak G, Kutarski A. Single-site Bachmann's bundle pacing is beneficial while coronary sinus pacing results in echocardiographic right heart pacemaker syndrome in brady-tachycardia patients. *Circ J* 2010;**74**:1380–15.
48. Verlato R, Botto GL, Massa R, Amellone C, Perucca A, Bongiorni MG et al. Efficacy of low interatrial septum and right atrial appendage pacing for prevention of permanent atrial fibrillation in patients with sinus node disease: results from the Electrophysiology-Guided Pacing Site Selection (EPASS) Study. *Circ Arrhythmia Electrophysiol* 2011;**4**:844–50.

IMAGES IN ELECTROPHYSIOLOGY

doi:10.1093/europace/eus032
Online publish-ahead-of-print 7 March 2012

Pulmonary vein tachycardia during atrial tachycardia in the context of atrial fibrillation ablation

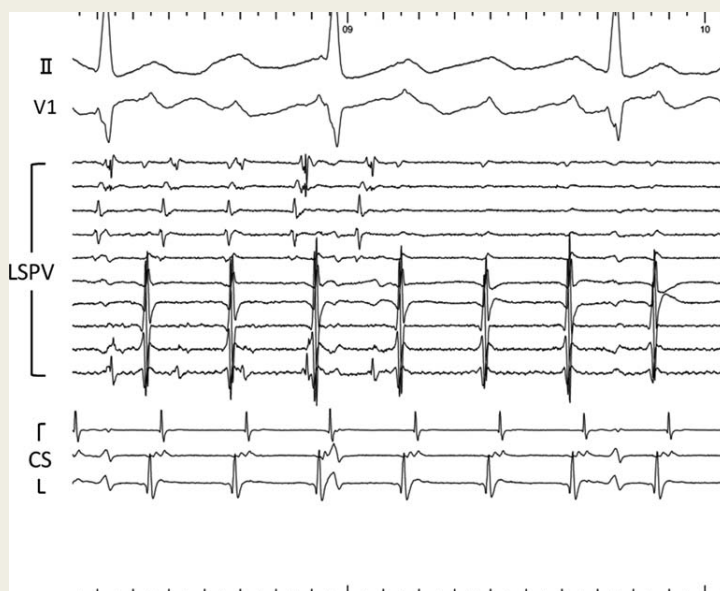
Shinsuke Miyazaki*, Hiroshi Taniguchi, and Yoshito Iesaka

Tsuchiura Kyodo Hospital, Ibaraki, Japan

*Corresponding author: Cardiology Division, Cardiovascular Center, Tsuchiura Kyodo Hospital, 11-7 Manabeshin-machi, Tsuchiura, Ibaraki 300-0053, Japan. Tel: +81 29 823 3111; fax: +81 29 826 2411. Email: mshinsuke@k3.dion.ne.jp

Although checking the pulmonary vein isolation (PVI) is an important first step to identify atrial tachycardia (AT) mechanism in the context of atrial fibrillation (AF) ablation, careful mapping is required to reach a precise diagnosis. A 68-year-old man with long-standing persistent AF underwent ablation. Atrial fibrillation converted to AT with a cycle length of 240 ms during left atrial (LA) ablation after PVI. During AT mapping, PV tachycardia with a cycle length of 180 ms was recorded in the left superior PV, which seemed four to three conductions from the PV to LA. However, the termination of this tachycardia did not have any impact on the AT, which suggested bystander tachycardia.

Conflict of interest: none declared.



Paper III

Diagnosis of atrial tachycardias originating from the lower right atrium: importance of P-wave morphology in the precordial leads V3–V6

Yan Huo^{1*}, Frieder Braunschweig², Thomas Gaspar¹, Sergio Richter¹, Robert Schönbauer¹, Philipp Sommer¹, Arash Arya¹, Sascha Rolf¹, Andreas Bollmann¹, Gerhard Hindricks¹, and Christopher Piorkowski¹

¹Department of Electrophysiology, Leipzig Heart Center, Leipzig University, 04289 Leipzig, Germany; and ²Department of Cardiology, Karolinska University Hospital, Stockholm, Sweden

Received 19 June 2012; accepted after revision 17 August 2012; online publish-ahead-of-print 10 October 2012

Aims

This study aimed to characterize P-wave morphology (PWM) in leads V3–V6 during focal atrial tachycardia (AT) originating from the lower right atrium (RA), and to investigate the role of interatrial conduction (IAC) pathways in the formation of PWM.

Methods and results

Twenty-eight consecutive patients with tachycardia foci in the lower RA underwent detailed atrial endocardial activation mapping and radiofrequency catheter ablation. P-wave configuration was analysed using standard 12-lead electrocardiogram. Atrial tachycardia originated from lower non-septal tricuspid annulus (LTA) ($n = 11$), coronary sinus ostium (CSo) ($n = 11$), lower crista terminalis (LCT) ($n = 4$), or lower free wall ($n = 2$). In leads V3–V6, PWM showed a negative pattern in at least two consecutive leads during AT originating from CSo (11/11) and LTA (9/11), with an associated sensitivity of 91%, specificity of 100%, positive predictive value (PPV) of 100%, and negative predictive value (NPV) of 75%. A positive PWM was observed in three of four ATs originating from LCT, with an associated sensitivity of 75%, specificity of 100%, PPV of 60%, and NPV of 96%. A negative PWM in V3–V6 was consistent with a preferential IAC through musculature in the vicinity of the CS and an activation of both atria in an antero-posterior direction. In contrast, a positive PWM was associated with the engagement of a posterior (non-CS-related) interatrial connection.

Conclusion

Characteristic PWMs in V3–V6 may accurately differentiate the anatomic sites of AT from the low RA with high PPVs and NPVs. P-wave morphology in V3–V6 is likely to be influenced by the engagement of the preferential IAC.

Keywords

Atrial tachycardia • Radiofrequency catheter ablation • P-wave morphology • Interatrial conduction pathway • Lower right atrium

Introduction

Focal atrial tachycardias (ATs) originating from single atrial sites outside the sinus node are found to be the underlying mechanism in 5–15% of adults with paroxysmal supraventricular tachycardia.¹ Foci responsible for focal AT tend to cluster at characteristic anatomical locations. The majority of focal AT stem from the right atrium (RA), with foci along the crista terminalis (CT) in over two-third of cases.² Less frequently, the foci are at the tricuspid

annulus (TA),^{3,4} the coronary sinus ostium (CSO),⁵ or the parahisian region.^{6,7}

A thorough analysis of P-wave morphology (PWM) in 12-lead electrocardiogram (ECG) during AT is a key to the non-invasive identification of arrhythmic foci. Generally, as a first step, right- and left-sided origins are distinguished. Further, if an RA origin is suggested, positive P-waves in the inferior leads typically indicate AT from the middle or superior CT in over 90% of focal ATs

* Corresponding author. Tel: +0049 341 865 1413; fax: +0049 341 865 1460, Email: dr.huoyan@googlemail.com

Published on behalf of the European Society of Cardiology. All rights reserved. © The Author 2012. For permissions please email: journals.permissions@oup.com.

What's New?

- Characteristic P-wave morphology in the precordial leads V3–V6 can accurately differentiate the anatomic sites of atrial tachycardia origin with high positive and negative predictive values in patients with atrial tachycardias from lower right atrium.
- Characteristic P-wave morphology in the precordial leads V3–V6 is likely to be influenced by the employment of preferential interatrial conduction pathways between right and left atria.

with CT origins.² Further ECG-based differential diagnosis of AT from the lower RA is difficult to perform. However, the PWM in ECG leads V3–V6 has not been sufficiently addressed in previous studies⁷ and may provide important additional information on the origin of the AT.

This study was performed to further establish ECG characteristics of focal AT originating from the lower RA. We hypothesized that the employment of the preferential interatrial conduction (IAC) pathways results in typical PWM in V3–V6. A number of factors may influence the PWM during AT originating from the RA such as: (i) activation sequence within the RA, (ii) preferential IAC pathways for activation from the RA to the left atrium (LA), and (iii) activation sequence of the LA.

Methods

Study population

Between October 2006 and April 2010, 144 consecutive patients underwent radiofrequency catheter ablation (RFCA) of focal AT with RA origins at our institution. In 28 (19%), a tachycardia with origin of lower RA was confirmed using three-dimensional (3D) electroanatomical (EA) activation mapping during the RFCA procedure. All patients had symptomatic tachycardias and proved refractory to at least one antiarrhythmic agent. All patients signed a written informed consent.

Electrophysiological study

Electrophysiological procedures were performed according to international standard routines using conventional equipment,⁸ and the tachycardia mechanism was defined by established criteria.⁹ The mode of tachycardia onset and termination was recorded together with the tachycardia cycle length, local activation time at the site of successful ablation, as well as the ratio of atrial to ventricular electrogram as recorded on the ablation catheter at the site of successful ablation.

All antiarrhythmic medications were discontinued at least five half-lives before the study. None of the patients were taking amiodarone or digitalis. If necessary, electrophysiological studies were performed using intravenous midazolam and/or fentanyl. Conventional 12-lead surface ECG and bipolar intracardiac electrogram recordings (filtered between 30 and 500 Hz) were amplified and displayed using the Prucka CardiLab System (GE Medical Systems, Milwaukee, WI, USA). A quadripolar catheter was placed via a left femoral vein in the RV and a decapolar catheter was placed in the CS with the

proximal pole at the ostium. High-rate atrial stimulation (or programmed stimulation) and intravenous isoproterenol and/or atropine were used for arrhythmia induction if spontaneous tachycardia was not present at the baseline.

Mapping of atrial tachycardia

A mapping and ablation procedure was performed using a 7-F Navistar catheter (Biosense Webster, Diamond Bar, CA, USA; 4 mm tip, two bipolar electrode pairs, inter-electrode distance 2 mm) and guided by a 3D-EA mapping system (CARTO-XP, Biosense Webster) in all patients. Activation mapping during tachycardia was used to identify sites of earliest endocardial activation in the RA and CS. Activation time in the CS relative to the RA activation was used to describe preferential conduction used for impulse propagation from the RA into the LA. The influence on PWM in V3–V6 was studied.

Activation time was measured from the onset of the first sharp component of the bipolar electrogram on the distal mapping catheter to the earliest deflection of the P-wave on the surface ECG. The target site of ablation was determined using the combination of the earliest bipolar activation and the shape of the unipolar electrogram (sharply negative pattern).

Radiofrequency catheter ablation and follow-up

Radiofrequency catheter ablation was performed in the RA with continuous temperature feedback control of the power output to achieve a target temperature of 70°C. The maximum power used was 50 W for a maximum of 60 s. An acute procedural success was defined by the inability to induce the tachycardia 15 min after the ablation despite the aggressive burst atrial pacing or programmed atrial stimulation and the use of isoproterenol. The patients were followed in their referring clinics in order to assess the recurrence of symptoms or documented tachycardia.

Section definitions

The RA location of the tachycardia focus was determined based on the findings from 3D-EA activation mapping and termination of the tachycardia using RFCA at the putative site.

- An AT was considered to arise from the CT when earliest activation was mapped in this region with the aid of fractionated electrograms and the anatomical position was tagged on the 3D-EA map; ablation in this region successfully eliminated the tachycardia.
- An AT was considered to arise from the CSo when earliest activation was recorded around the CSo and when ablation within 1 cm of this region successfully eliminated the tachycardia.
- An AT was considered to arise from the TA based on the following criteria:
 - Ablation catheter positioned in an annular location when viewed in right and left anterior oblique fluoroscopic views with characteristic annular motion of the catheter tip.
 - A–V ratio of <1.
 - Exclusion of sites around the CSo and parahisian region. The different sectors of the TA (Figure 1) are described using anatomic terminology contained in published guidelines.¹⁰
 - Ablation in this region successfully eliminated the tachycardia.
- An AT was considered to arise from the lower free wall:
 - Earliest activation was mapped in the region between non-septal TA and lower CT.

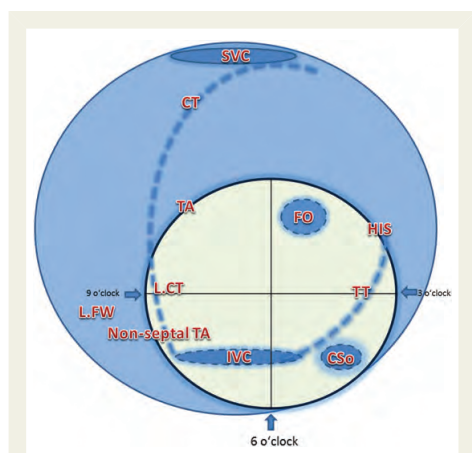


Figure 1 Localization of anatomical structures in the lower right atrium. SVC, superior vena cava; TA, tricuspid annulus; CT, crista terminalis; FO, fossa ovalis; LFW, lower free wall; LCT, lower crista terminalis; TT, tendon of tudaro; CSO: coronary sinus ostium.

- The local electrogram with the earliest activation did not contain either fractionated electrograms (suggests CT origin) or A–V ratio of <1 (suggests TA origin).
- Ablation in this region successfully eliminated the tachycardia.

P-wave analysis

The PWM on the surface ECG was assessed carefully to assist in the tachycardia localization. Particular attention was paid to assessment of an unencumbered P-wave during periods of atrioventricular block or after ventricular pacing. The definitions by Tang *et al.*¹¹ were used to analyse the surface 12-lead PWM and further modified based on our study findings in characterizing positive-isoelectric and negative-isoelectric morphologies. P-waves were described on the basis of the deviation from baseline during the T–P interval as being: (i) completely positive (+), (ii) completely negative (–), (iii) biphasic: when there were both positive and negative (+/– or –/+) deflections from baseline, (iv) isoelectric: when there were no P-wave deflections from baseline >0.05 mV, or (v) isoelectric-positive/ isoelectric-negative: isoelectric line after the onset of the P-wave 20 ms followed by a change to positive or negative. Alternatively, positive-isoelectric/negative-isoelectric was defined as positive or negative pattern followed by an isoelectric line 20 ms before the end of P-wave. Figure 2 illustrates these different PWM during tachycardia.

Statistical analysis

All data distributions were tested for normality using histograms and presented as mean \pm SD. Population proportions are presented as a percentage. The sensitivity, specificity, positive predictive value (PPV), and negative predictive value (NPV) were calculated according to standard definitions.

Results

Patient characteristics

The patient characteristics are described in Table 1. They were 52 ± 15 years of age and the majority was male ($n = 21$, 75%). None received amiodarone. All had normal cardiac anatomy on transthoracic echo with no Ebstein's anomalies. Left atrium diameters were measured as 34 ± 5 mm.

General findings

The AT origin was identified at the following sites: 11 patients (39%) along the TA (6–9 o'clock), another 11 (39%) around the CSO, 4 patients (14%) in the lower CT, and 2 patients (7%) in the lower RA free wall. Multifocal AT was found in two patients (7%) with AT originating from the CSO; in both cases the second focal tachycardia originated from the superior CT. In contrast to AT originating from the upper RA which typically shows at least two positive P-waves in the inferior (II, III, and aVF) leads, the ECG of all study patients with lower RA AT contained a maximum of one positive P-wave (up to one lead with exclusively positive pattern) in the inferior leads.

P-wave morphology and anatomic location

Non-septal tricuspid annulus origin

Nine of the 11 ATs originating at the non-septal TA (6–9 o'clock) had an exclusively negative pattern in the inferior and precordial (V3–V6) leads. However, the remaining two ATs originating from TA at 9 o'clock, had a negative–positive (patient 18) or positive (patient 19) pattern in lead II, an isoelectric pattern in lead III and aVF, and an exclusively positive pattern in precordial leads V3–V6 (Table 2, Figures 1 and 2).

Coronary sinus ostium origin

All eleven ATs originating from CSO had a positive pattern in aVR and aVL leads with an exclusively negative pattern in all inferior leads (II, III, and aVF). Nine of 11 ATs had an exclusively negative pattern in all four precordial leads (V3–V6). In the remaining two ATs, one (patient 14) had a biphasic pattern (–/+) in precordial leads V3 and V4. The other (patient 16) had a biphasic pattern (–/+) in precordial lead V3. All biphasic patterns contained an early negative component.

Lower crista terminalis

All ATs originating from the lower CT ($n = 4$), had isoelectric or biphasic patterns in the inferior leads (II, III, and aVF) and three had a positive pattern in all four precordial leads (V3–V6). The remaining one AT had a biphasic pattern (–/+) in all four precordial leads (V3–V6).

Lower free wall

Two ATs originated from the lower free wall of the RA. One exhibited a negative pattern in all inferior leads (II, III, and aVF) and biphasic patterns (–/+) in all four precordial leads V3–V6. The other exhibited an isoelectric pattern in all inferior leads (II, III, and aVF), a positive pattern in V3 and V4 and an isoelectric pattern in V5 and V6.

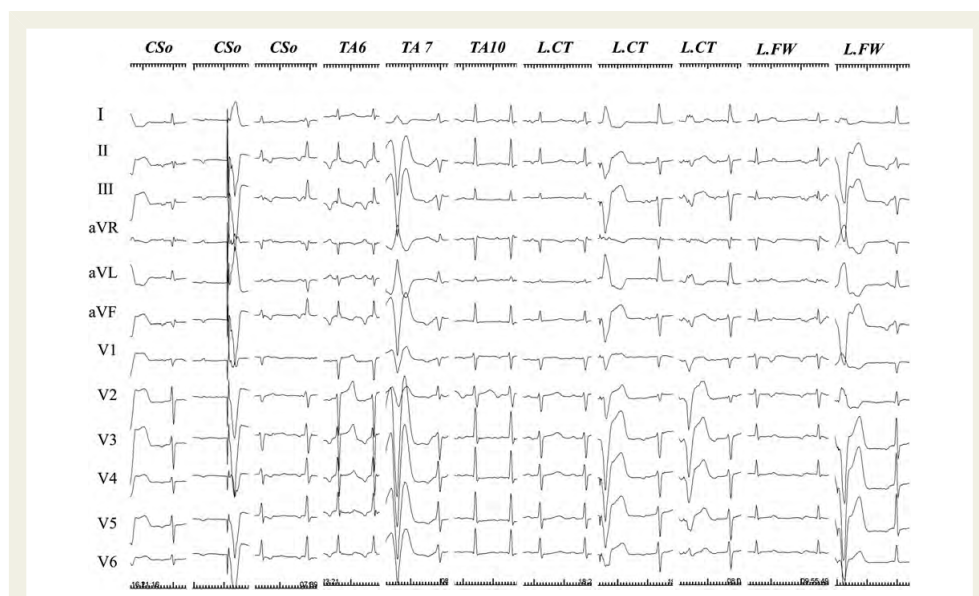


Figure 2 P-wave morphology during ectopic atrial tachycardias (25 mm/s). P-wave morphology was shown on a standard 12-lead ECG during ectopic atrial tachycardia originating from the lower right atrium. CSo, coronary sinus ostium; TA, tricuspid annulus; TA6, at 6 o'clock position of TA; TA7, at 7 o'clock position of TA; TA9, at 9 o'clock position of TA; LCT, lower crista terminalis; LFW, lower free wall.

Power of precordial leads (V3–V6) to discriminate the anatomical atrial tachycardia origin

Lower tricuspid annulus origin (annulus foci) vs. lower crista terminalis origin

P-wave morphology in the precordial leads (V3–V6) showed a negative pattern in at least two consecutive leads at the origins of AT from the non-septal TA (9 of 11 patients) or CSo (all 11 patients). In contrast, AT from the lower CT showed a positive pattern in V3–V6 in three of four patients. A negative P-wave in at least two consecutive leads in V3–V6 demonstrated a sensitivity of 91%, a specificity of 100%, a PPV of 100%, and an NPV of 75% for a focus at the TA, including CSo and non-septal TA. On the contrary, a positive P-wave in all V3–V6 demonstrated a sensitivity of 75%, a specificity of 100%, a PPV of 60%, and an NPV of 96% for a lower CT focus.

Non-septal tricuspid annulus origin vs. coronary sinus ostium origin

In the current study, the PWM in precordial leads V3–V6 was not able to discriminate between AT with CSo and non-septal TA origin. Both AT origins were associated with predominantly negative P-waves in the precordial leads (V3–V6).

Activation mapping and preferential interatrial conduction

Coronary sinus activation during AT was recorded from proximal to distal using the CS catheter and compared to the spread of RA activation described in the right atrial 3D map. During AT originating from the lower CT, the proximal CS (CS 9–10) was activated later than the lower mid-septum of RA, but slightly earlier (two of four patients) or simultaneously (one of four patients) in relation to the posterior CSo (Figure 3A). However, during AT originating from the lower TA (20 of 22 patients), including the non-septal TA (9 of 11 patients) (Figure 3B) and the CSo (all 11 patients) (Figure 3C), the proximal CS was activated earlier than the lower right atrial mid-septum. These activation patterns indicate differences in LA activation caused by different preferential conduction pathways used for interatrial impulse propagation.

Discussion

Main findings

In patients with AT from the lower RA, characteristic PWMs in V3–V6 leads could help to differentiate the anatomical site of AT origin with high PPVs and NPVs. A negative pattern in V3–V6 indicates an AT from annular aspects of the RA such as the

Table 1 Patients' characteristics

Patient number	Age (year)	Gender	LA (mm)	Hypertension	Diabetes	CAD	Arrhythmia
1	64	Male	37	–	–	–	PAF, EAT
2	47	Female	39	–	–	–	AVB III, EAT
3	45	Male	33	–	–	–	EAT
4	42	Male	35	–	–	–	EAT
5	58	Male	40	+	–	–	EAT
6	56	Male	41	+	–	–	EAT
7	72	Female	42	–	–	–	PAF, EAT
8	71	Male	39	–	–	–	EAT
9	70	Male	36	–	–	+	EAT
10	60	Male	29	+	–	–	EAT
11	60	Female	37	+	+	–	EAT
12	59	Male	36	+	–	–	EAT
13	56	Male	33	–	–	–	PAF, EAT
14	43	Male	31	+	–	–	EAT
15	48	Male	30	–	–	–	EAT
16	81	Male	40	–	+	–	EAT
17	38	Female	24	–	+	–	EAT
18	27	Male	26	+	–	–	EAT
19	36	Male	33	+	–	+	EAT
20	31	Male	30	+	–	–	EAT
21	33	Male	29	–	–	–	EAT
22	46	Female	34	+	–	+	EAT
23	52	Female	36	–	–	–	EAT
24	66	Male	35	–	–	–	PAF, EAT
25	78	Male	33	+	–	–	EAT
26	55	Male	34	+	–	–	EAT
27	53	Female	27	–	+	+	EAT
28	22	Male	35	–	+	–	EAT

LA-diameter was measured at parasternal long axis view (antero-posterior in the 2D echo-long axis).

LA, left atrium; CAD, coronary arterial disease; PAF, paroxysmal atrial fibrillation; EAT: ectopic atrial tachycardia; AVB III^o, third degree of atrioventricular block.

non-septal TA and around the CSo while positive P-waves in V3–V6 are associated with a lower CT focus. These different PWM patterns are likely to be influenced by the preferential conduction between RA and LA.

P-wave morphology in precordial leads V3–V6

The PWM in precordial leads V3–V6 provided high PPVs and NPVs for the localization of AT originating from the lower TA or CT. However, PWM in the precordial leads V3–V6 was not useful in distinguishing ATs of non-septal TA vs. CSo origin. Previous studies have described the PWM of ATs originating from non-septal TA and CSo, separately.^{4,5,7} Morton *et al.*⁴ reported either inverted or biphasic P-waves with an initial negative deflection in V2–V6 during ATs from TA and a predominantly negative PWM in lead V3 and V6 has been described in association with ATs from CSo.⁵ In another study from the same group,⁷ a positive P-wave in lead V3 and V6 during ATs originating from the lower CT was described, which supports our findings. It has also been suggested that PWM in leads I and V1 can differentiate between

non-septal TA and CSo origins.⁷ However, when we applied these criteria to our data, a positive pattern in lead I provided a sensitivity of only 27% with a specificity of 100%. Negative P-waves in lead V1 differentiated between a non-septal TA and CSo origin with a sensitivity of 23% and a specificity of 83%. It is possible to explain the low sensitivity of leads I/V1 criteria in our data by the anatomical distribution of ATs, as the majority of ATs in our patient cohort were located at TA 6–7 o'clock.

Considering the low prevalence of ATs originating from the lower free wall and the lower CT, we could not draw a solid conclusion on the reliability of PWM for distinguishing ATs with an origin from these sites. However, in contrast to a lower CT origin, none of the ATs from the lower free wall contained a completely positive P-wave in all leads V3–V6.

Preferential interatrial connections and formation of P-wave morphology in atrial tachycardias

The Bachmann bundle (BB), a region of rapid IAC connecting the superior RA and LA behind the ascending aorta, is recognized as

Table 2 Tachycardia cycle length and P-wave morphology during ectopic atrial tachycardia

No.	TCL	Localization	I	II	III	aVR	aVL	aVF	V1	V2	V3	V4	V5	V6
Lower freewall (2 patients)														
1	320–360 ms	LFW	+	-	-	+/-	+	-	-	-	-/+	-/+	-/+	-/+
2	280–310 ms	LFW	+	Iso	Iso	Iso	+	Iso	Iso	+	+	+	Iso	Iso
Lower CT (4 patients)														
3	400–450 ms	LCT	+/-	Iso/-	Iso	+	-	+/-	Iso	+	+	+	+	+
4	330–340 ms	LCT	+	Iso	Iso	-	+	-/+	Iso	+	+	+	+	+
5	310–320 ms	LCT	-/+	-/+	-/+	+	-/+	-/+	Iso	Iso	-/+	-/+	-/+	-/+
6	360 ms	LCT	-/+	-/+	-/+	-	+	-/+	Iso	+	+	+	+	+
CS ostium (11 patients)														
7	270 ms	CSo	-/+	-	-	+	+	-	Iso/+	-	-	-	-	-
8	290–320 ms	CSo	-/+	-	-	+	+	-	Iso	Iso	-	-	-	-
9	300–340 ms	CSo	Iso	-	-	+	+	-	-	-	-	-	-	-
10	250–270 ms	CSo	Iso	-	-	+	+	-	Iso	Iso	-	-	-	-
11	290 ms	CSo	-/+	-	-	+	+	-	-/+	Iso	-	-	-	-
12	380–390 ms	CSo	-/+	-	-	+	+	-	Iso	-	-	-	-	-
13	350–390 ms	CSo	-/+	-	-	+	+	-	-/+	-/+	-	-	-	-
14	330–360 ms	CSo	-/+	-	-	+	+	-	Iso	-/+	-/+	-/+	-	-
15	390–450 ms	CSo	-/+	-	-	+	+	-	+/-	-	-	-	-	-
16	380 ms	CSo	-/+	-	-	+	+	-	+	Iso	-/+	-	-	-
17	410–430 ms	CSo	Iso	-	-	+	+	-	+	Iso	-	-	-	-
Non-septal TA (11 patients)														
18	330–350 ms	TA 9	-/+	-/+	Iso	+	-/+	Iso	-	-/+	+	+	+	+
19	460 ms	TA 9	+	+	Iso	-	Iso	Iso	-	Iso	+	+	+	+
20	420–440 ms	TA 6	-/+	-	-	+	+	-	-/+	-/+	-	-	-	-
21	390–400 ms	TA 7	Iso	-	-	+	+	-	-	-	-	-	-	-
22	270 ms	TA 6	Iso/+	-	-	+	+	-	Iso	-	-	-	-	-
23	320 ms	TA 6	-/+	-	-	+	+	-	Iso	-	-	-	-	-
24	330–340 ms	TA 6	-/+	-	-	+	+	-	Iso	Iso/-	-	-	-	-
25	330–350 ms	TA 7	+	-	-	-	+	-	-	-/Iso	-	-	-	-
26	310–320 ms	TA 7	-/+	-	-	+	+	-	-	Iso	-	-	-	-
27	350 ms	TA 6	Iso/+	-	-	+	+	-	Iso	Iso	-	-	-	-
28	290 ms	TA 6	Iso	-	-	+	+	-	+	Iso	-	-	-	-

LFW, lower free wall; LCT, lower crista terminalis; CSo, coronary sinus ostium; TA, tricuspid annulus.

the preferential path of LA activation during sinus rhythm as demonstrated by both animal and human studies.^{12–14} Another pathway of IAC is located in the proximity of the CS ostium and utilizes the myocardial CS coat¹⁵ for electrical impulse propagation.^{14,16} Ho and Sanchez-Quintana¹⁷ also described small muscular bridges connecting the RA posterior wall with the LA posterior wall near the ostia of the right-sided pulmonary veins (PVs). The presence of these posterior interatrial connections was also confirmed by mapping during PV tachycardias,¹³ identifying a posterior breakthrough at the intercaval area of the RA. On the basis of the findings above, the pattern of IAC may differ depending on the relative proximity of the source of activation to each of the possible electrical pathways (posterior fibres, BB, or CS).¹⁸

The formation of PWMs during ATs depends on the activation sequence of both the RA and the LA which can also be described in terms of the original chamber (generator) and the secondary

chamber (follower). The activation pattern of the secondary chamber is determined by the insertion site of the preferential interatrial connection. In our study focusing on ATs from the lower RA, a superoanterior interatrial connection through the BB was unlikely due to its large anatomical distance from the focal arrhythmic origin. Conversely, the LA was activated using inferoanterior (musculature in the vicinity of CS) or posterior (posterior fibres behind foramen ovale) IAC pathways. Accordingly, the follower (LA) was activated either anteriorly/posteriorly or vice versa, resulting in a negative or positive PWM in precordial leads V3–V6.

Interpretation of characteristic P-wave morphology in precordial leads

The ATs of TA origin primarily showed P-waves that were either exclusively negative or with early negative components in leads V3–V6

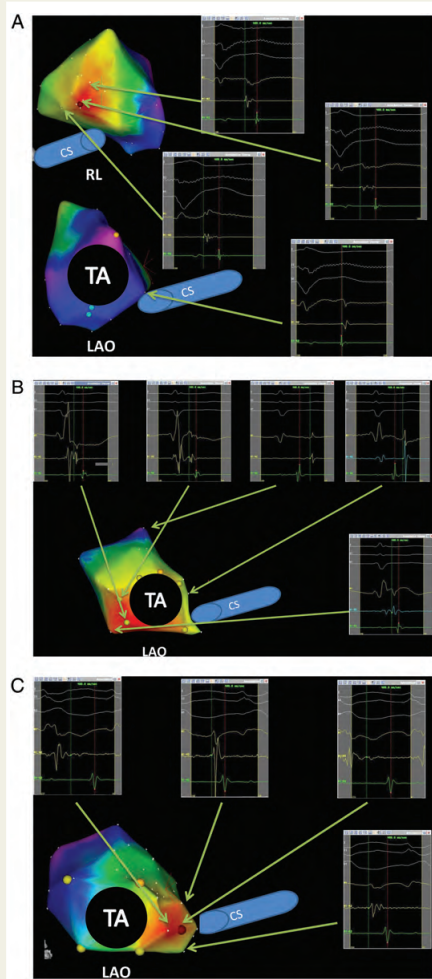


Figure 3 Three-dimensional electroanatomical mapping (activation map) and endocardial electrograms during ectopic atrial tachycardias. (A) The ectopic atrial tachycardia originated from the lower crista terminalis. The right inferior electrograms show mid-septum was activated later than coronary sinus ostium. The left superior activation map shows the earliest activation spot with fragmented potentials on the ablation catheter and sharply negative unipolar electrogram. (B) The activation map shows the ectopic atrial tachycardia originating from non-septal TA (7 o'clock). The right superior electrograms show mid-septum (posterior area of coronary sinus ostium) was activated later than coronary sinus ostium. (C) The activation map shows an ectopic atrial tachycardia originating from the coronary sinus ostium.

and were thus significantly different from ATs originating from the lower CT showing a positive PWM. Activation mapping suggested that the right atrial depolarization vector during ATs with TA origin pointed from the TA to the posterior wall; meanwhile, the LA was activated via musculature in the vicinity of the CS using one of the three possible IAC pathways with an antero-posterior LA depolarization vector. In contrast, activation mapping during ATs of lower CT origin showed a reverse pattern of the depolarization vector in both atria and, consequently a positive PWM in leads V3–V6. We speculate that this may be explained by a forward left atrial depolarization vector caused by a preferential IAC through posterior fibres near the ostia of the right-sided PVs. Neither of the two ATs of lower free wall origin had either negative or positive P-waves in all leads V3–V6 which may relate to different locations of AT origin relative to possible interatrial sites of conduction.

Distribution of localization of atrial tachycardia foci in lower right atrium

It needs to be kept in mind that foci within the lower RA are an uncommon source of AT. In fact, in the present study, only 19% of 144 right atrial ATs originated from the lower RA. Therefore, the described distribution of AT origins within the lower RA is limited by sample size. In the paper by Kistler *et al.*,⁷ lower RA foci were more commonly located at the TA ($n = 38$), while CSo and lower CT accounted for $n = 16$ and $n = 4$ cases, respectively. While the CT is a common anatomic origin of RA tachycardia overall, AT from the lower CT is rare (below 10% of all CT foci⁷).

Conclusion

Characteristic PWMs, in all inferior leads combined with a positive or negative pattern in V3–V6 leads, may help to differentiate annular vs. more posterior anatomical sites of ATs from the lower RA with high PPVs and NPVs. P-wave morphology in V3–V6 is likely to be influenced by the employment of preferential conduction pathways between RA and LA.

Limitation

Activation mapping of the LA was not carried out during the electrophysiological study. However, the activation sequence of LA was mapped using the CS catheter and the interrelation of RA and LA activation could be assessed using the combination of CS- and 3D-map of the RA. Yet, the exact localization of the LA breakthrough during AT cannot be provided.

Acknowledgement

We appreciate Hedi Razavi, PhD for improving our English. We also appreciate Pyotr G Platonov, MD, PhD, FESC for valuable advice.

Conflict of interest: none declared.

References

- Chen SA, Chiang CE, Yang CJ, Cheng CC, Wu TJ, Wang SP et al. Sustained atrial tachycardia in adult patients. Electrophysiological characteristics, pharmacological response, possible mechanisms, and effects of radiofrequency ablation. *Circulation* 1994;**90**:1262–78.
- Kalman JM, Olgin JE, Karch MR, Hamdan M, Lee RJ, Lesh MD. 'Cristal tachycardias': origin of right atrial tachycardias from the crista terminalis identified by intracardiac echocardiography. *J Am Coll Cardiol* 1998;**31**:451–9.
- Matsuoka K, Kasai A, Fujii E, Omichi C, Okubo S, Teramura S et al. Electrophysiological features of atrial tachycardia arising from the atrioventricular annulus. *Pacing Clin Electrophysiol* 2002;**25**:440–5.
- Morton JB, Sanders P, Das A, Vohra JK, Sparks PB, Kalman JM. Focal atrial tachycardia arising from the tricuspid annulus: electrophysiologic and electrocardiographic characteristics. *J Cardiovasc Electrophysiol* 2001;**12**:653–9.
- Kistler PM, Fynn SP, Haqqani H, Stevenson IH, Vohra JK, Morton JB et al. Focal atrial tachycardia from the ostium of the coronary sinus: electrocardiographic and electrophysiological characterization and radiofrequency ablation. *J Am Coll Cardiol* 2005;**45**:1488–93.
- Frey B, Kreiner G, Gwechenberger M, Gossinger HD. Ablation of atrial tachycardia originating from the vicinity of the atrioventricular node: significance of mapping both sides of the interatrial septum. *J Am Coll Cardiol* 2001;**38**:394–400.
- Kistler PM, Roberts-Thomson KC, Haqqani HM, Fynn SP, Singarayar S, Vohra JK et al. P-wave morphology in focal atrial tachycardia: development of an algorithm to predict the anatomic site of origin. *J Am Coll Cardiol* 2006;**48**:1010–7.
- Akhtar M, Williams SV, Achord JL, Reynolds WA, Fisch C, Friesinger GC 2nd et al. Clinical competence in invasive cardiac electrophysiological studies. A statement for physicians from the acp/acc/aha task force on clinical privileges in cardiology. *Circulation* 1994;**89**:1917–20.
- Blomstrom-Lundqvist C, Scheinman MM, Aliot EM, Alpert JS, Calkins H, Camm AJ et al. ACC/AHA/ESC guidelines for the management of patients with supraventricular arrhythmias—executive summary. A report of the American College of Cardiology/American Heart Association task force on practice guidelines and the European Society of Cardiology committee for practice guidelines (writing committee to develop guidelines for the management of patients with supraventricular arrhythmias) developed in collaboration with NASPE-Heart Rhythm Society. *J Am Coll Cardiol* 2003;**42**:1493–531.
- Cosio FG, Anderson RH, Kuck KH, Becker A, Benditt DG, Bharati S et al. ESCWGA/NASPE/P Experts Consensus Statement: living anatomy of the atrioventricular junctions. A guide to electrophysiologic mapping. Working group of arrhythmias of the European Society of Cardiology. North American Society of Pacing and Electrophysiology. *J Cardiovasc Electrophysiol* 1999;**10**:1162–70.
- Tang CW, Scheinman MM, Van Hare GF, Epstein LM, Fitzpatrick AP, Lee RJ et al. Use of p wave configuration during atrial tachycardia to predict site of origin. *J Am Coll Cardiol* 1995;**26**:1315–24.
- Lemery R, Soucie L, Martin B, Tang AS, Green M, Healey J. Human study of biaxial electrical coupling: Determinants of endocardial septal activation and conduction over interatrial connections. *Circulation* 2004;**110**:2083–9.
- Dong J, Zrenner B, Schreieck J, Deisenhofer I, Karch M, Schneider M et al. Catheter ablation of left atrial focal tachycardia guided by electroanatomic mapping and new insights into interatrial electrical conduction. *Heart Rhythm* 2005;**2**:578–91.
- Hertervig E, Li Z, Kongstad O, Holm M, Olsson SB, Yuan S. Global dispersion of right atrial repolarization in healthy pigs and patients. *Scand Cardiovasc J* 2003;**37**:329–33.
- Maros TN, Racz L, Plugor S, Maros TG. Contributions to the morphology of the human coronary sinus. *Anat Anz* 1983;**154**:133–44.
- Antz M, Otomo K, Arruda M, Scherlag BJ, Pitha J, Tondo C et al. Electrical conduction between the right atrium and the left atrium via the musculature of the coronary sinus. *Circulation* 1998;**98**:1790–5.
- Ho SY, Sanchez-Quintana D. The importance of atrial structure and fibers. *Clin Anat* 2009;**22**:52–63.
- O'Donnell D, Bourke JP, Furniss SS. Interatrial transeptal electrical conduction: comparison of patients with atrial fibrillation and normal controls. *J Cardiovasc Electrophysiol* 2002;**13**:1111–7.

Paper IV



Variability of P-wave morphology predicts the outcome of circumferential pulmonary vein isolation in patients with recurrent atrial fibrillation

Yan Huo, M.D.,^{a, b, *} Fredrik Holmqvist, M.D., Ph.D.,^a Jonas Carlson, MSc, Ph.D.,^a Thomas Gaspar, M.D.,^b Gerhard Hindricks, M.D.,^c Christopher Piorowski, M.D.,^b Andreas Bollmann, M.D., Ph.D., FESC,^{c, 1} Pyotr G. Platonov, M.D., Ph.D., FHRS, FESC^{a, 1}

^a Department of Cardiology and Center for Integrative Electrocardiology at Lund University (CIEL), Lund University, Lund, Sweden

^b Department of Electrophysiology, Heart Center—University Dresden, Dresden, Germany

^c Department of Electrophysiology, Heart Center—University Leipzig, Leipzig, Germany

Abstract

Introduction: Severe atrial structural remodeling may reflect irreversible damage of the atrial tissue in patients with atrial fibrillation (AF) and is associated with changes of P-wave duration and morphology. Our aim was to study whether variability of P-wave morphology (PMV) is associated with outcome in patients with AF after circumferential PV isolation (CPVI).

Methods and results: 70 consecutive patients (aged 60 ± 9 years, 46 men) undergoing CPVI due to symptomatic AF were studied. After cessation of antiarrhythmic therapy, standard 12-lead ECG during sinus rhythm was recorded for 10 min at baseline and transformed to orthogonal leads. Beat-to-beat P-wave morphology was subsequently defined using a pre-defined classification algorithm. The most commonly observed P-wave morphology in a patient was defined as the dominant morphology. PMV was defined as the percentage of P waves with non-dominant morphology in the 10-min sample. At the end of follow-up, 53 of 70 patients had no arrhythmia recurrence. PMV was greater in patients without recurrence ($19.5 \pm 17.1\%$ vs. $8.2 \pm 6.7\%$, $p < 0.001$). In the multivariate logistic regression model, $PMV \geq 20\%$ (upper tertile) was the only independent predictor of ablation success (OR = 11.4, 95% CI 1.4–92.1, $p = 0.023$). A $PMV \geq 20\%$ demonstrated a sensitivity of 41.5%, a specificity of 94.1%, a PPV of 96.7%, and an NPV of 34.0% for free of AF after CPVI.

Conclusions: We report a significant association between increased PMV and 6-month CPVI success. PMV may help to identify patients with very high likelihood of freedom of AF 6-months after CPVI.

© 2015 Elsevier Inc. All rights reserved.

Keywords: Atrial fibrillation; P-wave morphology; Circumferential PV isolation; Variability of P-wave morphology

Introduction

Our understanding of atrial fibrillation (AF) pathophysiology has advanced significantly over the years through increased awareness of the role of atrial remodeling in the development of persistent change in atrial structure or function.

Many studies have explored the mechanism of the initiation and maintenance of AF [1–8]. Over the last decade, studies of radiofrequency catheter ablation for treatment of AF reported higher efficacy rates than did studies of antiarrhythmic drug therapy [9–12]. Circumferential pulmonary vein isolation

(CPVI) has been proven as the cornerstone of treatment of AF, regardless of stage of AF. However, CPVI *alone* has been shown to be insufficient for a considerable proportion of patients with AF [13–15], especially for those with persistent or permanent AF. Optimal criteria for patient selection for CPVI still remain debatable.

In the last two decades, many conventional markers have been also studied and reported as markers of structural remodeling in patients with AF and predict outcome of AF ablation, such as left atrial diameter, P-wave duration (PWD) and morphology, etc. However, there is still a lack of a suitable marker, which could reflect the turning point of ‘reversible-to-irreversible’ remodeling during the whole development of AF.

Further experimental studies also suggest that interatrial conduction defects play a role in the development of AF

* Corresponding author at: Department of Cardiology, Lund University, SE-221 85, Lund, Sweden.

E-mail address: dr.huoyan@googlemail.com

¹ These two authors contributed equally.

[16–19]; the global conduction abnormalities during sinus rhythm in patients or animal models with AF or atrial tachycardia have been also studied [20,21]. It is also worth to notice that in certain regions conduction velocity was significantly reduced [22]. These changes are associated with significant increase in AF vulnerability.

As conventional wisdom, atrial remodeling is continuously evolving in patients with AF, such as increasing of PWD or LA-diameter, or altered P wave morphology. Furthermore, sequence of atrial depolarization and duration of entire atrial depolarization decided the final P-wave morphology beat by beat. Mild or moderate remodeling may not change the P-wave morphology constantly. So we decided to study variability of P-wave morphology instead of P-wave morphology directly. From methodological view, one previous study conducted by our group, shows that orthogonal P-wave morphology derived from standard 12-lead ECG can be used to identify the left atrial breakthrough site and the corresponding route of interatrial conduction beat-by-beat [23].

We hypothesized that beat-to-beat variability of atrial depolarization route during sinus rhythm (SR) may reflect the degree of atrial remodeling and thus might be associated with outcome of AF ablation.

Methods

Study group

Between January 2010 and June 2010, 70 consecutive patients (aged 60 ± 9 years, range 31–79 years, 46 men) undergoing clinically motivated CPVI due to highly symptomatic drug-refractory atrial fibrillation at heart center Leipzig were included in this study. All patients gave written informed consent on the investigational nature of the procedure that was approved by the institutional review committee. All antiarrhythmic drugs were discontinued at least five half-lives prior to the study, including beta-blocker and digitalis, and none of the patients were taking amiodarone.

Exclusion criteria were: (1) severe valve disease (e.g. greater than mitral insufficiency II°); (2) acute heart failure; (3) any previous ablation procedure affecting the atria; and (4) previous surgery on heart, esophagus or lung.

Data acquisition and P-wave analysis

After sedation using midazolam and propofol, standard 12-lead electrocardiogram (ECG) was recorded continuously using the Prucka CardioLab System (GE Medical Systems, Milwaukee, WI, USA) for 10 min at baseline, when patients were in SR at the beginning of the electrophysiological study. In patients with atrial fibrillation at baseline, electrical cardioversion was performed in order to achieve stable SR and analyze characteristics of P wave at SR. These data were stored for subsequent offline processing. Data were analyzed using custom-made software running on MATLAB (The MathWorks, Natick, MA, USA). To enable analysis of orthogonal P-wave morphology, orthogonal-lead ECG data were derived from the 12-lead ECG using the inverse Dower transform [24,25]. Unfiltered, signal-averaged P waves were analyzed to determine P-wave morphology [24,26–28].

Following high-pass (0.5 Hz) and band-stop (50 Hz) filtering, QRS complexes were automatically identified and grouped according to similarity (cross-correlation coefficient > 0.9). P waves were extracted using 250 ms-wide signal windows preceding each QRS complex. The signal windows were then shifted in time to estimate the maximal correlation in each lead. P waves with cross-correlation coefficient > 0.9 (analyzed separately in all leads) were grouped together and averaged. Actual P waves were defined by manual setting of onset and end. P wave duration was measured manually by two of the investigators without knowledge of the history of AF. Any differences between observers were resolved by consensus. The method used in this study is described in detail elsewhere [24,26,27].

Variability of orthogonal P-wave morphology and classification of orthogonal P wave morphology

After the ECGs were transformed to orthogonal leads, beat-to-beat P-wave morphology was defined automatically depending on P-wave polarity in orthogonal leads (positive/negative/biphasic) in accordance with a pre-defined classification algorithm. The morphology subsequently was classified into one of five pre-defined classes [23]:

- Type 1: Positive leads X and Y and negative lead Z
- Type 2: Positive leads X and Y and biphasic lead Z (-/+)
- Type 3: Positive lead X and biphasic signals in leads Y (-/+) and Z (-/+)
- Type 4: Positive lead X, Y and Z [29]
- Atypical: Any morphology in lead X, Y and Z, except type 1 to 4

The four different types are schematically illustrated in Fig. 1. The most common P-wave morphology observed in each patient during the 10-min recording was defined as the dominant morphology. Variability of orthogonal P-wave morphology (PMV) was defined as the percentage of P waves with non-dominant morphology in the 10-min sample. All analyses were performed in a blinded fashion. Standard transthoracic echocardiography was performed in association with ablation. Fig. 2 was a sample of change of orthogonal P-wave morphology during 10-min recording.

Mapping and ablation procedure

Transesophageal echocardiography was performed to exclude the presence of thrombus within the left atrium. Patients were studied under deep sedation. Standard catheters were placed in the right ventricular apex and the coronary sinus. Antiarrhythmic drugs were not given for peri-procedural rhythm stabilization.

Mapping and ablation were performed under the guidance of 3-D mapping systems (CARTO 3, Biosense Webster, Inc., Diamond Bar, CA, USA or Ensite-Velocity, Endocardial Solutions, Inc., St. Paul, MN, USA.) supplemented by 3-D image integration as described previously (CARTO: $n = 11$, NavX: $n = 59$) [30]. A temperature probe in the esophagus (FIAB, St. Jude Medical, Inc., Florence, Italy) at the level of the left atrium tagged the esophageal location and provided

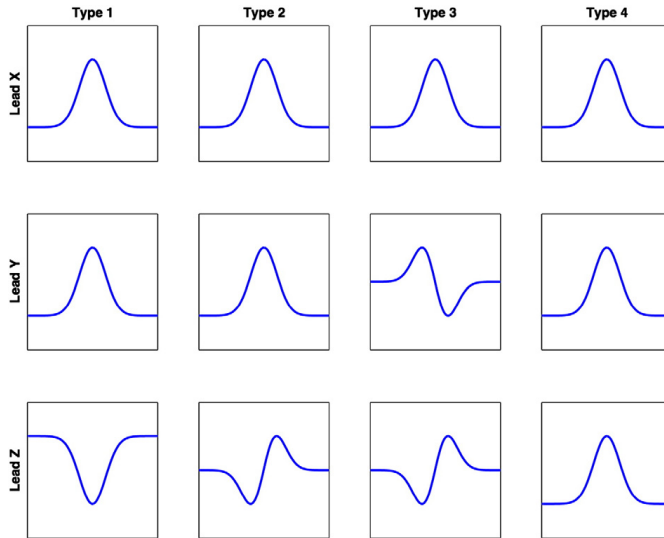


Fig. 1. The four different types are schematically illustrated.

intraesophageal temperature feedback during the procedure. Ablation lines were adapted to avoid RF delivery in close vicinity to the esophagus [31].

Radiofrequency alternating current was delivered in a unipolar mode between the irrigated tip electrode of the ablation catheter (F-Type, irrigated tip, Navi-Star Thermocool, Biosense Webster, Diamond Bar, California, USA; M-Curve IBI Therapy Cool-Flex, St. Jude Medical, Inc., St. Paul, Minnesota, USA) and an external back-plate electrode. The standard ablation setting consisted of pre-selected catheter tip temperature of 48 °C, power of 40 W, and flow rate of 30 ml/min (17 ml/min for IBI Therapy Cool-Flex catheter). Near the esophagus, power delivery was reduced to 30 W and 20 ml/min, and further adapted according to actual temperature increase.

Catheter navigation was performed with steerable sheath technology in all patients (Agilis, St. Jude Medical, Inc., St. Paul, Minnesota, USA) [32]. For initial ablation line placement, the catheter tip was dragged along the intended lesion line according to local bipolar amplitude reduction. Therefore, multiple sites were ablated with each initiation of RF energy delivery.

Ablation line concept and procedural end point

Circumferential ablation around both ipsilateral pulmonary veins (PVs) was performed in all patients. The level of ablation was chosen at the atrial side of the PV antrum as indicated by information combined from the integrated 3-D image, the fluoroscopic cardiac silhouette, tactile catheter feedback, catheter impedance changes, and PV–atrium electrogram characteristics.

Post-procedural care and follow-up

After ablation, a continuous 7-day Holter ECG (Lifecard CF, DelmarReynolds Medical Inc, Irvine, California, USA) was recorded in all patients. The continuous 7-day Holter ECG was repeated after 3 and 6 months. In case of symptoms outside the recording period, patients were advised to contact our institution or the referring physician to obtain ECG documentation. Documentations of AF and/or atypical atrial flutter (AFL) longer than 30 s were considered an episode of sustained AF and/or atypical AFL recurrence. As part of our study protocol, the antiarrhythmic medication was discontinued after ablation, and patients received a beta-blocker, if tolerated. Re-ablations for symptomatic drug refractory recurrences of AF and AFL were scheduled after at least 3 months of follow-up. Starting the day after the ablation procedure, patients received oral anticoagulation with an International Normalized Ratio of 2.0 to 3.0. Anticoagulation was discontinued after 3 months of follow-up according to CHADS2 score.

Statistics

All data with normal distribution are expressed as means \pm SD. Data without normal distribution are expressed as median and range. Sample distributions were tested using the Shapiro–Wilk test. Data without normal distribution were tested using a non-parametric test. Intergroup comparisons were performed using the Two-Independent-Samples test (Mann–Whitney U test). Possible correlations between variables were tested using the spearman correlation test (two-tailed test). Outcome-related values of a set of predictor variables were evaluated by multivariate logistic regression

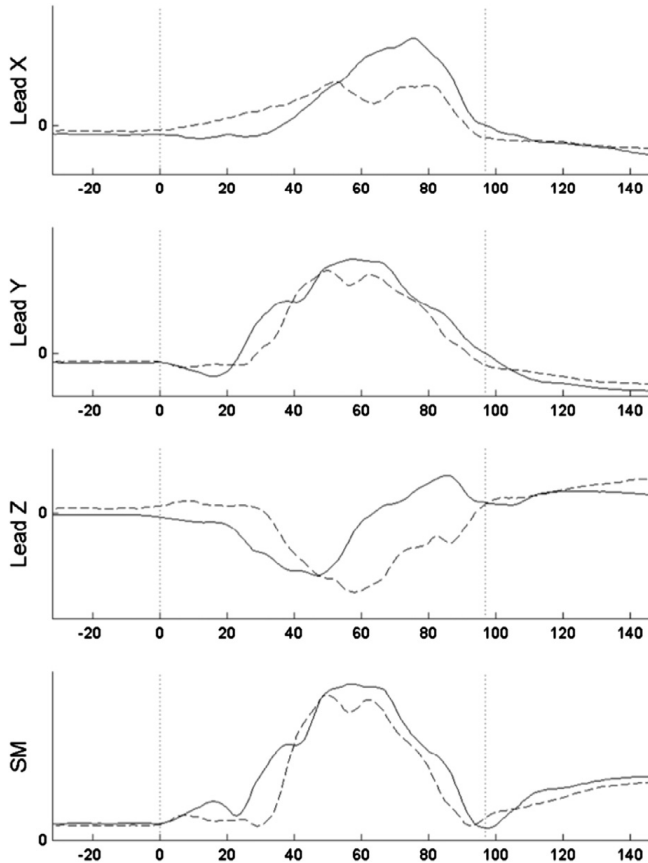


Fig. 2. Changing of orthogonal P-wave morphology. P-wave morphology in lead Z from negative/positive switched to completely negative, which presented the change of dominant type (Type 2 P-wave morphology, solid line) to the secondary type (Type 1 P-wave morphology, dashed line).

(binary logistic regression). Sensitivity was defined as a probability that a test result will be positive, when free of AF after CPVI is present (true positive rate). Specificity was defined as a probability that a test result will be negative, when free of AF after CPVI is not present (true negative rate). Positive predictive value (PPV) was defined as a probability that free of AF after CPVI is present when the test is positive. Negative predictive value (NPV) was defined as a probability that free of AF after CPVI is not present when the test is negative. A P value of < 0.05 was considered significant.

Results

Patients' characteristics and ablation outcome

The patient characteristics are described in Table 1. All patients ($n = 70$) received a CPVI alone without any extra linear ablation. Fifty (71%) patients suffered from paroxysmal

AF and 20 patients (29%) suffered from persistent AF. None of the patients with previous diagnosis of heart failure had decompensation during hospital admission or the 6-month follow-up. Forty-eight of 50 patients with paroxysmal AF had SR at the beginning of the procedure and 22 patients (2 with paroxysmal and all 20 with persistent AF) had AF at the beginning of the procedure. In all 70 patients (100%), acute successful PV-Isolation was achieved, and at least 6 months of follow-up was completed. Recurrence of atrial arrhythmias (including recurrence of AF and atypical atrial flutter) by 6-month follow-up was observed in 11 patients (22.9%) with paroxysmal AF, and in 6 patients (27.3%) with persistent AF ($p = 0.695$).

P-wave duration and type of P-wave morphology

The P-wave duration (PWD) was 150 ± 18 ms in all patients. The PWD in patients with SR at the beginning of

Table 1
Comparison between patients with recurrence and no recurrence of atrial arrhythmias.

	No Recurrence at 6 months (n = 53)	Recurrence at 6 months (n = 17)	p-value
Age (year)	60 ± 7	58 ± 12	0.356
Gender (male)	32 (60.4%)	14 (82.4%)	0.099
BMI	29 ± 4	28 ± 5	0.360
AF History (month)	56 ± 64	66 ± 74	0.574
Type of AF (paroxysmal AF)	40 (75.5%)	10 (58.8%)	0.189
Hypertension	42 (79.2%)	14 (82.4%)	0.782
Diabetes	8 (15.1%)	1 (5.9%)	0.327
Coronary artery disease	9 (17.0%)	2 (11.8%)	0.610
Chronic heart failure	1 (1.9%)	2 (11.8%)	0.070
Mitral valve insufficient	1 (1.9%)	1 (5.9%)	0.393
ECHO			
LA-diameter before CPVI (mm)	43 ± 6	45 ± 5	0.894
LA-diameter at 6 months after CPVI (mm)	40 ± 5	44 ± 7	0.330
LVEF% before CPVI	61 ± 8	54 ± 10	0.007 [#]
LVEF% at 6 months after CPVI	62 ± 5	59 ± 11	0.332
CPVI			
Initial Rhythm (SR)	37 (69.8%)	11 (64.7%)	0.695
Procedure Time (min)	138 ± 48	142 ± 52	0.773
Fluoroscopy Time (min)	27 ± 11	36 ± 19	0.087
Before CPVI			
Oral anticoagulation	30 (62.5%)	13 (76.5%)	0.285
Statin	21 (39.6%)	4 (23.5%)	0.232
ACEI/ARB	36 (67.9%)	10 (58.8%)	0.495
Antiarrhythmics			
Total	48 (90.6%)	17 (100%)	0.871
Class IC	1 (1.9%)	0	0.571
Class II	47 (88.7%)	17 (100%)	0.150

BMI: body mass index. AF: atrial fibrillation. LA: left atrium, CPVI: circumferential pulmonary vein isolation. LVEF: left ventricular ejection fraction. SR: sinus rhythm.

the procedure (n = 48) was significantly shorter than in patients with initial AF (n = 22) in whom the PWD was measured after cardioversion (144 ± 16 vs. 162 ± 17 ms, p < 0.001). The PWD in patients with diagnosis of paroxysmal AF (n = 50) was significantly shorter than with persistent AF (n = 20) (145 ± 16 vs. 162 ± 17 ms, p < 0.001). However, there was no significant difference in PWD between patients with recurrence (n = 17) and those with non-recurrence (n = 53) during the 6-month follow-up (155 ± 23 vs. 149 ± 16 ms, p = 0.241).

There was no significant difference in the type of P-waves observed between patients with paroxysmal vs. persistent

AF, initial SR vs. AF or recurrence vs. non-recurrence of atrial arrhythmias after CPVI during the 6-month follow-up. (Table 2)

Variability of orthogonal P-wave morphology

The PMV in patients (n = 53) without recurrence of atrial arrhythmias after CPVI during the 6-month follow-up was greater than in patients (n = 17) with recurrence (19.5 ± 17.1% vs. 8.2 ± 6.7%, p < 0.001). However, no significant difference was observed between patients with initial SR (n = 48) vs. initial AF (n = 22) (14.7 ± 14.0% vs. 21.3 ± 19.1%, p = 0.159) or with paroxysmal (n = 50) vs. persistent AF (n = 20) (15.7 ± 15.3% vs. 19.6 ± 17.5%, p = 0.351). In the univariate analysis, PMV significantly correlated to AF history duration and baseline LA diameter (R = -0.254, p = 0.036; R = -0.355, p = 0.005 respectively), but the correlations were weak.

Predictor of ablation outcome

A PMV ≥ 20% (upper tertile) demonstrated a sensitivity of 41.5%, a specificity of 94.1%, a PPV of 96.7%, and an NPV of 34.0% for free of AF after CPVI. In the multivariate logistic regression model, PMV ≥ 20% was the only independent predictor of ablation success (OR = 11.4, 95% CI 1.4–92.1, p = 0.023). None of other clinical characteristics such as age, gender, BMI, left atrial diameter, type of AF or AF history duration were associated with the outcome.

Discussion

Main findings

We report a significant association between increased variability of P-wave morphology and better outcome of CPVI at 6-months follow-up. A cut-off value of PMV ≥ 20% identifies patients with a very high likelihood of freedom of AF 6-months after CPVI. Reduced variability of P-wave morphology, probably meaning rigid and invariable propagation of atrial activation during SR in patients with recurrent AF, is likely to reflect severe structural remodeling.

Baseline P-wave duration

The baseline PWD in patients with persistent AF is prominently longer as compared to PWD in patients with paroxysmal AF, which is in agreement with previous studies

Table 2
Type of P-wave morphology.

	Type of P-waves				p value
	Type 1	Type 2	Type 4	Atypical	
Rhythm at baseline: SR (n = 48)	6 (12.5%)	32 (66.7%)	7 (14.6%)	3 (6.3%)	0.359
AF (n = 22)	1 (4.5%)	16 (72.7%)	0 (0%)	5 (22.7%)	
Clinical type of AF: Paroxysmal AF (n = 50)	5 (10%)	34 (68%)	7 (14%)	4 (8%)	0.937
Persistent AF (n = 20)	2 (10%)	14 (70%)	0 (0%)	4 (20%)	
Follow-Up at 6 months: No Recurrence (n = 53)	5 (9.4%)	36 (67.9%)	6 (11.3%)	6 (11.3%)	0.671
Recurrence (n = 17)	2 (11.8%)	12 (70.6%)	1 (5.9%)	2 (11.8%)	

SR: sinus rhythm, AF: atrial fibrillation.

[33,34]. Several studies also focused on baseline PWD and AF using either standard or signal-averaged ECG [35–38]. Notably, Magnani et al. [38] studied P-wave indices of maximum duration and dispersion in 1550 Framingham Heart Study participants ≥ 60 years old (58% women) from single-channel ECG recorded from 1968 through 1971. In that analysis, maximum P-wave duration at the upper fifth percentile was associated with long-term AF risk in an elderly community-based cohort. P-wave duration is an electrocardiographic endophenotype for AF. In our study, a vast majority of patients had normal LVEF; majority had PAF (71%) with mild LA dilatation, while the rest of the cohort had persistent AF (29%) with mild to moderate LA dilatation. This risk profile indicates that our patients had less diseased atria and lower risk of AF recurrence. Because of lack of significantly prolonged P-wave duration at baseline, we may not be able to detect the relationship between the outcome of CPVI and baseline PWD.

Orthogonal P-wave morphology

The dominant type of orthogonal P-wave morphology was characterized by the biphasic P-waves in the lead Z (type 2) regardless of the type of AF, with or without electrical cardioversion or recurrence after CPVI, which is also in accordance with our previous findings [39,40]. Moreover, baseline dominant P-wave morphology *per se* was not related to the recurrence of atrial arrhythmias after CPVI.

The distribution of P-wave morphology types was compared between patients with initial SR and AF, with paroxysmal and persistent AF, or with and without recurrence of atrial arrhythmias after CPVI. No notable difference was observed in any of the comparisons. We speculate that neither the main type nor the distribution of type of orthogonal P-wave morphology predicts the outcome after CPVI.

Variability of orthogonal P-wave morphology

In previous studies, interatrial conduction defects have been suggested to play a role in the development of AF [16–19]. Different P-wave morphologies during SR as displayed on standard ECGs have been postulated to correspond to differences in interatrial conduction [41–43]. A previous study from our group shows that orthogonal P-wave morphology can be used to correctly identify the left atrial breakthrough site and the corresponding route of interatrial conduction [23]. PMV may be related to a number of factors such as the origin of SR within the right atrium, its proximity to the interatrial connections and anatomical variability of those as reviewed recently [44]. In summary, the PMV in our method likely reflects switch between different interatrial paths (either due to functional block in any of them or due to variability in the sinus rhythm origin). Increasing fibrosis etc. would both limit the possibility to conduct through different paths and limit the potential number of exits from sinus node, both leading to a more stable or rigid activation pattern during sinus rhythm.

Based on the findings above, we introduced the current method to quantify the variability of employment of preferential

interatrial conduction pathways using pre-defined orthogonal P-wave morphologies in order to detect the relation between the beat-to-beat variability of atrial activation pattern and the outcome of CPVI at 6 months.

Atrial structural remodeling has been considered as the main contributor for initiation and persistence of AF, and might be present before start of AF caused by associated diseases [45–47]. Structural remodeling that is consistently seen in models of AF and in patients with AF includes atrial enlargement, cellular hypertrophy, dedifferentiation, fibrosis, apoptosis, and myolysis [48–57]. These structural changes are unlikely to be completely reversible [58].

Our method brings up a new ECG marker, which, in the context of AF, may reflect the level of AF substrate deterioration, and, if independently replicated, be able to detect the appropriate patients for CPVI alone, which could be sufficient for reaching clinical success. High PMV observed in patients who benefited from CPVI may reflect less advanced structural remodeling and greater amount of preserved atrial myocardium that allows variable propagation of sinus pulses across the atria. The exact reason for the high PMV may not be completely understood at this time. In our study, we sought to define variability as a switch between the distinct morphological classes of P-waves that have previously been linked to different left atrial breakthrough sites during SR and suggest variation in employment of different interatrial routes [23] that may occur on a beat-to-beat basis.

A recent pathology study has documented strong association between the persistency of AF and the extent of structural changes in atrial myocardium that affects both right and left atrium, so that the degree of fibro-fatty replacement of atrial myocardium may exceed 50% in patients with long-standing AF [59]. Along with progression of structural remodeling and fibro-fatty replacement of atrial myocardium, the number of uninterrupted myocardial fibers available for conduction is likely to be reduced, which may lead to reduced variability of atrial activation patterns, i.e. reduced PMV. The strong association between reduced PMV and failure of CPVI suggests that this novel ECG marker of atrial conduction may reflect the degree of atrial remodeling, which is especially important in view of the fact that conventional ECG markers of atrial abnormalities such as P-wave duration or dominant P-wave morphology appeared to be abnormal at baseline and failed to identify patients who would benefit from CPVI.

Clinical implications

Identifying reliable predictors of recurrence of atrial arrhythmias following CPVI may improve the patient selection strategy and therefore improve the overall success rate of the method. We have shown for the first time that a simple marker of the variability of propagation of atrial activation is significantly associated with recurrence of atrial arrhythmias. Damaged interatrial conduction has been suggested to play a role in the development of AF [16–19], and may therefore also be an indicator of the level of damaged

interatrial conduction to predict recurrence of atrial arrhythmias after CPVI. This is the first report, and further studies are required.

Limitations

Patients included in our study represent a relatively low risk cohort with *a priori* high probability of catheter ablation success and without advanced atrial remodeling, which affects generalizability of our study findings. Secondly, in a significant minority of patients, PMV was assessed following preprocedural cardioversion and could have been influenced by incomplete restoration of atrial electrophysiological properties. However, we did not observe any significant difference in PMV between patients who arrived to the electrophysiological lab in SR and those who underwent cardioversion. Nevertheless, we consider the study as hypothesis-generating and believe that it motivates further studies on larger samples in order to independently replicate our findings.

Conclusions

We report a significant association between PMV and 6-month CPVI success. PMV \geq 20% offers a low sensitivity and negative predictive value, but very high specificity and positive predictive value for freedom of AF after CPVI. Low PMV in patients with recurrent AF is likely to reflect severe structural remodeling and explain the failure of CPVI. Our findings warrant further studies of PMV as a marker of atrial remodeling that may be used to predict ablation success. The impact of interatrial conduction state on the overall success rate of CPVI needs further elucidation.

Conflict of interest

None declared.

References

- [1] Olsson SB, Omdahl G, Ernstrom S, Eskilsson J, Persson S, Grenner ML, et al. Spontaneous reversion from long-lasting atrial fibrillation to sinus rhythm. *Acta Med Scand* 1980;207:5–20.
- [2] Chen J, Mandapati R, Berenfeld O, Skanes AC, Gray RA, Jalife J. Dynamics of wavelets and their role in atrial fibrillation in the isolated sheep heart. *Cardiovasc Res* 2000;48:220–32.
- [3] Anyukhovsky EP, Sosunov EA, Chandra P, Rosen TS, Boyden PA, Danilo Jr P, et al. Age-associated changes in electrophysiologic remodeling: a potential contributor to initiation of atrial fibrillation. *Cardiovasc Res* 2005;66:353–63.
- [4] Roberts-Thomson KC, Stevenson IH, Kistler PM, Haqqani HM, Goldblatt JC, Sanders P, et al. Anatomically determined functional conduction delay in the posterior left atrium relationship to structural heart disease. *J Am Coll Cardiol* 2008;51:856–62.
- [5] Rha SW, Kim YH, Hong MK, Ro YM, Choi CU, Suh SY, et al. Mechanisms responsible for the initiation and maintenance of atrial fibrillation assessed by non-contact mapping system. *Int J Cardiol* 2008;124:218–26.
- [6] Yamazaki M, Vaquero LM, Hou L, Campbell K, Zlochiver S, Klos M, et al. Mechanisms of stretch-induced atrial fibrillation in the presence and the absence of adrenergic stimulation: interplay between rotors and focal discharges. *Heart Rhythm* 2009;6:1009–17.
- [7] Yamabe H, Morihisa K, Koyama J, Enomoto K, Kanazawa H, Ogawa H. Analysis of the mechanisms initiating random wave propagation at the onset of atrial fibrillation using noncontact mapping: role of complex fractionated electrogram region. *Heart Rhythm* 2011;8:1228–36.
- [8] Olgin JE, Sih HJ, Hanish S, Jayachandran JV, Wu J, Zheng QH, et al. Heterogeneous atrial denervation creates substrate for sustained atrial fibrillation. *Circulation* 1998;98:2608–14.
- [9] Reynolds MR, Zimetbaum P, Josephson ME, Ellis E, Danilov T, Cohen DJ. Cost-effectiveness of radiofrequency catheter ablation compared with antiarrhythmic drug therapy for paroxysmal atrial fibrillation. *Circ Arrhythm Electrophysiol* 2009;2:362–9.
- [10] Calkins H, Reynolds MR, Spector P, Sondhi M, Xu Y, Martin A, et al. Treatment of atrial fibrillation with antiarrhythmic drugs or radiofrequency ablation: two systematic literature reviews and meta-analyses. *Circ Arrhythm Electrophysiol* 2009;2:349–61.
- [11] Khaykin Y, Wang X, Natale A, Wazni OM, Skanes AC, Humphries KH, et al. Cost comparison of ablation versus antiarrhythmic drugs as first-line therapy for atrial fibrillation: an economic evaluation of the RAAFT pilot study. *J Cardiovasc Electrophysiol* 2009;20:7–12.
- [12] Jons C, Hansen PS, Johannessen A, Hindricks G, Raatikainen P, Kongstad O, et al. The Medical ANtiarrhythmic Treatment or Radiofrequency Ablation in Paroxysmal Atrial Fibrillation (MANTRA-PAF) trial: clinical rationale, study design, and implementation. *Europace* 2009;11:917–23.
- [13] Mulder AA, Wijffels MC, Wever EF, Boersma LV. Pulmonary vein isolation and left atrial complex-fractionated atrial electrograms ablation for persistent atrial fibrillation with phased radio frequency energy and multi-electrode catheters: efficacy and safety during 12 months follow-up. *Europace* 2011;13:1695–702.
- [14] Hayward RM, Upadhyay GA, Mela T, Ellinor PT, Barrett CD, Heist EK, et al. Pulmonary vein isolation with complex fractionated atrial electrogram ablation for paroxysmal and nonparoxysmal atrial fibrillation: a meta-analysis. *Heart Rhythm* 2011;8:994–1000.
- [15] Willems S, Klemm H, Rostock T, Brandstrup B, Ventura R, Steven D, et al. Substrate modification combined with pulmonary vein isolation improves outcome of catheter ablation in patients with persistent atrial fibrillation: a prospective randomized comparison. *Eur Heart J* 2006;27:2871–8.
- [16] O'Donnell D, Bourke JP, Furniss SS. Interatrial transeptal electrical conduction: comparison of patients with atrial fibrillation and normal controls. *J Cardiovasc Electrophysiol* 2002;13:1111–7.
- [17] Papageorgiou P, Monahan K, Anselme F, Kirchhof C, Josephson ME. Electrophysiology of atrial fibrillation and its prevention by coronary sinus pacing. *Semin Interv Cardiol* 1997;2:227–32.
- [18] Papageorgiou P, Anselme F, Kirchhof CJ, Monahan K, Rasmussen CA, Epstein LM, et al. Coronary sinus pacing prevents induction of atrial fibrillation. *Circulation* 1997;96:1893–8.
- [19] Agarwal YK, Aronow WS, Levy JA, Spodick DH. Association of interatrial block with development of atrial fibrillation. *Am J Cardiol* 2003;91:882.
- [20] Monigatti-Tenkorang J, Jousset F, Pascale P, Vesin JM, Ruchat P, Fromer M, et al. Intermittent atrial tachycardia promotes repolarization alternans and conduction slowing during rapid rates, and increases susceptibility to atrial fibrillation in a free-behaving sheep model. *J Cardiovasc Electrophysiol* 2014;25:418–27.
- [21] Lalani GG, Schrick A, Gibson M, Rostamian A, Krummen DE, Narayan SM. Atrial conduction slows immediately before the onset of human atrial fibrillation: a bi-atrial contact mapping study of transitions to atrial fibrillation. *J Am Coll Cardiol* 2012;59:595–606.
- [22] Medi C, Kalman JM, Spence SJ, Teh AW, Lee G, Bader I, et al. Atrial electrical and structural changes associated with longstanding hypertension in humans: implications for the substrate for atrial fibrillation. *J Cardiovasc Electrophysiol* 2011;22:1317–24.
- [23] Holmqvist F, Husser D, Tapanainen JM, Carlson J, Jurkko R, Xia Y, et al. Interatrial conduction can be accurately determined using standard 12-lead electrocardiography: validation of P-wave morphology using electroanatomic mapping in man. *Heart Rhythm* 2008;5:413–8.
- [24] Carlson J, Havmoller R, Herreros A, Platonov P, Johansson R, Olsson B. Can orthogonal lead indicators of propensity to atrial

- fibrillation be accurately assessed from the 12-lead ECG? *Europace* 2005;7(Suppl 2):39–48.
- [25] Edenbrandt L, Pahlm O. Vectorcardiogram synthesized from a 12-lead ECG: superiority of the inverse Dower matrix. *J Electrocardiol* 1988;21:361–7.
- [26] Havmoller R, Carlson J, Holmqvist F, Herreros A, Meurling CJ, Olsson B, et al. Age-related changes in P wave morphology in healthy subjects. *BMC Cardiovasc Disord* 2007;7:22–4.
- [27] Holmqvist F, Platonov PG, Carlson J, Havmoller R, Waktare JE, McKenna WJ, et al. Variable interatrial conduction illustrated in a hypertrophic cardiomyopathy population. *Ann Noninvasive Electrocardiol* 2007;12:227–36.
- [28] Holmqvist F, Platonov PG, Havmoller R, Carlson J. Signal-averaged P wave analysis for delineation of interatrial conduction — further validation of the method. *BMC Cardiovasc Disord* 2007;7:29–33.
- [29] Platonov PG, Christensen AH, Holmqvist F, Carlson J, Haunso S, Svendsen JH. Abnormal atrial activation is common in patients with arrhythmogenic right ventricular cardiomyopathy. *J Electrocardiol* 2011;44:237–41.
- [30] Piorkowski C, Kircher S, Arya A, Gaspar T, Esato M, Riahi S, et al. Computed tomography model-based treatment of atrial fibrillation and atrial macro-re-entrant tachycardia. *Europace* 2008;10:939–48.
- [31] Kottkamp H, Piorkowski C, Tanner H, Kobza R, Dorszewski A, Schirdewahn P, et al. Topographic variability of the esophageal left atrial relation influencing ablation lines in patients with atrial fibrillation. *J Cardiovasc Electrophysiol* 2005;16:146–50.
- [32] Piorkowski C, Kottkamp H, Gerdts-Li JH, Arya A, Sommer P, Dagues N, et al. Steerable sheath catheter navigation for ablation of atrial fibrillation: a case-control study. *Pacing Clin Electrophysiol* 2008;31:863–73.
- [33] Santoni-Rugin F, Verma R, Mehta D, Gopal A, Chan EK, Pe E, et al. Signal-averaged P-wave ECG discriminates between persistent and paroxysmal atrial fibrillation. *J Electrocardiol* 2001;34:189–95.
- [34] Vincenti A, Rota M, Spinelli M, Corciulo M, De Ceglia S, Rovaris G, et al. A noninvasive index of atrial remodeling in patients with paroxysmal and persistent atrial fibrillation: a pilot study. *J Electrocardiol* 2012;45:109–15.
- [35] Steinberg JS, Zelenkofske S, Wong SC, Gelernt M, Sciacca R, Menchavez E. Value of the P-wave signal-averaged ECG for predicting atrial fibrillation after cardiac surgery. *Circulation* 1993;88:2618–22.
- [36] Ogawa H, Inoue T, Yoshida A, Doi T, Ohga N, Ohnishi Y, et al. The signal-averaged electrocardiogram of P wave in patients with documented atrial fibrillation or flutter and in patients with left or right atrial overload without atrial fibrillation. *Jpn Heart J* 1993;34:29–39.
- [37] Van Beeumen K, Houben R, Tavernier R, Ketels S, Duytschaever M. Changes in P-wave area and P-wave duration after circumferential pulmonary vein isolation. *Europace* 2010;12:798–804.
- [38] Magnani JW, Johnson VM, Sullivan LM, Gorodeski EZ, Schnabel RB, Lubitz SA, et al. P wave duration and risk of longitudinal atrial fibrillation in persons \geq 60 years old (from the Framingham Heart Study). *Am J Cardiol* 2011;107:917–21 [e911].
- [39] Platonov PG, Carlson J, Ingemansson MP, Roijer A, Hansson A, Chreikin LV, et al. Detection of inter-atrial conduction defects with unfiltered signal-averaged P-wave ECG in patients with lone atrial fibrillation. *Europace* 2000;2:32–41.
- [40] Holmqvist F, Olesen MS, Tveit A, Enger S, Tapanainen J, Jurkko R, et al. Abnormal atrial activation in young patients with lone atrial fibrillation. *Europace* 2011;13:188–92.
- [41] Husson J, Froment C. Partial interatrial block due to a conduction defect of the preferential middle interatrial depolarization pathway. *Arch Mal Coeur Vaiss* 1985;78:1569–74.
- [42] Ariyaratna V, Apiyasawat S, Puri P, Spodick DH. Specific electrocardiographic markers of P-wave morphology in interatrial block. *J Electrocardiol* 2006;39:380–4.
- [43] Bayes de Luna A, Fort de Ribot R, Trilla E, Julia J, Garcia J, Sadurni J, et al. Electrocardiographic and vectorcardiographic study of interatrial conduction disturbances with left atrial retrograde activation. *J Electrocardiol* 1985;18:1–13.
- [44] Platonov PG. P-wave morphology: underlying mechanisms and clinical implications. *Ann Noninvasive Electrocardiol* 2012;17:161–9.
- [45] Anne W, Willems R, Roskams T, Sergeant P, Herijgers P, Holemans P, et al. Matrix metalloproteinases and atrial remodeling in patients with mitral valve disease and atrial fibrillation. *Cardiovasc Res* 2005;67:655–66.
- [46] Sanders P, Morton JB, Davidson NC, Spence SJ, Vohra JK, Sparks PB, et al. Electrical remodeling of the atria in congestive heart failure: electrophysiological and electroanatomic mapping in humans. *Circulation* 2003;108:1461–8.
- [47] Vaziri SM, Larson MG, Lauer MS, Benjamin EJ, Levy D. Influence of blood pressure on left atrial size. The Framingham Heart Study. *Hypertension* 1995;25:1155–60.
- [48] Ausma J, Wijffels M, Thone F, Wouters L, Allessie M, Borgers M. Structural changes of atrial myocardium due to sustained atrial fibrillation in the goat. *Circulation* 1997;96:3157–63.
- [49] Li D, Fareh S, Leung TK, Nattel S. Promotion of atrial fibrillation by heart failure in dogs: atrial remodeling of a different sort. *Circulation* 1999;100:87–95.
- [50] Schoonderwoerd BA, Ausma J, Crijns HJ, Van Veldhuisen DJ, Blaauw EH, Van Gelder IC. Atrial ultrastructural changes during experimental atrial tachycardia depend on high ventricular rate. *J Cardiovasc Electrophysiol* 2004;15:1167–74.
- [51] Anne W, Willems R, Holemans P, Beckers F, Roskams T, Lenaerts I, et al. Self-terminating AF depends on electrical remodeling while persistent AF depends on additional structural changes in a rapid atrially paced sheep model. *J Mol Cell Cardiol* 2007;43:148–58.
- [52] Morillo CA, Klein GJ, Jones DL, Guiraudon CM. Chronic rapid atrial pacing. Structural, functional, and electrophysiological characteristics of a new model of sustained atrial fibrillation. *Circulation* 1995;91:1588–95.
- [53] Everett TH, Li H, Mangrum JM, McRury ID, Mitchell MA, Redick JA, et al. Electrical, morphological, and ultrastructural remodeling and reverse remodeling in a canine model of chronic atrial fibrillation. *Circulation* 2000;102:1454–60.
- [54] Bauer A, McDonald AD, Donahue JK. Pathophysiological findings in a model of persistent atrial fibrillation and severe congestive heart failure. *Cardiovasc Res* 2004;61:764–70.
- [55] Moe GW, Laurent G, Doumanovskaia L, Konig A, Hu X, Dorian P. Matrix metalloproteinase inhibition attenuates atrial remodeling and vulnerability to atrial fibrillation in a canine model of heart failure. *J Card Fail* 2008;14:768–76.
- [56] Boyden PA, Tilley LP, Pham TD, Liu SK, Fenoglio Jr JJ, Wit AL. Effects of left atrial enlargement on atrial transmembrane potentials and structure in dogs with mitral valve fibrosis. *Am J Cardiol* 1982;49:1896–908.
- [57] Boyden PA, Tilley LP, Albalá A, Liu SK, Fenoglio Jr JJ, Wit AL. Mechanisms for atrial arrhythmias associated with cardiomyopathy: a study of feline hearts with primary myocardial disease. *Circulation* 1984;69:1036–47.
- [58] Kourliouros A, Savelieva I, Kiotseoglou A, Jahangiri M, Camm J. Current concepts in the pathogenesis of atrial fibrillation. *Am Heart J* 2009;157:243–52.
- [59] Platonov PG, Mitrofanova LB, Orshanskaya V, Ho SY. Structural abnormalities in atrial walls are associated with presence and persistency of atrial fibrillation but not with age. *J Am Coll Cardiol* 2011;58:2225–32.

